

Nociceptive Inputs to Brainstem Pain-modulating Neurons

Caitlynn C. De Preter

A DISSERTATION

Presented to the Department of Behavioral Neuroscience,
Behavioral and Systems Neuroscience Graduate Program,
and the Oregon Health and Science University School of Medicine
in partial fulfillment of
the requirements for the degree of

Doctor of Philosophy

October 2024

CERTIFICATE OF APPROVAL

School of Medicine
Oregon Health & Science University

This dissertation was presented on

10/02/2024

by

Caitlynn C. De Preter

This is to certify that the PhD dissertation of
Caitlynn C. De Preter has been approved by:

Dissertation Advisor: Mary M. Heinricher, PhD

Committee Chair: Tianyi Mao, PhD

Member: Matthew Butler, PhD

Member: Stephen David, PhD

Member: Susan Ingram, PhD

Reader: Michael Morgan, PhD

TABLE OF CONTENTS

LIST OF FIGURES	7
LIST OF ABBREVIATIONS	8
ACKNOWLEDGEMENTS	9
ABSTRACT	10
CHAPTER 1	11
ADAPTED FROM MANUSCRIPT # 1	11
1.1 OVERVIEW.....	12
1.2. MODULATION OF PAIN BY THE ROSTRAL VENTROMEDIAL MEDULLA.....	14
1.2.1. <i>Classification and function of RVM cell types</i>	15
1.2.2. <i>Mapping molecular markers to function</i>	19
1.3. OUTPUTS FROM THE RVM	21
1.4. INPUTS TO RVM PAIN-MODULATING NEURONS.....	23
1.4.1. <i>“Bottom up” inputs convey nociceptive information to RVM pain-modulating neurons</i>	23
1.4.2. <i>“Top-down” inputs to RVM</i>	25
1.4.3 <i>Sex differences in PAG-RVM circuitry and opioid-induced analgesia</i>	27
1.4.4. <i>PAG relays the influence of the mPFC on nociception</i>	28
1.5. RVM POPULATION DYNAMICS AND IMPLICATIONS FOR PAIN MODULATION.....	29
1.6. SUMMARY.....	31
1.6.1. <i>Chapter 2: Establish RVM cell responses to systemic morphine administration in female rats</i>	32
1.6.2. <i>Chapter 3: Nociceptive transmission pathways from Vi/Vc to RVM</i>	32
1.6.3. <i>Chapter 4: Establish the use of high-density silicon probe technology in RVM</i>	33
1.6.4. <i>Significance and Innovation</i>	34
CHAPTER 2	35
MANUSCRIPT # 2.....	35
2.1. ABSTRACT	36
2.2. INTRODUCTION.....	37
2.3. MATERIALS AND METHODS	38
2.3.1. <i>Surgical preparation and anesthesia for physiological characterization of RVM neurons</i>	38
2.3.2. <i>Inflammation</i>	39
2.3.3. <i>Characterization of RVM neurons under basal conditions and in persistent inflammation</i>	39

2.3.4. <i>Response of characterized RVM neurons to opioid administration</i>	40
2.3.5. <i>Histology</i>	41
2.4. RESULTS	44
2.4.1. <i>No differences in RVM cell ongoing firing and noxious somatic stimulus related responses in male and female animals</i>	44
2.4.2. <i>Persistent inflammation following CFA injection produces mechanical but not thermal hyperalgesia in female animals</i>	48
2.4.3. <i>Evoked responses of RVM neurons in female animals with persistent inflammation</i>	49
2.4.4. <i>Opioid response of RVM neurons in female animals</i>	50
2.5. DISCUSSION	53
CHAPTER 3	57
MANUSCRIPT # 3	57
3.1. ABSTRACT	58
3.2. INTRODUCTION	59
3.3. METHODS	60
3.3.1. <i>Viral vector injections</i>	61
3.3.2. <i>In vivo recording</i>	61
3.3.3. <i>Characterization of RVM neurons and response to Vi/Vc input</i>	62
3.3.4. <i>Recording sites and optical fiber placement</i>	63
3.3.5. <i>Anatomical tracing experiments</i>	63
3.3.6. <i>Analysis</i>	65
3.3.6.1. <i>Light-evoked responses in ChR2 experiments</i>	65
3.3.6.2. <i>Response to von Frey application and effect of inhibiting trigeminal terminals in RVM using ArchT</i>	66
3.3.6.3. <i>Statistical comparisons</i>	66
3.4. RESULTS	66
3.4.1. <i>Expression and validation of ChR2 or ArchT in Vi/Vc neurons and terminals in RVM and PB</i>	66
3.4.2. <i>RVM ON-cells are activated while RVM OFF-cells are inhibited by optogenetic activation of the Vi/Vc region</i>	68
3.4.3. <i>Ventral, but not dorsal, Vi/Vc projections to RVM recruit pain-modulating neurons</i>	70
3.4.4. <i>Optogenetic inhibition of ventral Vi/Vc terminals in RVM attenuates nociceptive responses of ON- and OFF-cells</i>	72
3.4.5. <i>Vi/Vc sends a GABAergic projection to RVM and PB neurons</i>	74
3.4.6. <i>Vi/Vc also recruits RVM pain-modulating neurons via PB</i>	76

3.4.7. <i>Direct and indirect recruitment results in different RVM response profiles</i>	79
3.5. DISCUSSION	80
3.5.1. <i>Direct pathway to RVM from ventral Vi/Vc and lamina V of Vc</i>	80
3.5.2. <i>Indirect pathway to RVM from dorsal Vi/Vc and more superficial laminae of Vc</i>	81
3.5.3. <i>Contribution to the OFF-cell pause</i>	82
3.6. SUMMARY AND CONCLUSIONS	83
CHAPTER 4	85
MANUSCRIPT # 4	85
4.1. ABSTRACT	86
4.2. SIGNIFICANCE STATEMENT	86
4.3. INTRODUCTION	87
4.4. METHODS	89
4.4.1. <i>Electrophysiological recordings</i>	89
4.4.2. <i>Histology</i>	90
4.4.3. <i>Spike sorters</i>	90
4.4.4. <i>Post-processing of sorter output and comparison</i>	90
4.4.5. <i>RVM neuron functional classification</i>	92
4.5. RESULTS	92
4.5.1. <i>Comparison of five sorters</i>	92
4.5.2. <i>Effect of manual curation</i>	95
4.5.3. <i>All five sorters identify physiologically classifiable units</i>	97
4.6. DISCUSSION	98
4.6.1. <i>Agreement among output of different sorters applied to RVM recordings</i>	99
4.6.2. <i>All sorters identified classifiable RVM units</i>	101
4.6.3. <i>MS5, IC, KS3, SC, and TDC can all be used to sort high-density RVM recordings</i>	102
4.6.4. <i>Conclusions</i>	103
CHAPTER 5	104
DISCUSSION	104
5.1. KEY FINDINGS	105
5.2. OVERVIEW	107
5.3. RVM NEURONS IN FEMALE ANIMALS RESPOND TO MORPHINE	108
5.4. VI/VC INPUT TO RVM	109
5.4.1 <i>Direct Vi/Vc input to RVM (Chapter 3)</i>	109

5.4.2. <i>Indirect Vi/Vc input to RVM (Chapter 3)</i>	111
5.4.3. <i>Differences in the direct and indirect circuits</i>	112
5.4.4. <i>Contribution to the OFF-cell pause</i>	112
5.5. HIGH-DENSITY SILICON PROBE RECORDINGS	114
5.6. TECHNICAL CONSIDERATIONS	115
5.6.1. <i>Anesthesia</i>	115
5.6.2. <i>Optogenetic methods</i>	116
5.6.3. <i>Withdrawal in a stereotaxic frame</i>	117
5.6.4. <i>Pause and burst activity in high-density silicon probe recordings</i>	117
5.7. FUTURE DIRECTIONS	118
5.7.1. <i>Role of GAD65+ neurons in the direct and indirect pathway</i>	118
5.7.2. <i>Synaptic characteristics of the Vi/Vc-RVM circuit</i>	118
5.7.3. <i>Identification of RVM cell types in slice</i>	118
5.7.4. <i>The role of Vi/Vc neurons in chronic inflammation</i>	119
5.8. CONCLUSIONS	120
REFERENCES	121

LIST OF FIGURES

FIGURES

Figure 1. Brainstem pain-modulation circuitry

Figure 2. The RVM functional cell types are defined by changes in firing associated with withdrawal from a noxious stimulus.

Figure 3. The RVM receives two parallel information streams from the dorsal horn with different temporal properties.

Figure 4. Firing of ON- and OFF-cells is reciprocal and coordinated.

Figure 5. Histologically verified recording locations within the RVM.

Figure 6. Representative OFF- and ON-cell responses associated with heat-evoked withdrawal in female animals.

Figure 7. Heat-evoked reflex-related responses in naïve males and females and paw withdrawal latencies.

Figure 8. Ongoing firing of ON- and OFF-cells.

Figure 9. Mechanically evoked cell response and withdrawal in naïve males and females.

Figure 10. Mechanical but not thermal hypersensitivity in females with persistent inflammation.

Figure 11. Shift in cell stimulus-response curve for mechanical stimulation of CFA treated paw.

Figure 12. Representative RVM cell response to systemic morphine administration in female animals.

Figure 13. Effects of systemic morphine administration on ongoing cell activity and withdrawal-evoked cell behaviors in naïve females.

Figure 14. Recording sites within RVM for ArchT and ChR2 experiments.

Figure 15. ChR2 and ArchT expression in Vi/Vc and terminal expression in RVM and PB.

Figure 16. ChR2-induced activation of trigeminal cell bodies mimics noxious stimulation, activating ON-cells and suppressing the firing of OFF-cells.

Figure 17. ChR2-induced activation of RVM terminals arising from ventral Vi/Vc and Vc Lamina V neurons, but not dorsal Vi/Vc, mimics noxious stimulation, activating ON-cells and suppressing the firing of OFF-cells.

Figure 18. ArchT-induced inhibition of RVM terminals arising from ventral Vi/Vc attenuates ON-cell and OFF-cell noxious evoked activity.

Figure 19. Both RVM and PB receive GABAergic projections from ventral Vi/Vc.

Figure 20. PB neurons are activated or inhibited by Vi/Vc cell body stimulation, while unaffected by RVM terminal activation.

Figure 21. RVM cell response timing differs with activation of Vi/Vc terminals in RVM versus PB.

Figure 22. Performance of different automated sorters in brainstem recordings.

Figure 23. Effect of curation and interaction with physiological classification.

LIST OF ABBREVIATIONS

ACC	Anterior cingulate cortex
Amg	Amygdala
ArchT	Archaerhodopsin
CFA	Complete Freund's adjuvant
ChR2	Channelrhodopsin-2
CTb	Cholera Toxin Subunit B
DMH	Dorsal medial hypothalamus
EKG	Electrocardiograph
EMG	Electromyograph
FG	Fluoro-gold
GABA	γ -Aminobutyric acid
GPER	G-protein-coupled estrogen receptor
Hyp	Hypothalamus
IC	IronClust
KS3	Kilosort3
MOR	μ -opioid receptor
mPFC	Medial prefrontal cortex
MS5	MountainSort5
PAG	Periaqueductal gray
PB	Parabrachial nucleus
RVM	Rostral ventromedial medulla
SC	SpyKING CIRCUS
SEM	Standard error of the mean
TDC	Tridesclous
VF	von Frey fibers
Vi/Vc	Trigeminal nuclei (interpolaris/caudalis)

ACKNOWLEDGEMENTS

I would like to thank my advisor Dr. Mary Heinricher for giving me the freedom to explore my interests and become an independent researcher during my PhD. Thank you to the members of the Heinricher lab that provided me tremendous support and feedback. A huge thank you to Melissa Martenson, Yangmiao Zhang, and Zhigang Shi for all your encouragement.

Thank you to my dissertation advisory committee for your important suggestions and insights: Dr. Tianyi Mao, Dr. Susan Ingram, Dr. Stephen David, and Dr. Matthew Butler. Thank you to Dr. Michael Morgan for being on my exam committee.

Thank you to the Abbas lab. Specifically thank you Dr. Alex Sonneborn for your time and help with getting the multi-channel work established.

Lastly, thank you to my family and friends. Mama and Papa, you inspired me at an early age to keep learning and persevering, and I would not have been able to do this without your support. Thank you, Alex Nevue, for doing loops around OHSU and listening to every talk. Thank you to my mentors at Merck, especially Julia Kahn. My short time as a co-op was one of the most rewarding experiences during my PhD, and I am forever grateful for everyone's time and mentorship.

This work was supported by the National Institutes of Neurological Disorders and Stroke (NS098660), the OHSU School of Medicine Exploratory Seed Grant program, and the Tartar Trust Foundation. I was supported by the National Institute of Dental and Craniofacial Research Fellowship (F31 DE030677) and Ashworth-Thomason Training Award.

ABSTRACT

The brain regulates nociceptive processing through descending projections from the brainstem to the spinal and trigeminal dorsal horns. This is accomplished through endogenous pain-modulating circuits that can amplify or suppress pain-related signals, and normally maintain a balance between facilitation and inhibition of pain. In chronic pain conditions, the system is dysregulated, contributing to a facilitated pain state. After opioid administration, the system turns into a pain inhibiting state. The output of this pain-modulating system, via the rostral ventromedial medulla (RVM) has been extensively studied. Bidirectional pain control from this region is mediated by two physiologically defined cell classes, “ON-cells” and “OFF-cells,” that respectively facilitate and inhibit nociceptive transmission. However, sensory inputs to RVM are only now receiving significant attention. Indirect inputs from the dorsal horn via the parabrachial complex (PB) convey nociceptive information to RVM and contribute to the sensitization of RVM neurons in persistent inflammatory pain. However, there also is evidence from anatomical studies for a direct input from the dorsal horn to RVM.

The data in this dissertation firstly established the use of female rodents for future RVM studies and found that ON- and OFF-cells respond similarly to morphine in both sexes. Second, these data established a functional link between the trigeminal horn, which relays sensory information from the face and neck, and RVM, revealing that RVM receives both direct inputs and indirect inputs via the PB. Lastly, this work established the use of high-density silicon probe technology in RVM, greatly increasing data output and providing the ability to answer questions about how ON- and OFF-cells work as a population. Collectively, these studies enhanced our understanding of the contribution of sensory inputs to the intrinsic pain-modulatory circuit and defined how nociceptive inputs gain access to the RVM. By identifying the drivers of pro-nociceptive brainstem outputs, we can gain new insights into how pain-modulating systems are recruited and modulated in acute pain, providing us with novel targets for therapies.

CHAPTER 1

INTRODUCTION

ADAPTED FROM MANUSCRIPT # 1

The 'in's and out's' of descending pain modulation from the rostral ventromedial medulla

Trends in Neurosciences. 2024 May 14.

Caitlynn C. De Preter^{1,2} and Mary M. Heinricher^{1,2}

Departments of Behavioral Neuroscience³ and Neurological Surgery⁴, Oregon Health & Science

University, Portland, OR, 97239

CDP and MMH –Wrote the paper

1.1 OVERVIEW

Nociception, the sensory processing of tissue damage, and pain, the sensory experience and suffering usually associated with tissue damage, are crucial for survival. While organisms can survive without sight, hearing, or olfaction, and have even regressively evolved to abandon these senses, all animal species possess nociceptors and the ability to sense injury [1-4]. Failure of the nociceptive system to detect damaging or potentially damaging somatic inputs can result in serious injury [5]. However, nociception and pain can be dissociated in that pain is not a direct function of tissue damage: tissue damage does not invariably lead to pain, and conversely, pain does not always reflect tissue damage.

The disparity between tissue damage and pain is due in large part to the actions of an intrinsic pain-modulating system that can suppress or amplify nociception and pain, and does so depending upon other biological needs and competing behavioral priorities [6-10]. The output node of this pain-modulating system is the rostral ventromedial medulla (RVM), which comprises the nucleus raphe magnus and adjacent reticular formation at the level of the facial nucleus. The RVM sends a diffuse projection to the trigeminal and spinal dorsal horns, where it interfaces with nociceptive transmission circuits (Fig. 1). The RVM integrates “bottom-up” (nociceptive sensory input) with “top-down” influences, notably from the midbrain periaqueductal gray (PAG) and medial prefrontal cortex (mPFC). The bottom-up influences support feedback control of nociceptive processing by RVM, while top-down inputs provide a potential substrate for modulation of pain by cognitive and emotional factors [11]. These emotional and cognitive factors can further influence nociceptive transmission via the RVM. Therefore, RVM plays one of the most important roles in the pain-modulating system, since it receives both top-down input to *modulate* pain, while also *responding* to bottom-up noxious input.

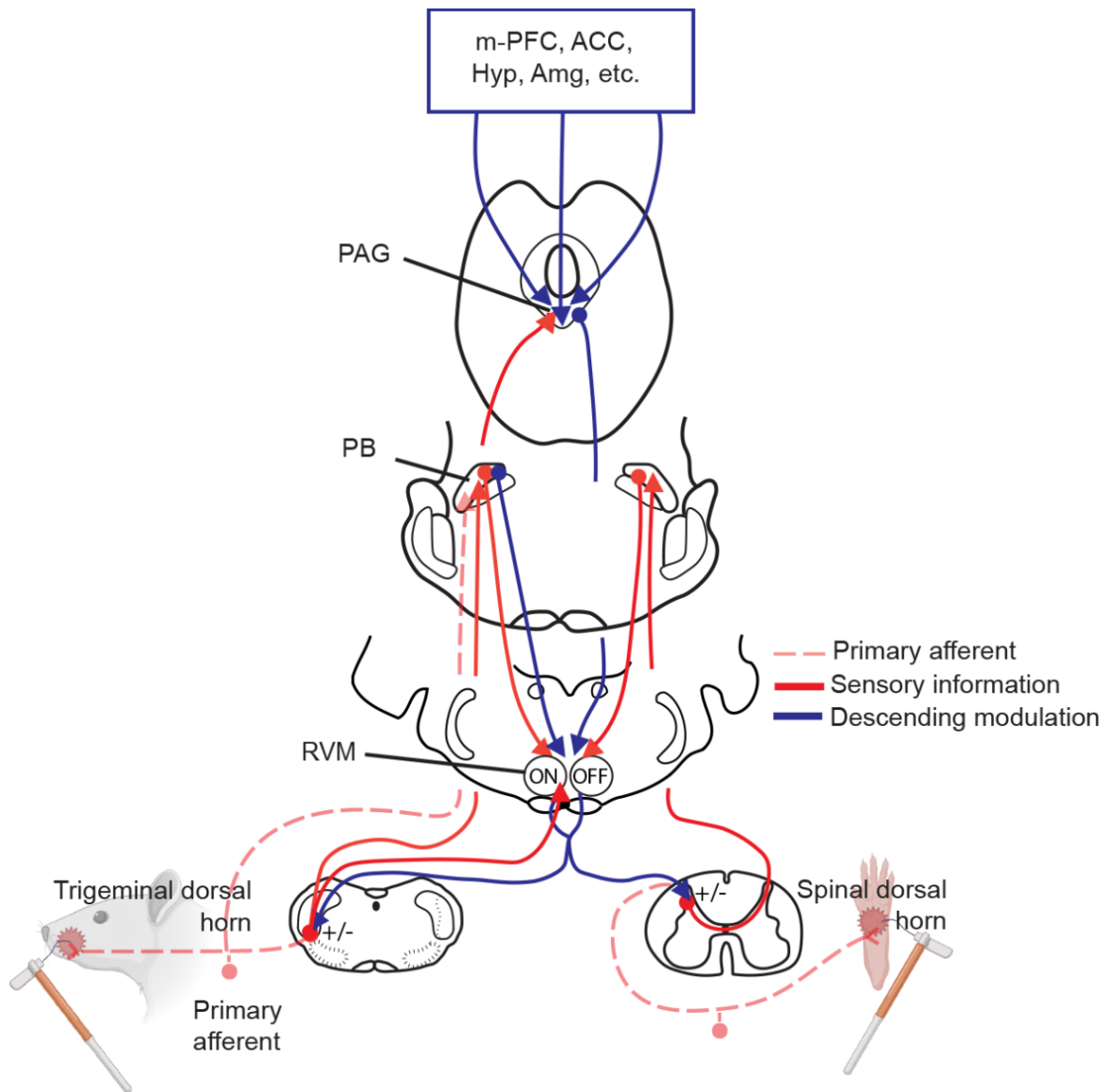


Figure 1. Brainstem pain-modulation circuitry

Ascending pathways: Primary afferents innervating the whisker pad or hindpaw convey nociceptive information to second order neurons in the trigeminal or spinal dorsal horns. Trigeminal pathway: Primary afferents can access neurons in the PB directly. Second order neurons in the trigeminal dorsal horn can relay nociceptive information to RVM directly and indirectly through PB. Spinal pathway: Second order neurons relay nociceptive information to RVM indirectly through PB.

Descending pathways: Cognitive and emotional processes mediated by higher brain structures influence RVM through the PAG. RVM output facilitates (ON-cells) or inhibits (OFF-cells) the transmission of nociceptive signals at the level of the trigeminal and spinal dorsal horns, in turn modulating the ascending sensory information pathway to PB, creating a feedback loop. ACC: anterior cingulate cortex; Amg: amygdala; Hyp: hypothalamus; m-PFC: medial prefrontal cortex; PAG: periaqueductal gray; PB: parabrachial complex; RVM: rostral ventromedial medulla.

While bottom-up inputs have been anatomically defined, these methods do not reveal whether a particular input is relevant to the pain-modulating functions of the RVM. This dissertation addresses 3 questions: 1) how do RVM neurons behave in females in response to opioids? 2) What are the pathways through which noxious information is relayed to pain-modulating neurons in RVM? and 3) Can new recording technologies be used to characterize the activity of multiple RVM neurons in a single recording? Collectively, the data in the current dissertation established the use of female animals in RVM pain-modulating studies (Chapter 2), defined a functional link between the trigeminal transition zone (Vi/Vc), a region of the brainstem involved in relaying noxious craniofacial input, and RVM (Chapter 3), and established high-density silicon probe recording technology (Chapter 4).

1.2. MODULATION OF PAIN BY THE ROSTRAL VENTROMEDIAL MEDULLA

The RVM was originally described as an “analgesia center” following demonstrations that low-intensity (< 10 μ A) electrical stimulation in this region produced potent antinociception and that opioids exerted their analgesic effects in part via an action in the RVM [12]. However, the functions of the RVM were subsequently shown to be significantly more complex. Contrary to that initial conceptual framework, the RVM not only inhibits pain but can also facilitate it, promoting hyperalgesia [6, 8, 13]. Moreover, the RVM is also implicated in autonomic function [14-16]. However, pain modulation by the RVM can be dissociated from autonomic control [17-19], suggesting that the different functions of the RVM are mediated by distinct cell populations. It is therefore imperative to identify the specific RVM cell types that mediate descending control of pain. This first section will describe how RVM exerts pain-facilitating or pain-inhibiting control through diffuse projections at multiple levels of the spinal and trigeminal dorsal horn [20-28] through distinct functionally defined cell classes, termed “ON-“ and “OFF-cells”, and discuss challenges with mapping these functional classes to molecular cell types.

1.2.1. Classification and function of RVM cell types

Functional cell types, defined by changes in activity associated with behavioral responses to noxious stimuli, have provided a productive and coherent explanatory framework for understanding the functions of the RVM. Two cell types, “ON-cells” and “OFF-cells,” exhibit abrupt state changes associated with nocifensive withdrawal: ON-cells enter a period of activity (“burst”), and OFF-cells a period of silence (“pause”) beginning just before the execution of nocifensor reflexes, such as the tail flick or paw withdrawal evoked by heat or mechanical stimulation (Fig. 2). This response occurs irrespective of the stimulation site, as seen in the response to mechanical stimulation of the whisker pad and hindpaw (see Technical considerations) [29-32]. At least some cells of both classes project to the dorsal horn [33, 34].

The noxious-related responses (burst and pause) could be taken to suggest that RVM pain-modulating neurons are simply modifying reflex behavior and are not relevant to pain as an aversive experience. This argument is based on the correlations between cell activity and the dynamics of the motor response [35]. Blocking RVM output reduces the magnitude of withdrawal, for example [36]. However, lesioning RVM alters the threshold for evoking behavior, without eliminating the motor response [37-39], and paralyzed animals still exhibit changes in RVM cell firing with stimuli that would normally elicit withdrawal [40]. Moreover, nociceptive withdrawal threshold is measurably lower during phases when ON-cells are active and OFF-cells inactive [41]. Additionally, RVM is implicated in many higher brain control functions than simple withdrawal. RVM output can be manipulated to induce conditioned place preference and avoidance [42-44]. These findings support RVM cells’ ability to modulate pain as a sensory experience, contributing to both the sensory reflexive component of pain, as well as the affective experience. Therefore, RVM should not be viewed as a sensory system, but as a modulatory system.

OFF-cells are responsible for the analgesic effects of manipulating the RVM, whereas ON-cells mediate the pro-nociceptive actions of this region (see [7, 8, 12, 45] for comprehensive

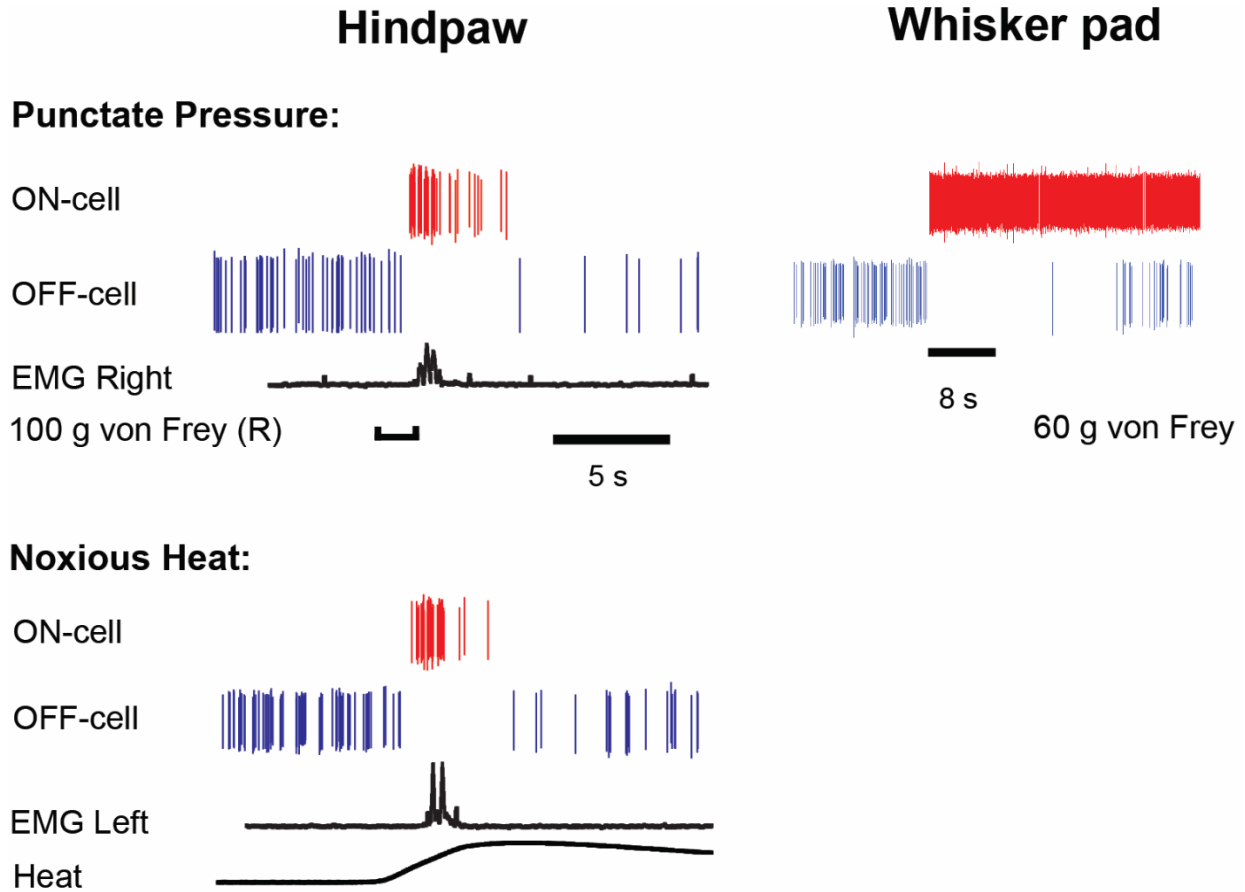


Figure 2. The RVM functional cell types are defined by changes in firing associated with withdrawal from a noxious stimulus

Representative recordings show Individual spikes emitted by an ON-cell (red) and an OFF-cell (blue) recorded simultaneously during application of noxious heat to the left hindpaw (top) and of a von Frey probe (100 g) to the right hindpaw (lower). Withdrawal is seen as deflections in the electromyogram (EMG) signal. **Punctate Pressure:** (Left) the OFF-cell pauses and ON-cell bursts immediately prior to the withdrawal from the von Frey probe to the paw. (Right) ON- and OFF-cell responses are similar in response to mechanical stimulation of the face. **Noxious Heat:** OFF-cell stops firing (“pauses”), while the ON-cell starts to fire (“bursts”) just prior to onset of the withdrawal. In both paw stimulation cases, the ON-cell burst was initiated immediately after the OFF-cell ceased firing. Heat stimulus (ramped from a hold temperature of 35 °C to a maximum of 53 °C at 1.5 °C/s) was delivered using contact Peltier device. The time of von Frey fiber application is indicated by a bracket below the trace. EMG trace was rectified and smoothed to show the magnitude and timing of the withdrawal. Recording was in a lightly anesthetized rat.

reviews). Experimental activation of OFF-cells produces analgesia, and it has been calculated that recruitment of fewer than 100 OFF-cells is sufficient to produce this effect [46, 47]. By

contrast, selective activation of ON-cells enhances nociceptive sensitivity [30, 48], and ON-cells have been shown to contribute to behavioral hypersensitivity in a number of rodent models of acute and chronic pain states [6, 13, 49, 50]. The validity of the OFF/ON-cell categorization for classifying RVM neurons has been further confirmed by the distinct pharmacological profiles exhibited by the different cell classes [30, 48, 51-61]. For example, opioids produce their analgesic effects in part by an action in the RVM, directly suppressing the firing of ON-cells while activating OFF-cells via disinhibition [51, 62].

Multiple lines of evidence indicate that the OFF/ON categorization reflects a stable and generalizable property of RVM pain-modulating neurons. OFF- and ON-cells have been described in unanesthetized animals [63-65], and in mouse as well as rat [66]. These cell classes are robust to stimulus modality and stimulation site (Fig. 2). Early reports that OFF- or ON-cells responded specifically to stimulation of select body parts [67, 68] suffered from technical limitations including repeated noxious stimulation of undefined intensity, lack of a behavioral correlate, and fluctuating anesthetic levels. Moreover, conclusions derived from electrophysiological studies using the OFF/ON framework have repeatedly been found to be congruent with behavioral observations by multiple groups in awake rats and mice [10, 69-79], and with functional imaging evidence in humans [80-83].

RVM neurons that display no changes in firing to noxious stimulation are considered a third class, "NEUTRAL-cells." NEUTRAL-cell classification has raised controversy, with some literature incorrectly classifying NEUTRAL-cells as a subgroup of ON- and OFF-cells that respond to craniofacial input alone [84], while more rigorous evidence using jaw-related behavioral reflex indicates NEUTRAL-cells do not respond to facial input when the appropriate behavioral withdrawal is recorded [32]. In contrast with our understanding of OFF- and ON-cell functions, the role of NEUTRAL-cells remains an enigma. Like OFF- and ON-cells, at least some NEUTRAL-cells project to the spinal cord, although it is not clear that the dorsal horn is a

specific target. It seems likely that NEUTRAL-cells are functionally heterogeneous, and contribute to the other known functions of the RVM, such as thermogenesis [14].

Serotonergic neurons, comprising ~20% of RVM neurons, have been considered either a subclass of NEUTRAL-cells, or a distinct fourth class [85]. Serotonergic neurons do not appear to be a subset of either OFF- or ON-cells, although some serotonergic neurons are weakly responsive to noxious stimuli [85-88]. Interestingly, early studies of the RVM as a pain-modulating system focused on serotonin as a molecular marker for analgesia-producing neurons in this region, primarily because the analgesic effects of stimulating the RVM were substantially attenuated or blocked by spinal administration of serotonin antagonists [89]. However, this straightforward and attractive concept lost its appeal when it was subsequently demonstrated that spinal administration of serotonin antagonists could similarly interfere with hyperalgesia in a range of persistent pain states. Further, selective activation of serotonergic neurons in the RVM can exacerbate or induce hyperalgesia [90-92], and serotonin levels at the trigeminal dorsal horn are tonically increased in mice subjected to a painful nerve injury [93].

Reconciling these disparate findings, it is now recognized that serotonergic outflow from the RVM has both pro-nociceptive and antinociceptive effects through an action in the dorsal horn, with the former mediated by the 5HT₃ receptor [94]. The variety of serotonin receptor subtypes and distinct anatomical targets in the dorsal horn may be relevant: medial RVM serotonergic neurons project more densely to the deeper laminae of the dorsal horn (laminae V through VI) and chemogenetic activation of midline serotonergic neurons produced mechanical (but not thermal) hyperalgesia, whereas lateral serotonergic RVM neurons project densely to superficial dorsal horn (laminae I and II) and chemogenetic activation of these more lateral neurons leads to thermal (but not mechanical) hyperalgesia [95, 96]. One possible resolution of these apparent discrepancies may be that serotonin acts as a modulator, enabling the functional effects of both OFF- and ON-cells at various sites under relevant conditions [97].

1.2.2. Mapping molecular markers to function

The OFF/ON/NEUTRAL-cell functional classes defined using a combination of *in vivo* electrophysiology, behavior, and pharmacology have not so far been successfully mapped to molecular cell-types defined by neurotransmitter content, e.g., GABA or glutamate. Indeed, none of these classes has a homogeneous molecular signature. A majority of spinally projecting OFF-cells were found to be GABAergic, but so were the majority of spinally projecting ON-cells and NEUTRAL-cells [98], and a substantial proportion of each class was presumably glutamatergic. Consistent with the fact that GABA is found in both OFF- and ON-cells, activation of RVM GABAergic neurons in the RVM using genetic tools has resulted in both pro-nociceptive [10, 74] and antinociceptive [75] effects in different experimental paradigms and rodent models. Indeed, it was clear as early as the mid-1980's that "no one neurotransmitter" mediates the different functional outputs from the RVM [99]. In addition to GABA, glutamate, and serotonin, there are a number of neuropeptides, including Substance P, somatostatin, enkephalin, cholecystokinin, and vasoactive intestinal peptide that co-localize with classical neurotransmitters in RVM neurons projecting to the dorsal horn [100, 101]. Glycine is also found in the RVM, including in projection neurons, and appears to be co-localized with GABA in many cases [102, 103]. Cholinergic neurons projecting to the dorsal horn have also been identified in the RVM [100, 104].

Another approach to defining molecular classes is to take advantage of the distinct pharmacological responses of different functional classes, which relates to their distinct receptor types. The μ -opioid receptor (MOR) is expressed only on ON-cells, and this cell class is the only one that expresses the MOR; further, *all* ON-cells respond to μ -opioid agonists [105]. Tools that take advantage of μ -opioid pharmacology, such as dermorphin-saporin, a neurotoxin selectively taken up by MOR-expressing neurons, have therefore been useful in confirming the pro-nociceptive function of ON-cells [73]. The G protein-coupled estrogen receptor (GPER) is another target linked specifically to ON-cells, although only a subset (~20% of ON-cells defined

by MOR expression) also express GPER. Exogenous estrogen or a GPER ligand applied directly within the RVM produces hyperalgesia, as does selective activation of GPER-expressing neurons. Conversely, local administration of a GPER receptor antagonist, or ablation of GPER-expressing neurons, reduces nociceptive responses in mice and rats [76, 106]. These findings with GPER raise the question of whether GPER-mediated activation of ON-cells is relevant to sex differences in pain or persistent pain. However, behavioral effects of GPER antagonism were seen in male as well as female mice and rats [76], which would argue against a *sex-specific* function of this receptor in the RVM.

Expression of the kappa opioid receptor (KOR) has also been proposed as a way to isolate the antinociceptive function of the RVM, and indeed, activation of KOR-expressing neurons in the RVM has been reported to have antinociceptive effects [78]. However, as with neurotransmitter content, KOR expression does not define a single functional population, since the majority of both OFF- and NEUTRAL-cells, as well as a small proportion of ON-cells express KOR [98]. The net antinociceptive effect of activating KOR-expressing neurons in the RVM therefore reflects the known behavioral potency of OFF-cells, which supersedes any behavioral effect of co-activating ON-cells and NEUTRAL-cells [62, 107]. Therefore, the KOR-expressing cells do not represent a functionally meaningful cell type.

More broadly, these analyses of RVM functions highlight some potential pitfalls involved in interpreting behavioral experiments based on candidate molecular markers. First, when a cell population expressing a specific marker is manipulated, it is possible that only a subset of that population is responsible for any measured behavioral effect. Without independent demonstration that neurons expressing the marker are functionally homogeneous, it can only be concluded that some unknown subset of that “type” is sufficient to elicit the behavior. Indeed, this experimental paradigm does not preclude the possibility that some subset of neurons expressing the relevant marker has no effect, different effects, or even opposing effects, since other outputs might be overridden and not manifest in behavior. A further concern is that a role

in other behaviors or physiological parameters that were not fully explored in the experimental paradigm cannot be ruled out. Finally, the possibility that additional cell populations defined by different, nonoverlapping, markers might also have the same net behavioral effect should be considered.

Because of the diverse functions and cell types of RVM and inconsistent molecular markers of RVM cell classes, functional characterization using electrophysiological approaches that allow single-neuron, single-spike resolution provides the most meaningful view into the circuitry and function of the RVM. Future studies using a combination of molecular dissection and *in vivo* recording, like Patch-seq for example, are necessary to determine RVM molecular cell types. It is likely that RVM neurons will need to be classified by both physiological and molecular types. For example, as described above, G-protein-coupled estrogen receptor (GPER) neurons likely represent a *subset* of GABAergic ON-cells and are important for itch and pain [108, 109]. Unfortunately, the reality is that functional types cannot be targeted as easily as molecular types for treatment currently. However, little is known about the inputs that drive changes in RVM cell activity, which may reveal other ways of defining RVM cell classes and reveal potential treatment targets.

1.3. OUTPUTS FROM THE RVM

RVM OFF- and ON-cells exert their effects on nociception and pain via descending projections to the dorsal horn [26, 34, 110, 111], where they respectively inhibit and facilitate the transmission of nociceptive signals relevant to local processing (e.g., nocifensor reflexes) and to the sensory experience of pain, including the affective dimension [112-114]. RVM terminals relevant to pain-modulation are concentrated in the superficial dorsal horn (laminae I/II), the neck of the dorsal horn (laminae IV/V) and surrounding the central canal (lamina X), and primarily contact somata and dendrites, rather than primary afferent terminals. These targets are for the most part excitatory neurons [115, 116]. Projections are diffuse, terminating bilaterally and at multiple levels [26, 96]. Moreover, dorsal horn neurons responding to RVM

input are heterogeneous in terms of location, morphology, and firing pattern [117, 118]. There is also preliminary evidence that the RVM can modulate other descending systems, such as the noradrenergic outputs of the locus coeruleus [119].

The diffuse nature of the RVM projection, together with the multiple dorsal horn targets imply that the RVM has the capacity to modulate nociceptive processing at multiple “touch points” in the dorsal horn, each of which will require detailed investigation. One recent focus has been on the *targets* of GABAergic RVM projection neurons. As already noted, up to about half of RVM neurons projecting to the dorsal horn are GABAergic [120]. Consistent with the fact that a substantial proportion of both OFF- and ON-cells are GABAergic [98], RVM GABAergic neurons exert both pro-nociceptive and antinociceptive effects, likely mediated by subsets of ON- and OFF-cells respectively. Thus, chemogenetic or optogenetic activation of RVM GABAergic neurons projecting to the dorsal horn or their terminals was reported to enhance mechanical nociception in both mice and rats, an effect attributed to RVM GABA-mediated inhibition of inhibitory interneurons in the dorsal horn [10, 74]. By contrast, selective activation of RVM inhibitory neurons (GABA and/or enkephalin) connecting with primary afferent terminals in the dorsal horn was found to induce mechanical and thermal hypoalgesia in mice [75]. Thus, the RVM-mediated inhibition of inhibitory interneurons was found to enhance nociception, whereas the RVM-mediated inhibition of transmission from primary afferents suppressed nociception. It is notable that manipulation of GABA-expressing RVM outputs with specific, distinct targets in the dorsal horn has opposing behavioral effects. Interestingly, RVM projections to the trigeminal dorsal horn also differ from projections to the spinal dorsal horn, with RVM projections to the spinal dorsal horn more likely being GABAergic than projections to the trigeminal dorsal horn [21]. Indeed, this work highlights the importance of considering connectivity in defining and implementing the functions of RVM neurons, beyond characterization of the neurons’ responses to noxious stimuli or molecular content.

1.4. INPUTS TO RVM PAIN-MODULATING NEURONS

As described earlier, the net functional roles of RVM OFF- and ON-cells are now well established, and their primary output, to the dorsal horn, is being delineated in increasing detail. With that foundation, defining the *inputs* to these neurons (understanding the parameters that influence their activity) should provide insights into how intrinsic and extrinsic factors that can influence pain exert their effects on the RVM. Factors known to influence RVM OFF- and ON-cell firing include noxious sensory information, circuits mediating opioid analgesia [121], autonomic status [16], environmental light levels [122], and stress leading to both stress-induced analgesia and hyperalgesia [18, 123]. Functional pathways through which this information is conveyed to the RVM are not yet well defined, but anatomical tracing studies have revealed numerous inputs to the RVM from across the neuraxis, including the dorsal horn, and higher structures such as midbrain periaqueductal gray (PAG), hypothalamus, anterior cingulate, and amygdala [7, 124]. Although anatomical studies by themselves do not reveal whether a particular input is relevant to the pain-modulating function of the RVM, several circuits are well defined, and will be considered here.

1.4.1. “Bottom up” inputs convey nociceptive information to RVM pain-modulating neurons

ON-cells are activated by noxious stimuli, whilst OFF-cell firing is suppressed. This acute, pain-related activation of pain-facilitating ON-cells and suppression of pain-inhibiting OFF-cells functions as a positive feedback loop, facilitating responses to subsequent sensory inputs [125]. Functional pathways through which nociceptive information gains access to RVM ON- and OFF-cells are only now being defined, but it has become clear that there are at least two parallel pathways that convey nociceptive information to the RVM.

One pathway is an *indirect* pathway with a relay in the parabrachial complex (PB). The PB is a major nociceptive, emotional, and autonomic processing and relay center that at least in

rodents is the target of the bulk of supraspinal projections from the superficial dorsal horn [126-128]. It also receives input from deep dorsal horn [129, 130]. The PB projects directly to the RVM [131-133], and optogenetic inhibition of PB terminals in the RVM demonstrates that a PB relay contributes to the OFF-cell pause and ON-cell burst [132]. This system demonstrates considerable plasticity in persistent inflammatory pain states [134].

There is also a *direct* pathway to RVM from the trigeminal dorsal horn [103, 135-137]. The trigeminal dorsal horn is located in the lateral medulla of the brainstem. The trigeminal dorsal horn relays sensory input, primarily pain and temperature, from the face and head. Nociceptive information from the craniofacial region is first carried by peripheral sensory fibers to the spinal trigeminal nuclear complex where it is integrated. This complex is divided into the subnuclei oralis, interpolaris (Vi) and caudalis (Vc), from the rostral to caudal end [138, 139]. These subnuclei process pain from semi-discrete areas of the face: injection of cholera toxin B (CTb) in the three trigeminal nerve branches, maxillary, ophthalmic, and mandibular, reveal specific axonal terminations in the different subnuclei [140].

Nociceptive input had long been thought to be processed primarily in the Vc, but now attention has shifted to the Vi/Vc transition zone, as neurons in this region display increased excitability and sensitization in persistent pain states [141-143]. This transition zone comprises the rostral end of Vc dorsally, with the caudal end of Vi ventrally. Nociceptive neurons in both dorsal and ventral Vi/Vc send projections to PB [128, 144, 145], potentially relaying nociceptive information to RVM indirectly. PB neurons also exhibit prolonged responses to mechanical stimulation in models of trigeminal neuropathic pain [146] and receive direct nociceptive information from primary afferents innervating the whisker pad [147].

Combined tracing and immunohistochemistry experiments revealed nociceptive neurons in ventral Vi/Vc project to RVM [22]. However, given the diverse cell classes in RVM, how Vi/Vc recruits the different cell classes was explored in Chapter 3. The optogenetic studies in Chapter 3 show that both indirect Vi/Vc projections to RVM via PB and direct Vi/Vc projections contribute

to nociceptive responses of OFF- and ON-cells [136]. Direct GABAergic input to OFF-cells from the dorsal horn may contribute to the characteristic pause that defines these neurons, since it is known that this pause is mediated by GABA, and that the relevant input is not a local interneuron [148-150].

It is reasonable to assume that the direct and indirect nociceptive pathways are not mutually exclusive. Indeed, some neurons in the trigeminal complex project to both RVM and PB. However, the RVM response to activation of the two pathways was found to be not identical (Chapter 3; Fig. 3), with selective activation of the indirect pathway producing a prolonged response in RVM compared to that elicited by activation of the direct pathway [136]. This raises the possibility that these parallel input pathways play distinct functional roles, and contribute to the complexity of modulating both acute and chronic pain. For example, PB may link RVM to the affective dimension of pain, and modulating nocifensive behaviors through RVM, while RVM is directly engaged by Vi/Vc to promote immediate nocifensive responses. It is important to piece apart this circuit to understand how pain-transmission systems interact with pain-modulatory networks, especially in both male and female animals, given that trigeminal chronic pain conditions disproportionately impact women.

1.4.2. "Top-down" inputs to RVM

"Top-down" inputs to the RVM provide a potential substrate through which cognitive and emotional factors can influence pain [11]. The most prominent input to the RVM from higher structures arises from the PAG, which also relays information from cortical regions and amygdala to RVM. The influence of the PAG on RVM, and how PAG is recruited by medial prefrontal cortex (mPFC) will be considered here.

Like the RVM, the PAG is a heterogeneous region with multiple functions, but it plays a prominent role in pain, stress, and defensive behavior [151-153]. As with the RVM, electrical stimulation or focal injection of μ -opioid agonists in PAG produces antinociception. Importantly, electrical stimulation has been used clinically for pain relief, confirming that this system

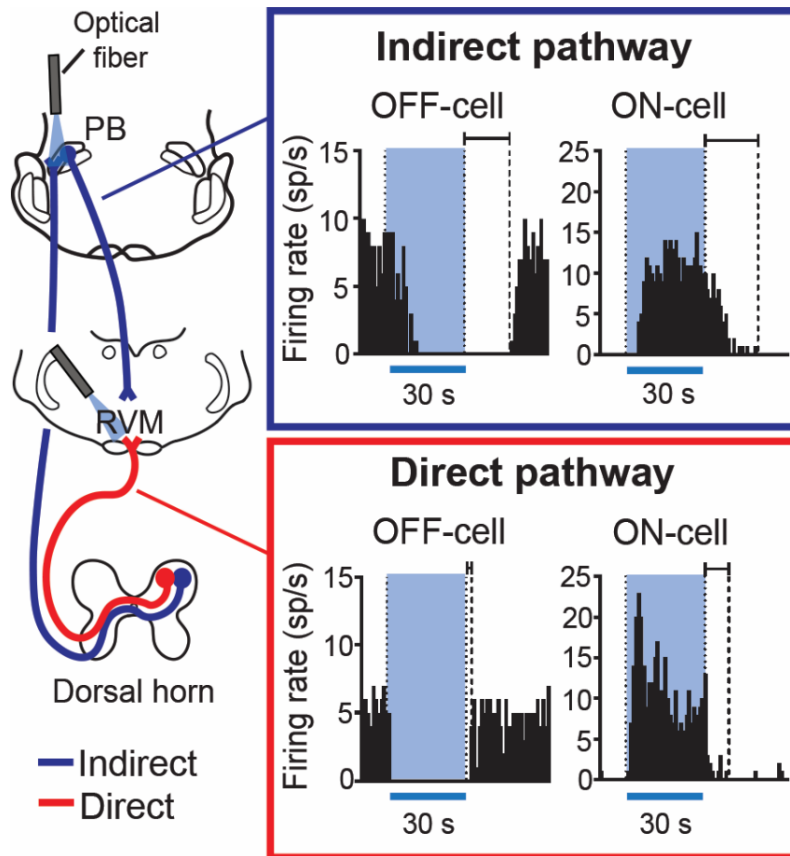


Figure 3. The RVM receives two parallel information streams from the dorsal horn with different temporal properties.

Left: the schematic illustrates indirect input to the RVM from the dorsal horn, via a relay in the PB (blue), and a parallel, direct projection from the dorsal horn (specifically the trigeminal dorsal horn, red). Right: firing rate histograms show representative responses of OFF-cells and ON-cells to optogenetic activation of dorsal horn terminals in the PB (indirect pathway) and in the RVM itself (direct pathway, stimulation sites shown in schematic at left). Blue overlay indicates periods of light delivery (30 s). The response to activation of the indirect pathway through the PB evokes a delayed response in the RVM that outlasts the stimulus, whereas the response to activation of the direct pathway is time-locked to light delivery. Recording in lightly anesthetized rat, histogram bins 1 s. Light delivered to trigeminal dorsal horn terminals in the PB (indirect pathway) and the RVM (direct pathway). Abbreviations: PB, parabrachial complex; RVM, rostral ventromedial medulla; sp/s, spikes/s.

modulates pain processing, and is not simply suppressing motor output [154]. Antinociception produced by activation of PAG is mediated by the RVM, via the latter's descending output to the dorsal horn [7]. Electrical stimulation of the circuit elicits analgesia in humans [155-157], just as it does in rats [158, 159]. Although the pain-modulating functions of the PAG have been studied most intensively in the context of analgesia, it can exert a pro-nociceptive effect [160-162].

As with the RVM itself, attempts to define molecular cell-types in the PAG have proved challenging [163]. Activation of GABAergic neurons leads to increased nociceptive behaviors [164, 165]. This is unlikely to represent a straightforward circuit however, since anatomical studies demonstrate that PAG neurons projecting to RVM include both GABAergic and glutamatergic populations, and there is no consensus as to the relative densities of the two projections [166-168].

Opioid engagement of the PAG-RVM system to produce analgesia has long been explained using the “disinhibition hypothesis,” in which opioids act presynaptically to inhibit GABA release onto PAG output neurons projecting to the RVM [121, 169]. This certainly occurs, but is also becoming clear that the disinhibition hypothesis is not a *complete* explanation of the link between PAG and RVM. Opioids can inhibit PAG neurons post-synaptically via activation of G protein-coupled inwardly rectifying potassium (GIRK) channels [121] and some PAG-RVM output neurons express mu opioid receptors [170, 171], suggesting that direct inhibitory effects of opioids in the PAG are also important. Moreover, MOR expressed by both GABAergic and glutamatergic PAG populations has been implicated in different forms of stress-induced analgesia [172]. These data suggest that there are at least two parallel, opioid-sensitive outputs from the PAG to RVM.

1.4.3 Sex differences in PAG-RVM circuitry and opioid-induced analgesia

Opioids are one of the most powerful classes of analgesics. Opioids interact with opioid receptors to modulate the release of neurotransmitters that are involved in the transmission of pain signals. This results in decreased perception of pain and overall analgesia. While incredibly effective in many acute settings, opioids have a long list of risks and side effects that become more severe with longer term use. Chronic opioid administration can lead to adaptations in RVM, contributing to opioid tolerance and hyperalgesia [173]. In acute settings, opioids act directly and indirectly to change RVM cell activity, resulting in the inhibition of pain signals as

they travel from the spinal and trigeminal dorsal horn to higher brain structures. As described earlier, RVM cell types can be defined by their response to systemic opioid administration.

Biological and social factors can influence pain experiences and responses to treatment. Thus, sexual dimorphisms in opioid metabolism contribute to disparities in the effectiveness of opioids [174]. At the same time, women are more likely to seek out treatment for pain and receive opioid prescriptions than men. However, literature in humans and rodents is conflicting. In humans, μ -opioids are more potent in women [175, 176], while in rats, μ -opioids are more potent in males than females [177-186]. Moreover, human studies can be influenced by psychological factors or social expectations, and rat studies are influenced by methodological factors such as dosing, administration route, and pain testing assays.

While the PAG-RVM descending modulatory system is engaged in both sexes [187, 188], pharmacological properties or anatomical differences in this circuit could contribute to the differential opioid effects in men and women. In male rats, there is a greater activation of PAG output neurons during systemic morphine administration, even though there is a reported greater number of PAG-RVM output neurons in females [189, 190]. Sex differences in opioid receptor expression and signaling in the pain-modulation circuit may also contribute to differences in opioid response [177, 186, 191-193]. Physiologically defined RVM cell classes in female rats have been identified, and compared to males, they demonstrate similar firing patterns and responses to noxious stimulation in both naïve and persistent inflammatory conditions [61, 194, 195]. In Chapter 2, experiments revealed RVM cells in female animals responded to systemic administration of opioids in the same direction as in male animals.

1.4.4. PAG relays the influence of the mPFC on nociception

The PAG receives a major cortical input from the mPFC, and there is accumulating evidence that dysfunction of this circuit underlies diminished descending control in chronic pain states, particularly neuropathic pain models. Stimulation of mPFC produces analgesia under basal conditions, but more important, inhibition of mPFC neurons projecting to the PAG has an

effect by itself, and results in hyperalgesia in rats [196, 197]. This suggests that mPFC maintains a tonic anti-nociceptive influence via the PAG, and raises the possibility that loss of this tonic anti-nociceptive influence via PAG contributes to chronic pain states. Consistent with this latter idea, excitability of mPFC neurons projecting to PAG is reduced after nerve injury, a change due at least in part to alteration in the balance of inhibitory and excitatory drive from the basolateral amygdala, as well as changes in endocannabinoid function in mPFC [198-201]. Confirmation that mPFC engages descending control comes from the observation that activation of mPFC depresses noxious-evoked responses of dorsal horn neurons [197].

It is worth noting that not all cortical influences on pain are mediated by engaging descending control. Manipulations of anterior cingulate cortex (ACC) can alter pain behaviors, and even activity of nociceptive dorsal horn neurons [202]. Like the mPFC, the ACC sends a substantial projection to the PAG. However, opioids applied directly in the ACC do not alter pain behaviors in animals subjected to nerve injury, although this procedure does induce a conditioned place preference in these animals (and not in controls that are not experiencing neuropathic pain). By contrast, opioids applied in RVM not only produce a CPP, but also attenuate pain behaviors [114, 203]. These findings imply that ACC plays a role in the affective dimension of pain after nerve injury, but that unlike mPFC, it does not recruit the RVM to modulate activity at the level of the dorsal horn.

1.5. RVM POPULATION DYNAMICS AND IMPLICATIONS FOR PAIN MODULATION

The foundational data defining the physiology and function of RVM neurons have for the most part come from studies of single, functionally characterized neurons. This approach has provided insights into how information is processed in RVM, and how and when pain-modulating neurons are recruited to exert their effects. However, codes implemented at the level of a neuronal population may not be evident at the level of individual neurons. This is not only because of variability when looking at individual neurons, but because variation and co-variation within and between populations may be functionally meaningful.

As noted earlier, single- and dual-electrode recordings suggest that cells within the OFF- and ON-cell classes fire in phase, and conversely, that cells of the two classes fire out of phase, such that activity in the OFF- and ON-cell populations is reciprocal (Fig. 4) [41, 204]. This reciprocal pattern is observed even in the absence of any noxious stimulation that would entrain activity in these neurons. This implies that there are integrating mechanisms that coordinate the activity of all members within each class and that this integration is functionally significant.

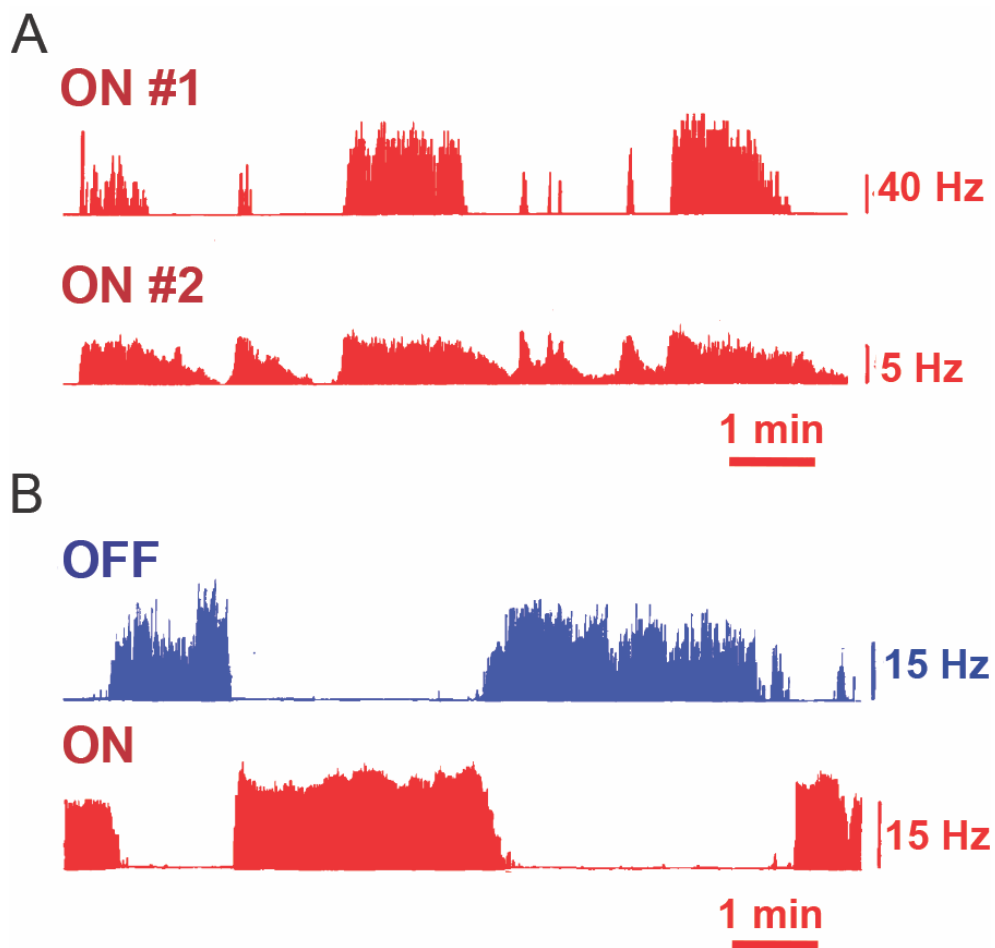


Figure 4. Firing of ON- and OFF-cells is reciprocal and coordinated

(A) Spontaneous firing of two ON-cells recorded simultaneously illustrates in-phase activity within this class. (B) Firing of an OFF-cell and ON-cell recorded simultaneously illustrates out-of-phase activity of the two cell classes: spontaneous active periods exhibited by the OFF-cell coincide with periods of lower or no activity of the ON-cell. The individual neurons were recorded simultaneously on two electrodes placed into the RVM of a lightly anesthetized rat. Ratemeter records with 1 s bins.

Little is known, however, about functional connectivity within the RVM. ON-cells likely do not inhibit the OFF-cells, given that selective inhibition of ON-cells does not reduce the OFF-cell pause and that the ON-cell burst does not precede the OFF-cell pause [148, 149]. These observations imply that ON-cells, as a population, do not function as an inhibitory interneuron within the RVM. Indeed, ON-cells are thought to lack local connections with the RVM, although OFF-cells give off local collaterals in addition to their projections to the dorsal horns [205].

Understanding the integrating mechanisms that coordinate activity within and between OFF- and ON-cell classes thus remains a significant challenge. Recent advances in silicon-probe technology to allow large-scale recordings from multiple cells with single-cell resolution in deep brain structures are employed in Chapter 4 to answer future population-level questions.

1.6. SUMMARY

Interactions between pain transmission and pain modulation happen at multiple levels in the pain-modulating circuit. The transmission of nociceptive information from the spinal and trigeminal dorsal horns is subject to bidirectional control by brainstem pain-modulation systems. This is mediated through two physiologically identified cell classes within the RVM, which is the output of this system. These cells, termed “ON-” and “OFF-cells”, respectively facilitate or inhibit the transmission of noxious information. After systemic morphine administration, the output of these neurons is modulated by both direct and indirect action which interferes with the transmission of nociceptive information. However, primary use of male rodents in research created a gap in knowledge about how these neurons respond to morphine and noxious information in both male and female animals. In addition, the ascending pathway through which noxious inputs gain access to RVM is only now receiving attention, and RVM population dynamics could not be described using traditional single-electrode recordings. This dissertation describes experiments that delineated RVM responses to morphine in female animals, elucidated an indirect and direct relay from Vi/Vc, a major relay of craniofacial nociceptive

information in the brainstem, and describe the novel application of high-density silicon probe recordings in the brainstem to investigate RVM population activity.

1.6.1. Chapter 2: Establish RVM cell responses to systemic morphine administration in female rats

The focus of the second Chapter of this dissertation was to characterize RVM cell activity in response to systemic morphine administration in female animals. Historically, single-unit electrophysiological recordings have been primarily conducted in male rodents, leaving a major gap in our knowledge of RVM physiology in female animals. RVM cells are defined in two ways: by their response to noxious stimulation and their response to opioids. While literature in humans and animals on basal pain sensitivity is conflicting and controversial, pharmacological responses to opioids are one of the few consistently reported differences between the sexes [206]. Previous research from the Heinricher lab demonstrated that firing properties of RVM ON- and OFF-cells are comparable between the sexes, and both cell classes exhibited sensitized responses to somatic stimuli in females subjected to persistent inflammation. Therefore, I investigated RVM responses to opioid administration and measured the change in ON- and OFF-cell activity in response to systemic morphine administration. *I found, that in response to systemic morphine administration, RVM cells in female rats respond in the same direction as RVM cells in male rats.*

1.6.2. Chapter 3: Nociceptive transmission pathways from Vi/Vc to RVM

The focus of Chapter 3 of this dissertation was to determine the direct and indirect pathways through which noxious signals reach RVM pain-modulating neurons. Previous research from the Heinricher lab demonstrated RVM receives indirect spinal and trigeminal nociceptive information from the cords through PB. However, anatomical evidence suggests a direct input from the trigeminal dorsal horn (Vi/Vc). If Vi/Vc relays nociceptive information directly to RVM, then activation of Vi/Vc terminals should mimic RVM responses to noxious

stimulation of the face, while inhibition of Vi/Vc terminals in RVM should attenuate RVM nociception-related activity. In addition, given that PB relays nociceptive information to RVM and that Vi/Vc projects to PB, activation of the indirect pathway through stimulation of Vi/Vc terminals in PB while recording from physiologically identified RVM neurons should mimic RVM responses to noxious stimulation of the face. Having established a foundation for the use of female animals in studies of RVM in Chapter 2 and given that trigeminal chronic pain disorders disproportionately affect females, I investigated this circuitry in both male and female animals.

In Chapter 3, I measured the change in RVM cell activity in response to optogenetic manipulation of Vi/Vc terminals in RVM. *I found that activation of both direct and indirect Vi/Vc pathways to RVM increased ON-cell activity and decreased OFF-cell activity, mimicking RVM cell responses to noxious stimulation in both male and female animals. NEUTRAL-cells remained unchanged. Interfering with Vi/Vc inputs attenuated the nociception-related responses of ON- and OFF-cells.*

1.6.3. Chapter 4: Establish the use of high-density silicon probe technology in RVM

The goal of Chapter 4 was to determine if high-density silicon probes can be used in RVM. The past 40 years of recordings in RVM have utilized single-unit electrodes, providing a thorough and careful definition of RVM functional cell types. However, by nature, this recording technique relies on a biased search approach and results in low data output. Additionally, there are many reasons to believe that the coordinated activity of RVM cells is functionally significant, and single- and dual-electrode recordings have relied on chance paired or distant neurons in RVM to observe this coordinated activity. High-density silicon probes can overcome these challenges by recording from multiple neurons in RVM in a single recording and location.

In Chapter 4, I successfully recorded RVM activity using a recently commercially available silicon probe that could reach RVM. 6 recordings were used to compare the performance of automated spike sorters, a necessary step as multi-channel recordings cannot be feasibly sorted using the previous semi manual and manual curation methods used for

single-unit recordings. *I found that each spike-sorter had varying degrees of agreement between sorters. However, each spike-sorter tested was able to identify ON-, OFF-, and NEUTRAL-cells, and manual curation of the output was necessary to reduce the number of false positives. These studies established the experimental tools for future investigations of RVM population activity.*

1.6.4. Significance and Innovation

The brainstem pain-modulating system maintains normal pain processing, and alterations in the normal functioning of this system contribute to many chronic pain states. RVM, the output center of this system, can facilitate or inhibit the transmission of noxious sensory information to help animals escape from pain. RVM neurons are directly affected by μ -opioid agonists, producing analgesia, but they also enhance nociception, facilitating hypersensitivity and spontaneous pain in chronic pain conditions. RVM neurons are defined by their response to noxious somatic input and opioids, yet the pathways through which pain-related information reaches these neurons is unknown, and sex disparities in research have created a gap in our understanding of how these neurons respond to opioids in females.

In this dissertation, I established the use of female animals in future RVM studies, defined a direct nociceptive relay from the dorsal horn to RVM, and established the use of high-density silicon probe technology for future investigations in RVM population dynamics. The experiments in this dissertation utilize a combination of optogenetic methods, single-unit in vivo recordings, multi-channel high density silicon probe recordings, behavior, tract tracing, and pharmacology. These approaches allow me to make direct conclusions about RVM circuitry and opioid responses.

CHAPTER 2

MANUSCRIPT # 2

Physiological properties of pain-modulating neurons in rostral ventromedial medulla in female rats, and responses to opioid administration

Neurobiology of Pain. 2021 September 27.

Gwen Hryciw*^{1, 2, 4, 5}, Caitlynn C. De Preter*^{3, 4, 5}, Jennifer Wong^{4, 5}, and Mary M. Heinricher^{3, 4, 5}
School of Dentistry¹, Departments of Biomedical Engineering², Behavioral Neuroscience³, and
Neurological Surgery⁴, Oregon Health & Science University⁵, Portland, OR, 97239

*These authors contributed equally to this work

GH, CCDP – Designed and performed experiments, analyzed data, and wrote the paper

JW – Performed experiments, analyzed data, and wrote the paper

MMH – Designed experiments, analyzed data, and wrote the paper

2.1. ABSTRACT

Functional pain disorders disproportionately impact females, but most pain research in animals has been conducted in males. While there are anatomical and pharmacological sexual dimorphisms in brainstem pain-modulation circuits, the physiology of pain-modulating neurons that comprise a major functional output, the rostral ventromedial medulla (RVM), has not been explored in female animals. The goal of this study was to identify and characterize the activity of RVM cells in female, compared to male, rats. ON- and OFF-cells were identified within the RVM in females, with firing properties comparable to those described in males. In addition, both ON- and OFF-cells exhibited a sensitized response to somatic stimuli in females subjected to persistent inflammation, and both ON- and OFF-cells responded to systemically administered morphine at a dose sufficient to produce behavioral antinociception. These data demonstrate that the ON-/OFF-cell framework originally defined in males is also present in females, and that as in males, these neurons are recruited in females in persistent inflammation and by systemically administered morphine. Importantly, this work establishes a foundation for the use of female animals in studies of RVM and descending control.

2.2. INTRODUCTION

Chronic pain disorders disproportionately impact females, and while studies in healthy humans indicate that there are likely few sex differences in basal pain threshold, males and females may experience pain differently [206-208]. One factor that could contribute to sex differences in pain experience is sexual dimorphisms in brainstem pain-modulation circuits. The rostral ventromedial medulla (RVM) is the functional output of the best-studied pain-modulating circuit. The RVM has been well-characterized anatomically, physiologically, pharmacologically, and functionally in male animals. Although there is evidence for anatomical and pharmacological sexual dimorphism in brainstem pain-modulating circuits [183, 185, 189, 190, 209], the physiology of pain-modulating neurons in females has been almost entirely unexplored.

A large body of evidence based on almost exclusively on findings in males indicates that the RVM modulates nociceptive transmission through projections to the spinal and trigeminal dorsal horns. Two classes of neurons, termed “ON-cells” and “OFF-cells”, have been identified physiologically in males: activity of ON-cells increases, whereas activity of OFF-cells ceases prior to behavioral responses evoked by noxious stimuli [29]. These two cell classes respectively amplify and suppress nociceptive transmission. A shift in the balance between ON- and OFF-cell population output can therefore produce enhanced or diminished nociception and pain behaviors [6, 7]. RVM receives information via sensory pathways, including noxious somatic input, forming a recurrent circuit [45, 134]. Input from higher structures to RVM forms a circuit through which cognitive and emotional factors can influence pain [7].

Given the evidence for anatomical and pharmacological differences in this brainstem pain-modulating circuit between males and females, it is surprising that few studies have considered the physiological properties of pain-modulating neurons in females [194, 195]. The purpose of the present study was to identify and fully characterize the activity of RVM cells in female compared to male animals.

We first compared RVM neuronal activity in naïve males and females to establish if there are any basal differences. Second, since women report higher prevalence of chronic pain than men, we extended these studies of RVM neuronal properties to a model of persistent, localized inflammation (injection of Complete Freund's Adjuvant into the plantar surface of one hindpaw). Finally, since the analgesic actions of opioids are reported to differ between women and men [210, 211], we determined the responses of RVM neurons to systemically administered morphine.

We found the basic physiological properties of RVM neurons to be similar between the sexes, in both the naïve state and during persistent inflammation, and that responses to systemic morphine administration were comparable. Taken as a whole, these data imply that the same fundamental “machinery” for descending control of pain is in place in females as well as males.

2.3. MATERIALS AND METHODS

All experiments followed the guidelines of the National Institutes of Health and the Committee for Research and Ethical Issues of the International Association for the Study of Pain, and were approved by the Institutional Animal Care and Use Committee at the Oregon Health & Science University. Male and female Sprague Dawley rats from Charles River were used in all experiments, weighing <380 and 260 g, respectively, at time of recording. Animals were acclimated for at least 12 days in the vivarium before testing.

2.3.1. Surgical preparation and anesthesia for physiological characterization of RVM neurons

Rats were housed in 12 h light/12 h dark cycles, and experiments were performed during the light phase. Following previously described methods [122, 212], animals were anesthetized (4% isoflurane) and a catheter placed in the external jugular vein for subsequent infusion of methohexital. Animals were then transferred to a stereotaxic apparatus and kept deeply anesthetized while a small craniotomy posterior to the lambda suture was drilled to gain access to RVM. After surgery, anesthesia was adjusted so that the animal withdrew its hindpaw to

noxious heat exposure but did not display spontaneous movement. Animals were maintained at this stable anesthetic plane for the duration of the experiment by infusion of methohexital at a constant rate. Heart rate and body temperature were also monitored. There was no significant difference in heart rate or body temperature between males and females (HR: $t_{36} = 0.76$, $p = 0.46$, Temp: $t_{36} = 0.63$, $p = 0.53$). Experimental protocol was initiated once the methohexital flow rate was not adjusted for a minimum of 20-30 min. Males required a higher anesthetic rate compared to females ($t_{35} = 2.84$, $p = 0.0076$, males: 60.89 ± 1.09 mg/kg/h, females: 56.18 ± 1.19 mg/kg/h) to achieve a similar anesthetic plane [213]

2.3.2. Inflammation

Persistent inflammation was induced in a subset of female animals prior to experiments. Rats were briefly anesthetized with isoflurane (4%, 4–5 min) and CFA (0.1 ml) was injected subcutaneously into the plantar surface of the right hindpaw. Rats were returned to their home cage for 3 to 6 days to model persistent inflammation, since inflammation peaks at this time [214, 215]. There was no significant difference in anesthetic dose required to maintain CFA-treated females at an anesthetic depth similar to that employed for naïve females ($t_{41} = 0.74$, $p = 0.46$, F CFA: 57.8 ± 1.82 mg/kg/h, F naïve: 56.18 ± 1.19 mg/kg/h). There was also no effect of treatment on heart rate or body temperature (HR: $t_{41} = 1.42$, $p = 0.16$, Temp: $t_{41} = 0.84$, $p = 0.41$).

2.3.3. Characterization of RVM neurons under basal conditions and in persistent inflammation

All testing was performed in low ambient light conditions (< 5 lux). A gold- and platinum-plated stainless-steel microelectrode was placed in the RVM to record cell activity. Signals were amplified and band-pass filtered (Neurolog, Digitimer) then transmitted to a computer for real-time spike detection and monitoring using Spike2 (CED, Cambridge, UK). EMG activity, heart rate, and paw heat-stimulus temperature were also recorded using Spike2. Identified neurons were classified as ON-, OFF-, or NEUTRAL-cells based on changes in firing rate associated

with nocifensive withdrawal [29, 122, 212]. ON-cells are defined by a burst in activity beginning just prior to withdrawal from a noxious stimulus. OFF-cells stop firing just prior to withdrawal.

After isolating and identifying a cell as an ON- or OFF-cell, one heat trial was performed on each hindpaw approximately 4 min apart (some trials were delayed in order to capture an ON-cell in a quiet state or an OFF-cell in an active state). Noxious heat was applied by lightly resting a Peltier device (Yale Instruments, New Haven, CT) on the plantar surface of the paw. Paw surface temperature was held at 35 °C before heat onset, and temperature then increased at a rate of approximately 1.5 °C to a maximum of 53 °C. To avoid damage to the paw, the Peltier device was removed upon limb movement, determined using EMG. von Frey fibers (4, 15, 26, 60, and 100 g) were applied to the webbing between the toes. Each fiber was applied three times to each paw, in ascending order, for 8 s. Three interdigital testing sites were alternated, with a minimum of 30 s between each trial. Longer inter-trial intervals (up to 5 min) were sometimes necessary to capture an ON-cell in a quiet state or an OFF-cell in an active state. Paw withdrawal was monitored visually as well as with EMG. In experiments using CFA, inflammation was confirmed visually in CFA-treated animals and paws were measured with calibrated calipers applied at the widest point across the dorsal-plantar surface. The treated hindpaw was significantly larger than those of untreated females ($t_{35} = 17.84$, $p < 0.0001$, CFA: 7.97 ± 0.16 , Naïve: 4.46 ± 0.089). In experiments using systemic morphine administration, a thermal stimulus (cut-off temperature of 53 °C, 12 s) was also used.

2.3.4. Response of characterized RVM neurons to opioid administration

Surgical preparation was as above. Opioids were administered systemically via either a second jugular catheter (n = 10) or intraperitoneal injection (n = 25). After isolating and identifying a cell, one heat trial was performed every 5 min as described above. After a minimum of 3 trials to establish baseline cell and behavioral response, morphine sulfate was given in increments of 0.5 mg/kg every 10 min until there was no behavioral response on two of

three successive heat trials (12-s cut-off). Naloxone (1 mg/kg i.v. or i.p.) was then administered, and ongoing firing and paw withdrawal-related changes in activity were recorded for a minimum of three trials. The average dose required to produce analgesia in these experiments in female animals was 1.86 mg/kg, which falls within the range of doses that are sufficient to suppress noxious evoked reflexes in lightly anesthetized male animals [216-218].

2.3.5. Histology

At the end of each experiment, the recording site was marked with an electrolytic lesion (Fig. 5). Animals were euthanized by methohexital overdose and perfused transcardially with saline and 10% formalin. Brains were removed, and the lesion site reconstructed. The RVM was defined as the nucleus raphe magnus and adjacent reticular formation medial to the lateral

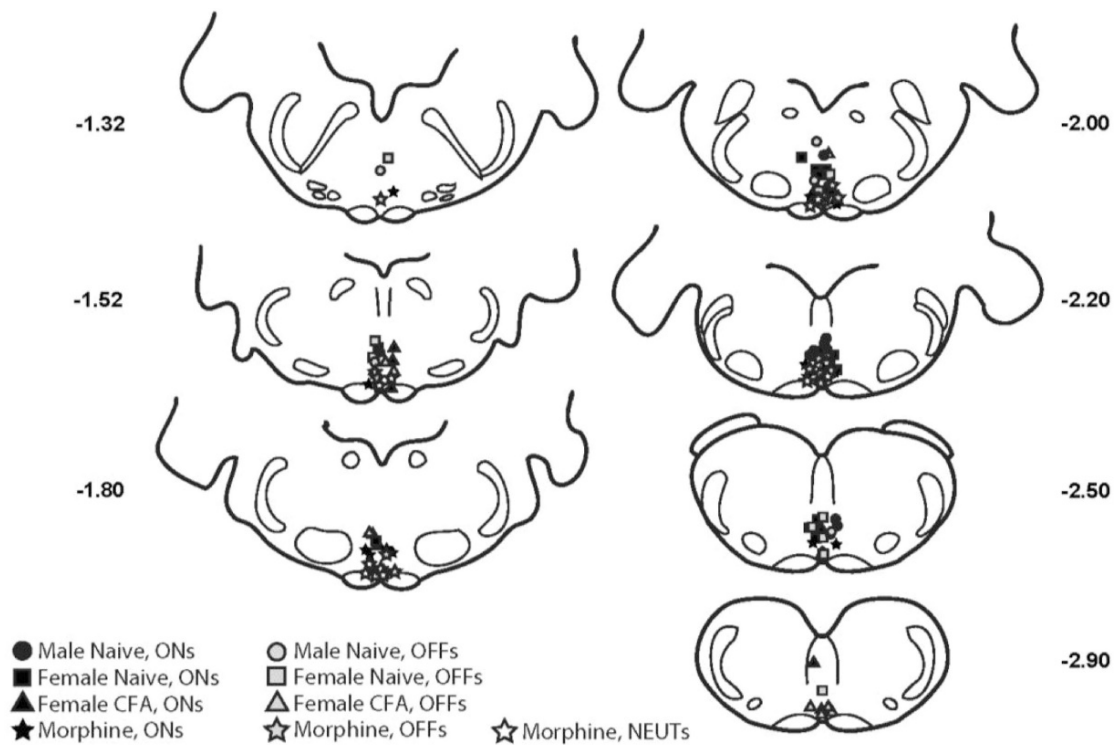


Figure 5. Histologically verified recording locations within the RVM.

Recording sites were distributed between -1.32 and -2.90 mm (relative to the interaural line). The majority of cells were distributed between -1.52 and -2.50 mm caudal to the interaural line.

boundary of the of the pyramids at the level of the facial nucleus. For characterization of RVM physiology, a total of 21 cells from 17 males, 26 cells from 21 naive females, and 25 cells from 22 CFA-treated females were recorded (1–2 cells per animal, although only one protocol was performed in each animal, two identifiable cells were isolated in some experiments). In experiments focused on opioid responses, a total of 45 cells was recorded from 35 females (1–2 cells per animal). Cells were distributed throughout RVM in both males and females (Fig. 5).

2.3.6. Data processing and analysis

At the conclusion of each experiment, action potential waveforms were individually examined to verify correct waveform sorting. Thermal-evoked paw withdrawal latency was defined as the average time from heat onset till paw withdrawal based on EMG activity. Mechanical withdrawal thresholds for each paw were determined based on the minimum force at which a withdrawal was observed in at least two out of three trials.

Ongoing activity was defined as the average firing rate during the two 30-s periods prior to each heat trial. Evoked firing for ON-cells was defined as the total number of spikes in the longest burst during heat, or as the total number of spikes in all bursts initiated during mechanical stimulation. A “burst” was defined as the first action potential after stimulus onset until the last action potential that preceded a 2-s quiet period. However, if an ON-cell was already active prior to heat stimulus onset, then the number of action potentials in the 3-s period around the paw withdrawal was used as the evoked response. Similarly, if an ON-cell was active prior to application of the von Frey fiber, the number of action potentials during the 8-s stimulation was considered the evoked response. Peak firing rate during stimulation was also determined for ON-cells. The stimulus-evoked pause exhibited by OFF-cells was quantified as the percent suppression. In heat trials, this was the firing rate in the 3-s period around the paw withdrawal relative to the firing rate 10-s prior to heat onset. For mechanical stimulation trials, this was the firing rate in the 8-s during mechanical stimulation relative to that in the 8-s period

prior to mechanical stimulation. The longest pause duration during stimulation was also determined. A “pause” was defined as the time-period between one spike that was preceded within 2 s by another action potential and terminated when two action potentials occurred within 2 s. Cell response threshold was also determined by finding the force required to elicit a minimum 50% change in cell in activity in at least two out of three trials.

Behavioral and cellular data from naïve animals were averaged between the left and right paw for subsequent data analysis. Behavioral data and reflex-related cell parameters were compared between naïve males and females using unpaired *t*-tests, and between the contralateral and ipsilateral paw of CFA-treated females using paired *t*-tests. For tests with von Frey fiber stimulation, data from naïve males and females were compared using 2-factor ANOVA with repeated measures on force. Data from CFA-treated females was analyzed using a 2-factor ANOVA with paw and force as within-subject factors.

In a separate set of experiments looking at effects of morphine administration on activity of RVM neurons in females, three time periods were defined for the purpose of analysis. The “baseline” was defined as the three heat trials prior to the first dose of morphine, the “morphine” period as the final three trials prior to naloxone (two of three consecutive trials with no withdrawal within the 12-s cut-off, as described above), and the “naloxone” period was the three trials after naloxone administration that resulted in at least two paw withdrawals. Ongoing activity was defined as the average firing rate during three 30-s periods prior to the heat trial in each time period. Evoked firing for ON- cells was defined as the total number of spikes in the longest burst during heat. In the morphine time-period when the paw-withdrawal was completely lost, cell activity around the average paw-withdrawal temperature at baseline + 0.5 °C was collected to define stimulus-related cell activity. Behavioral and cellular data obtained in the baseline period were compared with the averages of the three post-morphine trials and the three post-naloxone trials using repeated-measures ANOVA. Quantitative data are presented as mean ± SEM, unless otherwise specified. Parameters with highly skewed distributions were

log-transformed for analysis, and back-transformed data presented as geometric mean \pm 95% confidence intervals.

2.4. RESULTS

2.4.1. No differences in RVM cell ongoing firing and noxious somatic stimulus related responses in male and female animals

The first set of experiments compared the firing properties of RVM OFF- and ON-cells in female and male animals. Examples of the reflex related changes in firing of an OFF-cell and ON-cell recorded from a female animal during heat-evoked withdrawal are shown in Fig. 6.

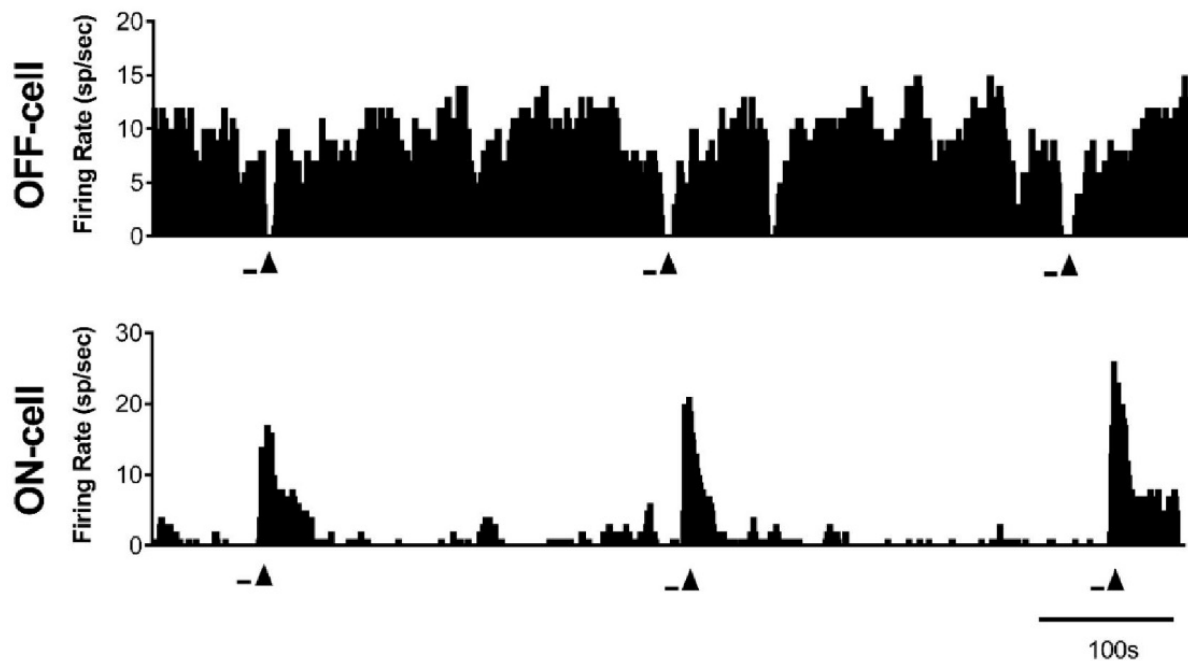


Figure 6. Representative OFF- and ON-cell responses associated with heat-evoked withdrawal in female animals.

Ratemeter records (1 s bins) show cell firing rate, with heat onset (black bars) and paw withdrawal (black triangles) shown below each trace. The OFF-cell firing ceased at the time of paw withdrawal, while the ON-cell responded with a burst of activity.

Quantification of reflex-related changes in activity is shown in Fig. 7. There was no difference in heat-evoked OFF-cell suppression and pause duration (Fig. 7a,b) or ON-cell total evoked spikes

and peak-firing rate (Fig. 7c,d) between the sexes. There was no significant difference in heat-evoked withdrawal latency (Fig. 7e).

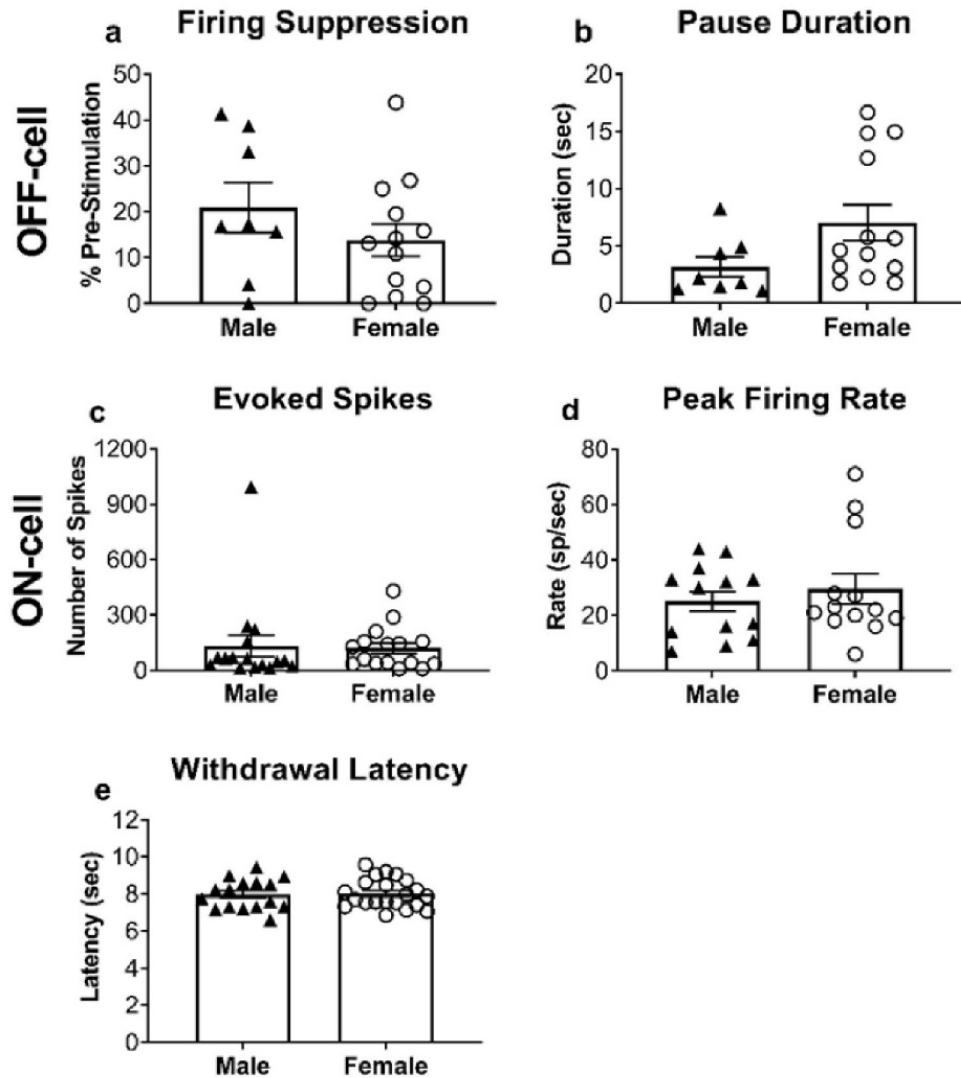


Figure 7. Heat-evoked reflex-related responses in naïve males and females and paw withdrawal latencies.

There was no significant effect of sex on any cell parameter. **a.** OFF cell suppression ($t_{19} = 1.15$, $p = 0.27$, $n = 8$ M, 13F). **b.** OFF cell pause duration ($t_{19} = 1.84$, $p = 0.082$, $n = 8$ M, 13F). **c.** ON-cell evoked spikes in burst ($t_{24} = 0.21$, $p = 0.84$, $n = 13$ M, 13F). **d.** ON-cell peak firing rate ($t_{24} = 0.69$, $p = 0.50$, $n = 13$ M, 13F). **e.** There was also no significant difference in thermal withdrawal latency between males and females ($t_{35} = 0.16$, $p = 0.88$, $n = 16$ M, 21F).

Comparison of ongoing firing rates (Fig. 8) similarly demonstrated no significant differences between males and females.

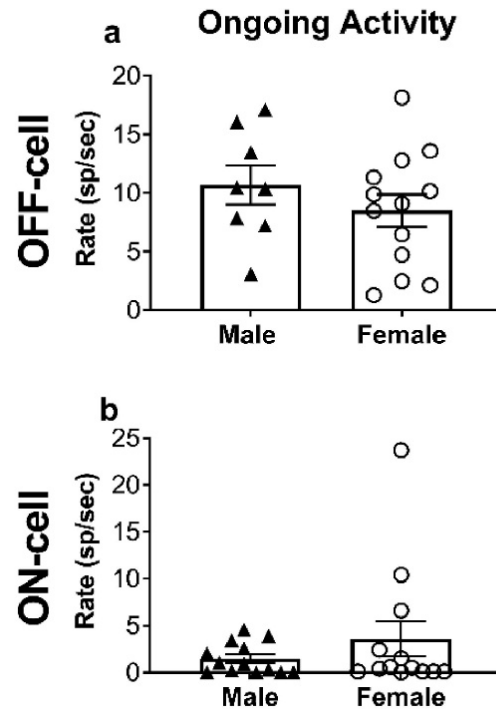


Figure 8. Ongoing firing of ON- and OFF-cells.

a. There was no significant difference in OFF-cell ongoing firing rate between male and female animals ($t_{19} = 1.0$, $p = 0.33$, $n = 8$ M, 13F). **b.** There was no significant difference in ON-cell ongoing firing rate between male and female animals ($t_{24} = 1.09$, $p = 0.29$, $n = 13$ M, 13F).

We then compared OFF- and ON-cell responses during stimulation with von Frey fibers at forces ranging from 4 to 100 g. In naive female and male animals, OFF- and ON-cells responded to forces in the frankly noxious range (60 and 100 g) that were sufficient to evoke a withdrawal reflex in either sex (Fig. 9 a-d). As with heat stimulation, there was no difference between the sexes in cell responses or behavioral threshold (Fig. 9e).

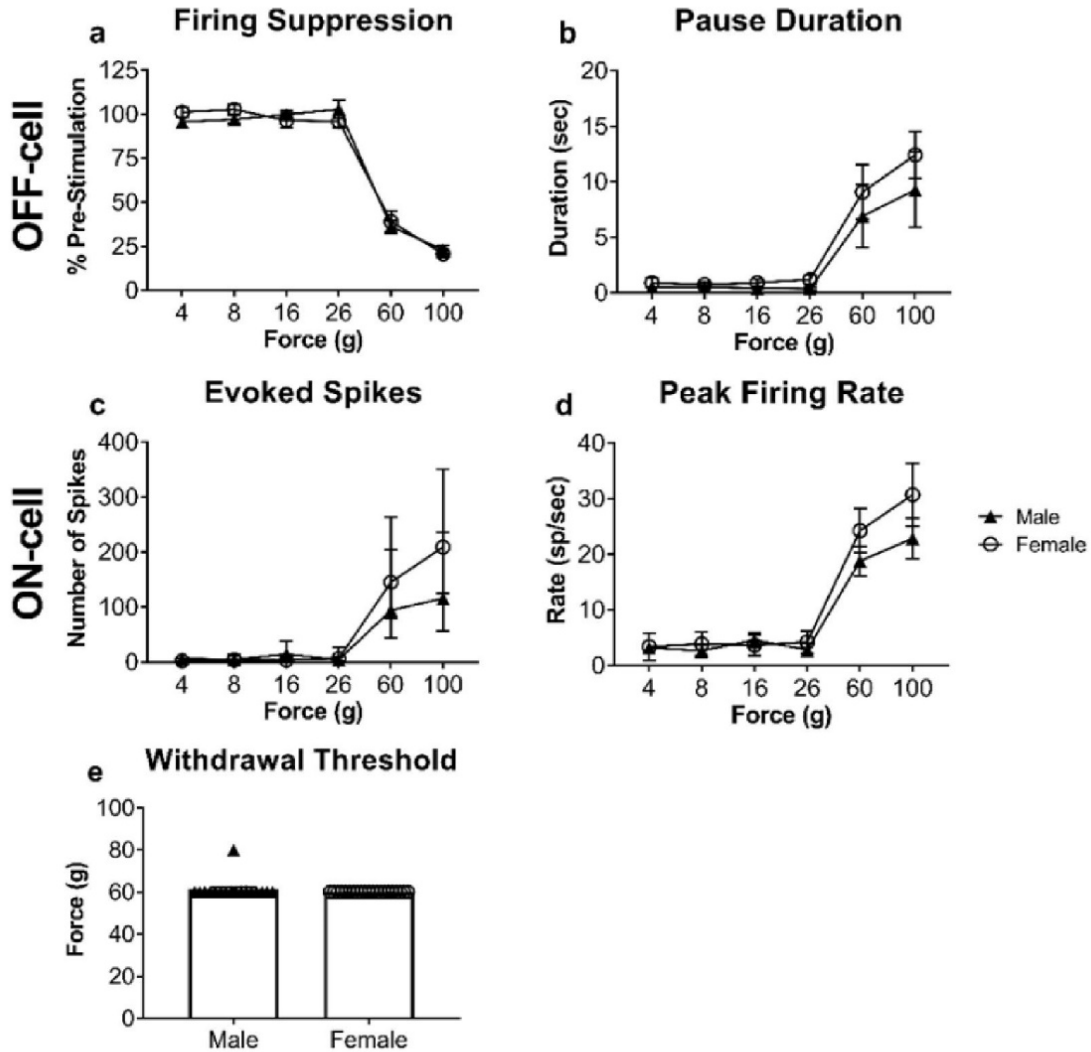


Figure 9. Mechanically evoked cell response and withdrawal in naïve males and females.

For all cell parameters, there was no significant effect of sex, although there was a significant effect of force. **a.** OFF-cell suppression (Sex: $F_{1,19} = 0.0057$, $p = 0.94$; Force: $F_{5,95} = 220$, $p < 0.0001$; Interaction: $F_{5,95} = 1.14$, $p = 0.34$; $n = 8$ M, 13F). **b.** OFF-cell pause duration (Sex: $F_{1,19} = 0.85$, $p = 0.37$; Force: $F_{5,95} = 21.47$, $p < 0.0001$; Interaction: $F_{5,95} = 0.35$, $p = 0.88$; $n = 8$ M, 13F). **c.** Evoked spikes in ON-cell burst (Sex: $F_{1,24} = 0.023$, $p = 0.88$; Force: $F_{5,120} = 76.21$, $p < 0.0001$; Interaction $F_{5,120} = 2.38$, $p = 0.042$; $n = 13$ M, 13F; data are displayed as geometric mean \pm 95% CI). **d.** ON-cell peak firing rate (Sex: $F_{1,24} = 0.65$, $p = 0.43$; Force: $F_{5,120} = 71.87$, $p < 0.0001$; Interaction: $F_{5,120} = 1.77$, $p = 0.12$; $n = 13$ M, 13F). **e.** There was no significant difference in mechanical withdrawal threshold between males and females ($t_{36} = 1.12$, $p = 0.27$, $n = 17$ M, 21F).

2.4.2. Persistent inflammation following CFA injection produces mechanical but not thermal hyperalgesia in female animals

We next characterized RVM cell responses during persistent inflammation in females. Animals were treated with an injection of CFA in the right hindpaw 3 to 6 days prior to recording. We found that local administration of CFA produced mechanical hyperalgesia in the treated paw (Fig. 10a) in female animals, with a statistically significant decrease in threshold when tested 3 - 6 d after CFA injection. This decrease was substantial in that stimulation of the inflamed paw even with an innocuous force (≤ 26 g) evoked a withdrawal response in 81.8% of the animals tested, whereas this was never seen with stimulation of the contralateral paw. Females did not exhibit thermal hyperalgesia at 3-6 d post-injection (Fig. 10b), with no difference in heat-evoked withdrawal latency between the inflamed and contralateral paw. These data are consistent with prior work in males [212].

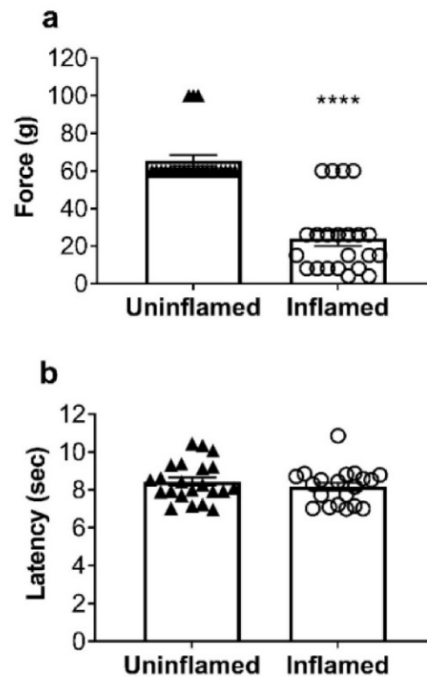


Figure 10. Mechanical but not thermal hypersensitivity in females with persistent inflammation.

a. There was a significant difference between paws for mechanically-evoked paw withdrawal threshold (paired t -test, $t_{21} = 11.61$, $p < 0.0001$, $n = 22$). **b.** No significant difference between paws for heat-evoked paw withdrawal latency (paired t -test, $t_{19} = 0.95$, $p = 0.35$, $n = 20$).

2.4.3. Evoked responses of RVM neurons in female animals with persistent inflammation

Stimulus-response functions for the OFF- and ON-cell responses evoked by von Frey fiber stimulation in females with persistent inflammation are shown in Fig. 11. The OFF-cell pause (cell suppression and pause duration, Fig. 11a,b) and ON-cell burst (total evoked spikes and peak firing, Fig. 11c,d) for stimulation of the inflamed and contralateral paw were compared. OFF- and ON-cells developed both increased responses to noxious (60–100 g) stimulation of the inflamed paw compared to the control paw, and novel responses to innocuous stimulation (≤ 26 g) of the inflamed paw (Fig. 11a,b,d,e). Thresholds were lowered for stimulation of the

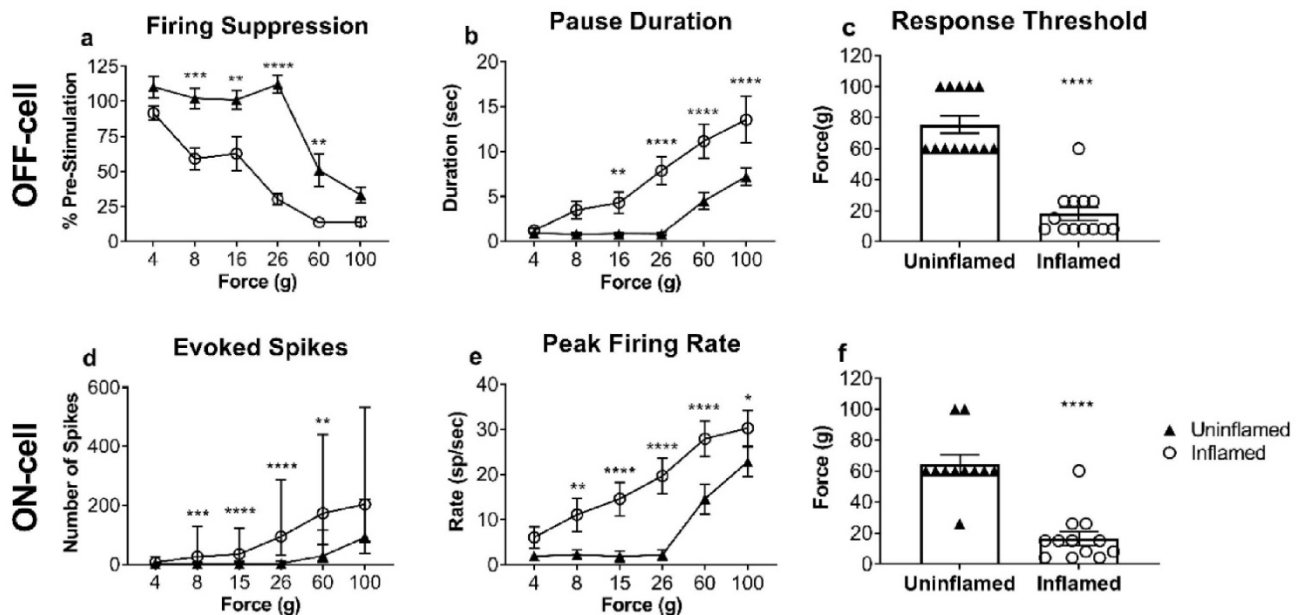


Figure 11. Shift in cell stimulus–response curve for mechanical stimulation of CFA treated paw. For all cell parameters, there was a significant effect of force, paw, and force × paw interaction.

a. OFF-cell suppression: force ($F_{5,60} = 47.28$, $p < 0.0001$), paw ($F_{1,12} = 51.71$, $p = 0.00012$), force × paw ($F_{5,60} = 5.58$, $p = 0.0003$), $n = 13$ cells. **b.** OFF-cell pause duration: force ($F_{5,50} = 22.61$, $p < 0.0001$), paw ($F_{1,10} = 21.31$, $p = 0.0010$), force × paw ($F_{5,50} = 7.12$, $p < 0.0001$), $n = 11$. **c.** OFF-cell response threshold was significantly lower in the inflamed paw ($t_{12} = 7.88$, $p < 0.0001$). **d.** ON-cell burst: force ($F_{5,55} = 28.34$, $p < 0.0001$), paw ($F_{1,11} = 28.5$, $p = 0.0002$), force × paw ($F_{5,55} = 4.26$, $p = 0.0024$), $n = 12$. **e.** ON-cell peak firing rate: force ($F_{5,55} = 31$, $p < 0.0001$), paw ($F_{1,11} = 21.06$, $p = 0.0008$), force × paw ($F_{5,55} = 3.81$, $p = 0.0049$), $n = 12$. **f.** ON-cell response threshold was significantly lower in the inflamed paw ($t_{10} = 6.77$, $p < 0.0001$).

inflamed paw, but not the contralateral paw (Fig. 11c,f). The responses of RVM cells are thus consistent with the mechanical hypersensitivity seen in these animals.

2.4.4. Opioid response of RVM neurons in female animals

In a third set of experiments, we determined the response of RVM ON-, OFF-, and NEUTRAL-cells to systemic administration of morphine in female animals. NEUTRAL-cells were defined by an absence of response during noxious-evoked withdrawal. Fig. 12 shows firing of

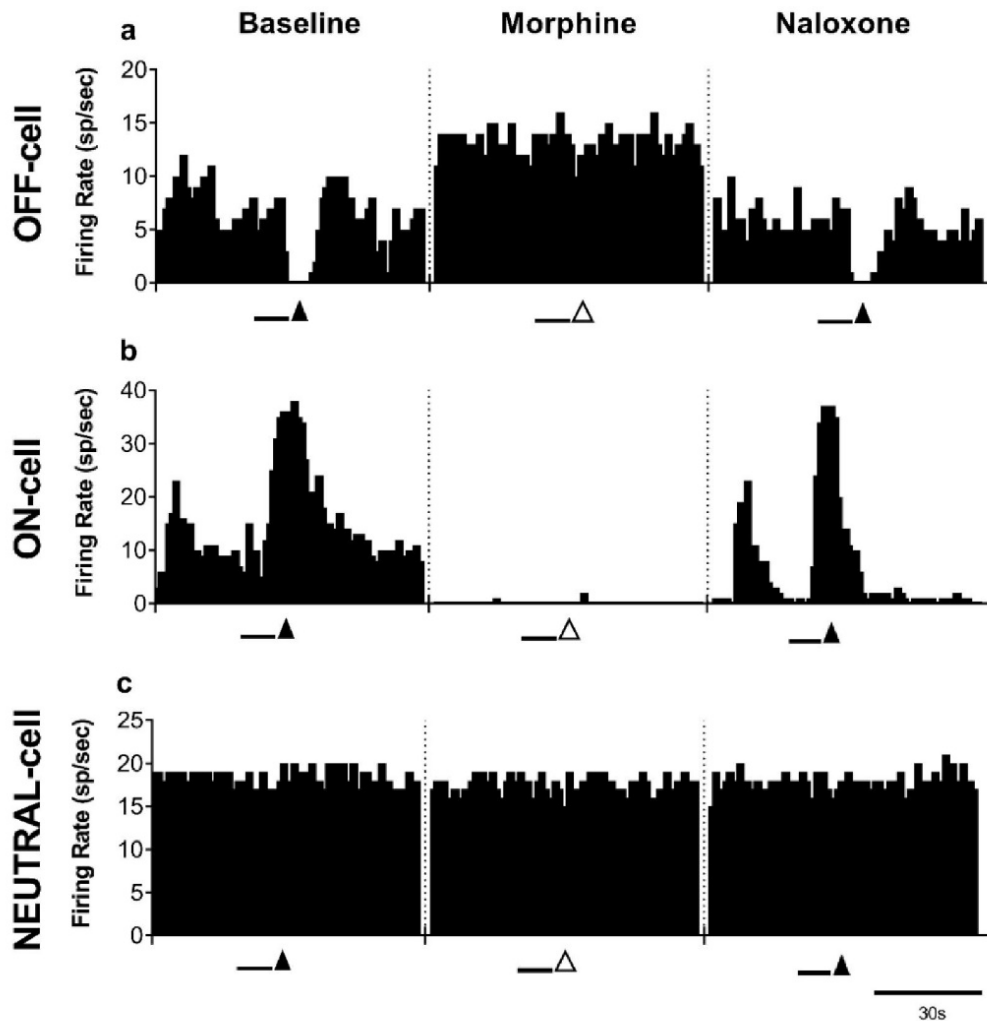


Figure 12. Representative RVM cell response to systemic morphine administration in female animals.

Ratemeter records (1 s bins) show the effect of systemic morphine administration on the activity of an **a.** OFF-cell, **b.** ON-cell, and **c.** NEUTRAL-cell. Heat onset (black bars) prior to morphine administration and after naloxone administration resulted in paw withdrawal (black triangles). Analgesic doses of morphine resulted in a loss of paw withdrawal (open triangles).

an OFF-, ON-, and NEUTRAL-cell in baseline, after systemic administration of morphine sufficient to inhibit heat-evoked withdrawal, and following reversal of the morphine effect with naloxone. In baseline, the OFF-cell exhibits the defining “pause” in activity at the time of the paw withdrawal, and the ON-cell exhibits a substantial increase in firing rate. NEUTRAL-cell firing is unchanged. After morphine, the paw withdrawal itself is eliminated. The OFF-cell becomes continuously active and during application of heat to the paw, and ON-cell firing is almost completely suppressed, with no burst of activity during the heat stimulus. NEUTRAL-cell firing continues as in baseline. These effects were reversed by systemic naloxone administration.

Group data are shown in Fig. 13. Overall, there was a statistically significant increase in the ongoing firing of OFF-cells and decrease in that of ON-cells. Two of fifteen OFF-cells studied, both with very low ongoing activity prior to morphine, became inactive after morphine, and two of fifteen ON-cells showed an overall increase in activity. The OFF-cell pause and ON-cell burst during noxious heat application were significantly depressed, however, one ON-cell failed to show a suppression of activity during noxious heat. NEUTRAL-cells exhibited ongoing activity at 19.4 spike/s on average, ranging from 11 to 36 spikes/s for individual neurons in the present sample. The firing rate was unchanged following morphine administration. These observations are consistent with the effects of systemically administered morphine on the activity of RVM cells in males [216, 219].

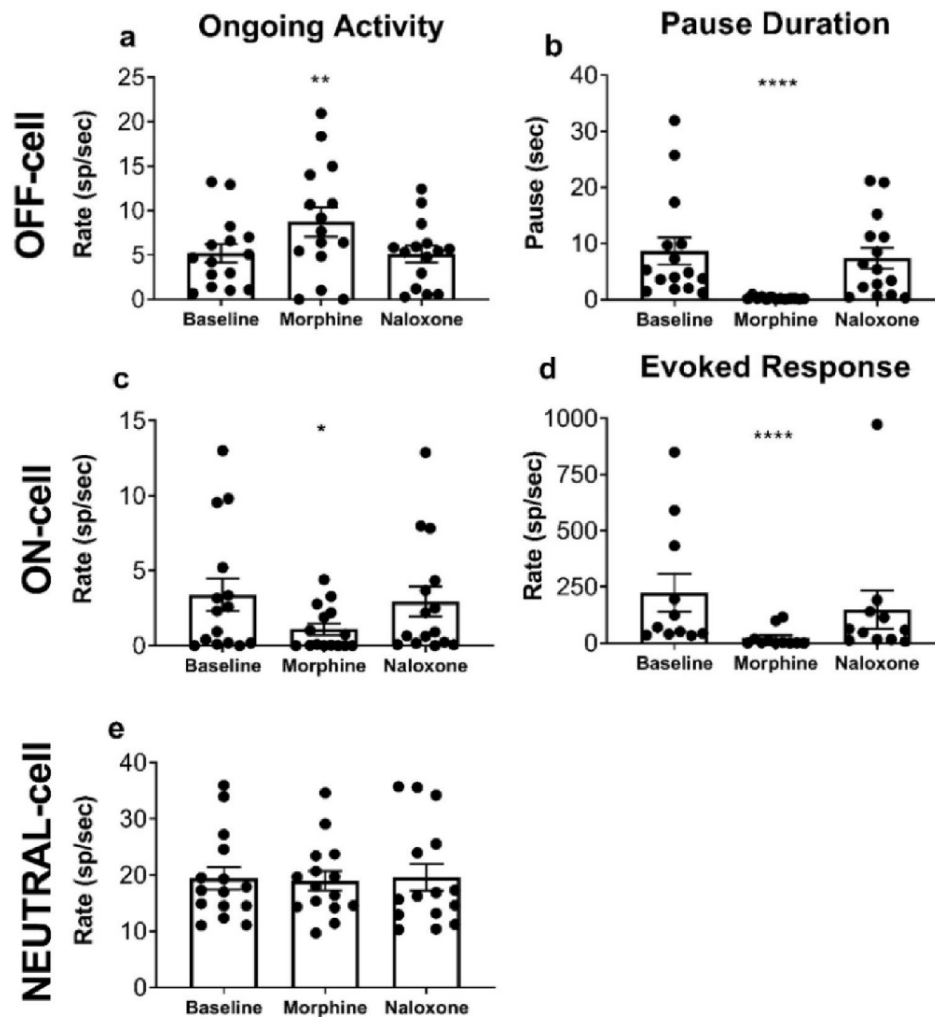


Figure 13. Effects of systemic morphine administration on ongoing cell activity and withdrawal-evoked cell behaviors in naïve females.

a. Systemic morphine administration significantly changed OFF-cell ongoing activity ($F_{2,28} = 7.76$, $p = 0.0021$), with post-morphine increased compared to baseline ($p = 0.0043$). **b.** Morphine significantly decreased the OFF-cell pause ($F_{2,26} = 25.43$, $p < 0.0001$) with post-morphine significantly different from baseline ($p < 0.0001$). **c.** There was a significant change in ON-cell ongoing activity ($F_{2,28} = 5.078$, $p = 0.013$), and morphine significantly decreased ongoing activity compared to baseline ($p = 0.016$). **d.** There was a significant difference in the total evoked spikes in the ON-cell burst ($F_{2,16} = 21.30$, $p < 0.0001$) with the post-morphine time point depressed compared to baseline ($p < 0.0001$). **e.** No significant change in NEUTRAL-cell ongoing activity ($F_{2,28} = 0.18$, $p = 0.84$). One-way ANOVA with repeated measures and *post-hoc* Dunn's multiple comparisons test, $n = 15$ OFF-cells, 15 ON-cells, 15 NEUTRAL cells. There was no significant difference between baseline and naloxone for any cell measure.

2.5. DISCUSSION

The goal of this study was to identify and characterize pain-modulating neurons in females. Since RVM is the physiological output of a major pain-modulation circuit and can amplify or suppress pain-transmission [6, 7], sex-related differences in the organization and activity of this system could in principle predispose females to develop chronic pain conditions. As in prior work in males, we were able to identify ON- and OFF-cells in the RVM in females. Firing properties in females were comparable to those in males. In addition, both ON- and OFF-cells exhibited a “sensitized” response to somatic stimuli in females subjected to persistent inflammation, responding to normally innocuous stimuli. As in males, both ON- and OFF-cells responded to systemically administered morphine at a dose sufficient to produce behavioral antinociception. Thus, there are not qualitative differences between males and females in the physiology of RVM neurons.

We first considered ongoing activity levels and noxious-evoked responses of RVM cells in naïve animals. There was no significant difference between the two sexes in cell firing parameters between the two sexes, showing that RVM cells in females have similar response properties to those in males under basal conditions. Thus, despite anatomical and pharmacological differences in pain-modulation circuitry upstream of RVM and in RVM itself [183, 185, 189, 190, 209], the output from the pain-modulation system is comparable in males and females under basal conditions. Moreover, since the RVM contributes to basal nociceptive “tone” [41], this observation of similar output from RVM in males and females is consistent with our own observation of no difference between males and females in thermal or mechanical nociception, and more generally, the lack of a robust sex difference in basal nociceptive responding [206-208].

We next looked at the effects of persistent inflammation on RVM output and behavioral sensitivity in female animals. When tested 3 to 6 days after localized injection of CFA in a single hindpaw, mechanical hyperalgesia was prominent in the CFA-treated paw, consistent with

previous reports in lightly anesthetized males [134, 212, 220, 221]. Both OFF- and ON-cells were sensitized to mechanical stimulation of the inflamed paw. Under basal conditions, OFF- and ON-cells responded to von Frey probes only in the noxious range. By contrast, they responded to innocuous stimulation of the inflamed paw, a response that paralleled the behavioral hypersensitivity to mechanical stimulation. This is consistent with prior findings in males [212] demonstrating that behavioral hypersensitivity, and the corresponding shifts in cell response, are confined to the inflamed paw, and validates the defining features of RVM cells in females.

We did not observe thermal hyperalgesia in female animals at the time points studied here, which again is in agreement with previous findings in male animals, that thermal hyperalgesia begins to resolve within the first 24 h after CFA injection [212, 221-226]. In any case, there is little evidence for substantial sex differences in CFA-induced hyperalgesia [178, 181, 227-229]. Overall, our findings are consistent with literature indicating that differences in either acute nociceptive sensitivity or hyperalgesia during persistent inflammation are likely nonexistent or minor.

Despite the similarity in behavioral endpoints and neuronal output in persistent inflammation, there are qualitative differences in pain-modulation circuitry between the sexes that could in principle underlie observed discrepancies in prevalence and presentation of chronic pain disorders. For example, periaqueductal gray (PAG) input to RVM is critical to pain-modulation, and Loyd and colleagues [178] have reported increased activation of PAG-RVM output neurons in males compared to females during persistent inflammation. However, these authors also reported no differences in inflammation-induced *hyperalgesia* between the two sexes. These apparently inconsistent observations raise the possibility that the similar behavioral outcome in males and females ultimately reflects comparable recruitment of RVM ON- and OFF-cells by the PAG during inflammation. Our finding that ON- and OFF-cells are sensitized in females, as in males, is consistent with this possibility. This argument would also

imply that molecular and anatomical differences between males and females at the level of the PAG are compensated for at the level of the RVM, leading to similar output from the pain-modulating system and comparable behavior.

We also investigated the effects of systemic opioid administration on behavioral analgesia and RVM cell response in female animals. Opioids are thought to produce analgesia in part by engaging the PAG-RVM descending modulatory system. Thus, sex differences in the anatomical and pharmacological properties of this circuit could result in differential opioid effects in men and women [185, 190, 191]. However, animal and human literature related to the impact of sex on opioid analgesia is not entirely consistent [210, 211]. Notably, μ -opioids are more potent in women [230, 231], while male rats are more sensitive to the antinociceptive properties of morphine [183, 232, 233]. In the present experiments, RVM OFF- and ON-cells responded to opioid administration in the same direction as shown previously in males: the OFF-cell populations showed increased activity, and the ON-cell population decreased activity. Although a small number of cells showed disparate results, this may be due to the cumulative dosing approach and the greater sensitivity of females to the anesthetic than males. However, conclusions are difficult without a direct comparison to contemporaneous experiments in males. Nevertheless, our findings in females are generally consistent with previous reports in males [219, 234], and suggest that recruitment of OFF-cells and suppression of ON-cells firing contribute to analgesia as in males.

While a greater prevalence of chronic pain disorders in women is well documented, evidence that women are more responsive to experimental pain is less convincing, and in general effects are small, with a host of confounding factors [206, 235-237]. Studies of sex differences in basal nociceptive sensitivity in rodents have also reported conflicting results. Sex differences are found in either direction, or not at all, and results are highly variable, both between different nociceptive assays, and within a given nociceptive assay [211]. Results also appear to depend on methodological details such as animal strain, laboratory environment, and

experimenter. Moreover, the field is likely highly biased by the tendency to report only positive results. On the whole, it appears unlikely that there are fundamental sex differences in basal nociceptive sensitivity. Our data provide physiological evidence consistent with this idea, demonstrating that the fundamental machinery of the pain-modulation system is comparable in males and females under basal conditions, and that this system is similarly recruited in the two sexes in persistent inflammation and by systemically administered morphine.

Overall, our findings provide a foundation for the use of female animals in understanding the RVM and pain-modulation more generally. Given the strong evidence for altered descending control in individuals with chronic pain, and the greater prevalence of chronic pain in women, the task of future studies will be to determine whether this system is differentially recruited in the two sexes in relevant models of chronic pain.

CHAPTER 3

MANUSCRIPT # 3

Direct and indirect nociceptive input from the trigeminal dorsal horn to pain-modulating neurons in the rostral ventromedial medulla

Journal of Neuroscience. 2023 August 9.

Caitlynn C. De Preter^{1,2,3} and Mary M. Heinricher^{1,2,3}

Departments of Behavioral Neuroscience¹ and Neurological Surgery², Oregon Health & Science University³, Portland, OR, 97239

CCDP – Designed and performed research, analyzed data, wrote the paper

MMH – Designed research, analyzed data, and wrote the paper

3.1. ABSTRACT

The brain is able to amplify or suppress nociceptive signals by means of descending projections to the spinal and trigeminal dorsal horns from the rostral ventromedial medulla (RVM). Two physiologically defined cell classes within RVM, “ON-cells” and “OFF-cells”, respectively facilitate and inhibit nociceptive transmission. However, sensory pathways through which nociceptive input drives changes in RVM cell activity are only now being defined. We recently showed that *indirect* inputs from the dorsal horn via the parabrachial complex (PB) convey nociceptive information to RVM. The purpose of the present study was to determine whether there are also *direct* dorsal horn inputs to RVM pain-modulating neurons. We focused on the trigeminal dorsal horn, which conveys sensory input from the face and head, and used a combination of single-cell recording with optogenetic activation and inhibition of projections to RVM and PB from the trigeminal interpolaris-caudalis transition zone (Vi/Vc) in male and female rats. We determined that a direct projection from ventral Vi/Vc to RVM carries nociceptive information to RVM pain-modulating neurons. This projection included a GABAergic component, which could contribute to nociceptive inhibition of OFF-cells. This approach also revealed a parallel, indirect, relay of trigeminal information to RVM via PB. Activation of the indirect pathway through PB produced a more sustained response in RVM compared to activation of the direct projection from Vi/Vc. These data demonstrate that a *direct* trigeminal output conveys nociceptive information to RVM pain-modulating neurons with a parallel *indirect* pathway through the parabrachial complex.

3.2. INTRODUCTION

The brain regulates nociception and pain through descending projections from the brainstem to the spinal and trigeminal dorsal horns. These endogenous pain-modulating circuits can amplify or suppress the transmission of pain-related signals. Under normal conditions, pain-modulating circuits maintain a balance between facilitation and inhibition of pain, but they can be dysregulated in chronic pain states and contribute to abnormal hypersensitivity.

The primary output node of the brainstem pain-modulating circuits is the rostral ventromedial medulla (RVM). Neurons within the RVM are diverse and have their own distinct functions: pain-modulating “ON-” and “OFF-cells” facilitate or suppresses nociceptive transmission, respectively, while neurons with no known role in pain-modulation, “NEUTRAL-cells”, likely mediate thermogenesis and cardiovascular and respiratory regulation [18, 238-240]. Because of the diverse functions of RVM, understanding inputs to identified RVM pain-modulating neurons would provide insights into when and how the brain controls pain.

The RVM receives top-down inputs from cortex, amygdala, and hypothalamus to allow cognitive and emotional factors to influence pain by recruiting ON- and OFF-cells [18, 45, 123, 241]. However, pain-modulating ON- and OFF-cells also respond to noxious stimulation of the head and body: ON-cells exhibit an increase in firing or a “burst” of activity, while OFF-cells are characterized by a GABA-mediated “pause” in ongoing firing just prior to nocifensive withdrawal [32, 242, 243]. However, the pathways through which noxious inputs drive changes in the activity of these pain-modulating cells are only now beginning to be defined.

One route through which nociceptive information is relayed to the RVM is via the parabrachial complex (PB). The PB is a major target of nociceptive transmission neurons in the superficial dorsal horn [244-246], and can relay this information to RVM pain-modulating neurons [247, 248]. While anatomical studies describe projections from the dorsal horn to the RVM as a region [22, 249], the goal of the present study was to determine whether this direct projection from the dorsal horn conveys nociceptive information to RVM pain-modulating

neurons. We focused on the trigeminal dorsal horn, which processes sensory information from the face and head.

Nociceptive information from the craniofacial region is carried by peripheral sensory fibers to the spinal trigeminal nuclear complex, divided into subnuclei oralis, interpolaris (Vi) and caudalis (Vc) [138, 139]. Nociresponsive neurons are concentrated in Vc and at the junction between Vi and Vc, a region referred to as the Vi/Vc transition zone [141-143]. This junction comprises the rostral end of Vc dorsally, with the caudal end of Vi ventrally. Nociresponsive neurons in Vi/Vc and Vc proper send projections to PB [128, 144, 145], which has the potential to convey craniofacial input to RVM pain-modulating neurons indirectly. However, Vi/Vc neurons also project directly to RVM, and RVM-projecting neurons in the ventral, but not dorsal, aspect of Vi/Vc are activated during persistent inflammation [22]. These anatomical studies raise the possibility that Vi/Vc conveys nociceptive information to RVM pain-modulating neurons both via a direct projection to RVM, and by means of an indirect pathway, relayed through PB.

The present experiments used optogenetics and electrophysiological methods in lightly anesthetized rats to define the functional connections from the trigeminal complex to identified RVM pain-modulating neurons. These studies revealed a direct input to RVM pain-modulating neurons from ventral Vi/Vc. Retrograde tracing combined with fluorescent labeling of GABAergic neurons and electrophysiological data suggests that ventral GABAergic Vi/Vc neurons contribute to the OFF-cell pause. In addition, Vi/Vc can influence RVM pain-modulating neurons indirectly, through PB.

3.3. METHODS

All experiments followed the guidelines of the National Institutes of Health and the Committee for Research and Ethical Issues of the International Association for the Study of Pain, and were approved by the Institutional Animal Care and Use Committee at the Oregon Health & Science University (OHSU).

3.3.1. Viral vector injections

Male and female Sprague-Dawley rats (Charles River; 75-125 g) were deeply anesthetized using isoflurane (4%). The rat was placed in a stereotaxic apparatus, and temperature was maintained with a circulating warm-water pad throughout the procedure. A craniotomy was performed 0-0.5 mm caudal to the lambdoid suture and 2.6 mm lateral to the sagittal suture. The dura was removed to allow placement of a glass micropipette into the ventral trigeminal transition zone (Vi/Vc) to inject AAV9-hSyn-hChR2(H134R)-eYFP (2.1E+13 vg/ml) or AAV9-CAG-ArchT-eGFP (1E+12 vg/ml, 1:10 dilution) (200-400 nl, Addgene # 26973 and 29777). The injection was performed over 3 - 5 min using a Picospritzer. The micropipette was left at the injection site for 10 min before retraction to minimize back-flow. Lidocaine ointment was applied to the injection site, and animals received penicillin G (1 mg/kg, intramuscular) and meloxicam (5 mg/kg, subcutaneous). Rats were returned to their home cages for 2 – 3 weeks to allow expression of opsin (channelrhodopsin 2, ChR2 or Archaeorhodopsin, ArchT).

3.3.2. In vivo recording

Two to three weeks after vector injection in the Vi/Vc, animals were anesthetized (4 – 5% isoflurane) and a catheter placed in the external jugular vein for subsequent infusion of methohexital. They were then transferred to a stereotactic frame and small craniotomies were made to gain access to RVM, PB, and Vi/Vc. Heart rate was monitored using EKG, and body temperature was monitored and maintained at 36-37°C with a heating pad. There was no significant difference in heart rate or body temperature between males and females. Males required a higher anesthetic rate compared to females ($p < 0.0001$, $t_{98} = 7.27$) to achieve a similar anesthetic plane, as described previously [61]. After preparatory surgery, the anesthetic plane was set at a depth that allowed a stable mechanical-evoked paw withdrawal reflex, while preventing spontaneous movement [61, 248]. All testing was performed in low ambient light conditions (< 5 lux).

Extracellular single-unit recordings were made using an optoelectrode, constructed by pairing a stainless-steel microelectrode (Frederick Haer & Co) with an optical fiber [200 μm diameter, ThorLabs, 247]. Signals were amplified (10k) and band-pass filtered (400 Hz to 15 kHz, Neurolog, Digitimer) before analog-to-digital conversion at 32k samples/s for real-time spike detection and monitoring using Spike2 software (CED, Cambridge, UK). Correct waveform identification was verified on an individual spike basis at the conclusion of the experiment using Spike2 template matching and cluster analysis. Optical fibers (200 – 400 μm) were also placed in Vi/Vc (for optogenetic activation of Vi/Vc cell bodies) and in PB (for optogenetic activation of Vi/Vc terminals in PB). EMG activity (to monitor withdrawal reflexes) and heart rate were also recorded using Spike2.

3.3.3. Characterization of RVM neurons and response to Vi/Vc input

An RVM neuron was isolated and characterized as an ON-, OFF-, or NEUTRAL-cell based on changes in firing rate associated with withdrawal of the paw from a noxious mechanical stimulus applied to the hindpaw [40, 216]. Hindpaw, rather than face, stimulation was used to classify the neurons since animals in a stereotactic frame cannot withdraw the head from a noxious stimulus. ON-cells are defined by a burst of activity beginning just prior to withdrawal from a noxious stimulus. OFF-cells stop firing just prior to withdrawal or remain silent if inactive. NEUTRAL-cells do not respond. Withdrawals were recorded by means of electromyographic (EMG) electrodes placed 1 cm apart in the hamstring muscles. The von Frey fibers were applied to the interdigital webbing for a period of either 8 s or until a withdrawal was elicited. Once a cell was thus characterized, stimulation of the face (application of 60 g and 100 g von Frey filaments to the whisker pad for 8 s) was used as the trigeminal noxious stimulus. ON- and OFF-cells that did not respond to both face and paw stimulation were not tested further in these experiments.

For ChR2 experiments, RVM responses to optogenetic manipulations of cell bodies in Vi/Vc, Vi/Vc terminals in RVM, and Vi/Vc terminals in PB were determined. Five different

stimulation protocols were used for all isolated RVM neurons: 50 ms pulses at 7 Hz, 20 ms at 9 Hz, 10 ms at 10 Hz, 20 ms at 15 Hz, and 20 ms at 28 Hz for 8 to 60 s at 2 to 5 min intervals. A von Frey Fiber (60 g) was applied to the whisker pad intermittently between light trials.

For ArchT experiments, continuous light was used to inhibit Vi/Vc terminals in RVM. In order to consistently stimulate the whisker pad across animals and reduce error, a 100 g von Frey filament was attached to a hydraulic microdrive and positioned on the whisker pad ipsilateral to the vector injection site. The fiber was advanced at a rate of 50 $\mu\text{m/s}$ for 17 s, reaching a terminal force of 100 g. The filament was kept in place for 10 s and then retracted at 50 $\mu\text{m/s}$. Trials with and without light delivery to the terminals were delivered in alternation. For light trials, continuous light was delivered beginning 30 s before von Frey stimulus onset and maintained throughout the stimulus.

3.3.4. Recording sites and optical fiber placement

Recording sites in RVM were marked with an electrolytic lesion at the conclusion of the experiment. Animals were overdosed with methohexital, and perfused transcardially with saline followed by 10% formalin. Brains were removed and post-fixed for 24 h in 10% formalin, then equilibrated for 24 – 72 h in 30% sucrose in PBS at 4 °C. Brains were sectioned at 40 to 60 μm , and recording sites were plotted (Fig. 14). The RVM was defined as the nucleus raphe magnus and adjacent reticular formation medial to the lateral boundary of the pyramids at the level of the facial nucleus. Locations of optical fibers were also verified.

3.3.5. Anatomical tracing experiments

To identify Vi/Vc neurons projecting to the RVM and PB, retrograde tracers Fluoro-Gold (FG; Fluorochrome) and cholera toxin subunit B (CTb; List Biological Solutions) were injected into RVM and PB in 2 male and 2 female animals. To identify GABAergic neurons in Vi/Vc, AAV9-mGAD65(delE1)-GFP (titer, 1.28E+13 vg/ml, Addgene #177316) was generated in the Molecular Virology Core at OHSU using plasmid from Hoshino et al. [250] and injected into

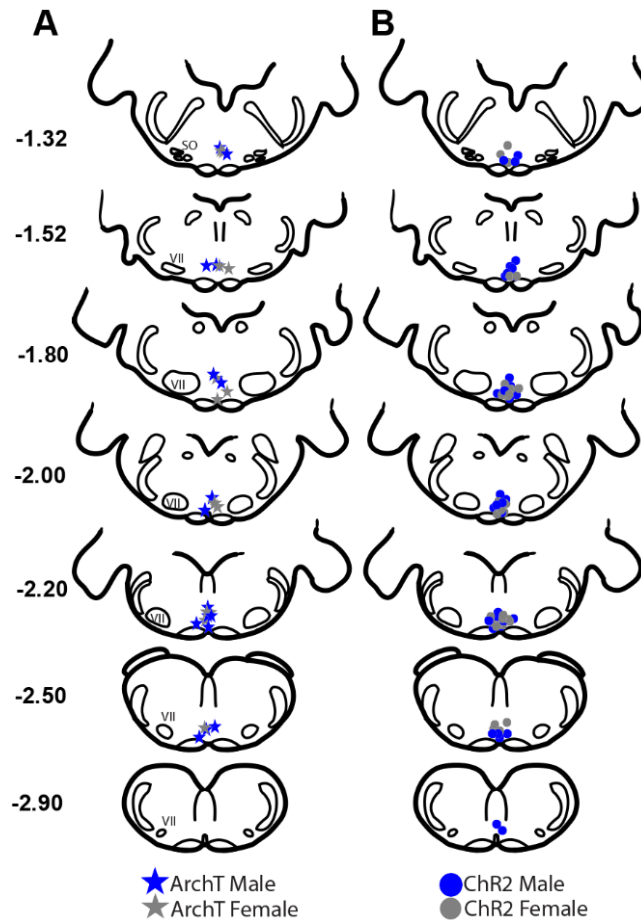


Figure 14. Recording sites within RVM for (A) ArchT and (B) ChR2 experiments.

Sites were distributed through the rostro-caudal extent of the RVM between -1.32 and -2.90 mm relative to interaural line. SO: superior olive, VII: nucleus of the facial nerve.

Vi/Vc. Small craniotomies were drilled to allow access to RVM (1.5 – 2.3 mm caudal to interaural line, within 0.3 mm of midline, 9 – 10 mm below brain surface) and PB (0.2 mm caudal to interaural line, 2 – 2.3 mm lateral to the sagittal suture, and 6.5 – 7 mm below brain surface) and two separate glass injectors were used to inject 4% FG into RVM and 1% CTb into PB (200 nl at each site). Two weeks after surgery, animals were deeply anesthetized and perfused transcardially before brain collection.

Sections including Vi/Vc and PB were incubated overnight at room temperature in primary antibody solution consisting of goat anti-CTb (1:5,000, List Biological Laboratories), 1%

skim milk, and 0.3% Triton X-100 (Sigma-Aldrich) in 0.1 M PBS. To visualize CTb, sections were incubated in secondary antibodies for 2 h at room temperature (donkey anti-goat Alexa Fluor 555, 1:5,000, ThermoFisher Scientific). The sections were then rinsed in PBS and mounted and coverslipped. For each animal, a total of three sections taken at -5.16 mm, -5.04 mm, and -4.92 mm from interaural were chosen for plotting of co-localization. Label was observed using a BZ-X710 Keyence fluorescence microscope and plotted according to the Paxinos & Watson rat brain atlas.

3.3.6. Analysis

3.3.6.1. Light-evoked responses in ChR2 experiments.

All light stimulation parameters were capable of evoking a response, and the resulting light-evoked changes were therefore pooled for analysis as previously described [247]. Firing rates before and during light application were determined. ChR2 responses were defined as the firing rate during light stimulation, and pre-light activity was defined as the firing rate in the equivalent time-period before light presentation, up to 30 s. Percent change in activity was calculated by taking the mean number of spikes in the pre-light stimulation periods and comparing it to the mean number of spikes during light-stimulations. A ceiling of 500% increase was applied to limit the impact of neurons with low spontaneous activity [251]. If the ON-cell was silent before all light stimulation trials, an increase of < 20 spikes was considered no difference.

The timing of the light-evoked response was also quantified, since, like the response to noxious stimulation [148], the RVM response to light could outlast the light stimulus. The duration of this “after-response” was calculated for trials when the ON-cells were inactive prior to light stimulation and were active in the last 2 s of light stimulation, and for trials when the OFF-cells were active in the 2 s period immediately preceding light onset and silent in the last 2 s of light stimulation. These measures were chosen to limit the impact of trials with undefinable or minimal terminal response. For RVM terminal stimulation, 20 ON-cells and 12 OFF-cells were included for after-response analysis. For PB terminal stimulation, the after-responses of 12 ON-

cells and 8 OFF-cells were analyzed. 13 ON- and 11 OFF-cells were included in analysis of the after-response to trigeminal cell body stimulation. The duration of the ON-cell after-response was calculated as the time between light termination and the last spike before a silent period lasting at least 2 s, while the OFF-cell after-response duration was calculated as the time between light termination and the first recovery spike that had another spike occurring within 2 s.

3.3.6.2. Response to von Frey application and effect of inhibiting trigeminal terminals in RVM using ArchT.

The single longest silent period (OFF-cells) and total number of evoked spikes (ON-cells) were used to quantify responses to the von Frey stimuli [61]. If the ON-cell was already active when the stimulus was applied, the number of action potentials during advancement and hold of the fiber was used as the evoked response.

3.3.6.3. Statistical comparisons.

Neuronal firing rate, durations of the OFF-cell pause and ON-cell burst, and number of spikes in the ON-cell burst before and during light presentation were compared using paired *t*-test. Because these parameters were not normally distributed (right-skewed), they were log-transformed for analysis. Effect size is reported as Cohen's *d*. Percent change in activity compared to the pre-light firing rate in male and female animals and effects of light applied at different sites were compared using *t*-tests for independent means. Prism v. 9.4.1 (GraphPad) was used for statistical analyses. Data are presented as mean \pm SEM.

3.4. RESULTS

3.4.1. Expression and validation of ChR2 or ArchT in Vi/Vc neurons and terminals in RVM and PB

AAV vectors encoding ChR2 or ArchT were injected in the trigeminal complex to drive opsin expression in ventral and dorsal Vi/Vc and in Vc (laminae I – V) in different animals.

Example showing fluorescent reporter in cell bodies in Vi/Vc and in terminals in RVM and PB are shown in Fig. 15. Positive fibers were seen to project along the entire length of the RVM, from the caudal end of the facial nucleus to the level of the facial nerve (Fig. 15B). Dense fibers were also found in the ipsilateral parabrachial complex (Fig. 15C), consistent with previous studies documenting projections from Vi/Vc and Vc to PB [128, 145, 246, 252].

In a subset of ChR2- or ArchT-injected animals, light-induced activation and inhibition of Vi/Vc neurons were tested to validate opsin function (Fig. 15D, E). Vi/Vc neurons that responded to noxious mechanical stimulus applied to the whisker pad using von Frey filaments were tested. For ChR2 activation of these neurons, a light source with a mean wavelength of

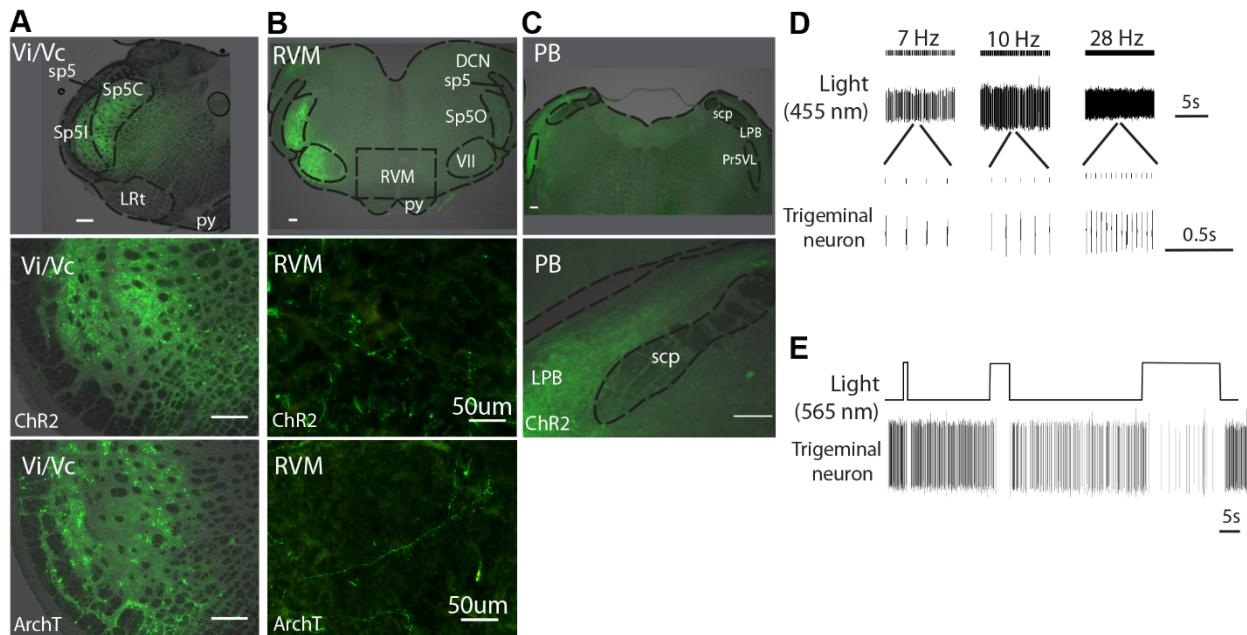


Figure 15. ChR2 and ArchT expression in Vi/Vc and terminal expression in RVM and PB.

(A) Expression of ChR2 and ArchT in Vi/Vc cell bodies. (B) Expression of ChR2 and ArchT in terminals in RVM. (C) Expression of ChR2 in PB. Terminals were densely distributed throughout lateral PB complex. (DCN = dorsal cochlear nucleus, IPB = lateral parabrachial nucleus, LRt = lateral reticular nucleus, Pr5VL = principal sensory ventrolateral trigeminal nucleus, py = pyramids, scp = superior cerebellar peduncle, sp5 = spinal trigeminal tract, Sp5C = spinal trigeminal nucleus, caudalis, Sp5I = spinal trigeminal nucleus, interpolaris, Sp5O = spinal trigeminal nucleus, oralis, VII = nucleus of the facial nerve). Scale bars are 200 μ m unless otherwise noted. (D) Trigeminal nucleus neuronal firing induced by light activation of ChR2 (10- to 50-ms pulses at 7, 10, or 28 Hz). Firing of the neuron reliably followed the light trains. (E) Suppression of activity of a trigeminal neuron during light-induced activation of ArchT.

455 nm (1.2 mW maximum power) was used. Vi/Vc neurons fired with each light pulse at all frequencies tested (7 to 28 Hz, 10 – 50 ms pulses). For ArchT-mediated inhibition, a light source with a mean wavelength of 565 nm (0.8 mW maximum power, continuous light for up to 30 s) was used, resulting in depression and complete cessation of cell firing.

3.4.2. RVM ON-cells are activated while RVM OFF-cells are inhibited by optogenetic activation of the Vi/Vc region

To determine whether RVM pain-modulating neurons receive input from the trigeminal complex, we recorded from identified RVM neurons while delivering light to cell bodies expressing ChR2 throughout the Vi/Vc region (Fig. 16A and B). We compared the pre-light firing rate to light-evoked firing rate in fourteen ON-cells in 6 male and 5 female animals, 14 OFF-cells in 6 male and 4 female animals, and 8 NEUTRAL-cells in 3 male and 3 female animals. Light activation of trigeminal cell bodies mimicked noxious mechanical peripheral stimulation of the face, as seen in examples in Figs. 16C-E. This was seen in animals with vector restricted to either dorsal Vi/Vc (5 ON-, 4 OFF-, 4 NEUTRAL-cells) or with vector present in ventral Vi/Vc region (9 ON-, 10 OFF-, and 4 NEUTRAL-cells). ON-cell firing was significantly increased ($p < 0.0001$, $t_{13} = 9.64$, paired t -test, Cohen's $d = 1.76$, Fig. 16F) with a mean increase of 14.7 ± 2.7 spikes/s, while OFF-cells exhibited a significant decrease in firing ($p < 0.0001$, $t_{13} = 8.55$, paired t -test, Cohen's $d = 2.35$, Fig. 16G) with a mean decrease of 6.0 ± 0.9 spikes/s as compared to the pre-light firing rate. NEUTRAL-cells did not show a significant change in firing ($p = 0.59$, $t_7 = 0.57$, paired t -test Fig. 16H) with a mean change of 0.2 ± 0.3 spikes/s. There was no difference in the magnitude of the change in firing in ON-cells ($p = 0.19$, $t_{12} = 1.39$, % of pre-light period, unpaired t -test) or OFF-cells ($p = 0.075$, $t_{12} = 1.95$, unpaired t -test) between animals with vector expressed in dorsal versus ventral Vi/Vc. Cells from both male and female animals responded in the same direction (Fig. 16F-H), and there was no significant difference in the percent change in ON-cell ($p = 0.19$, $t_{12} = 1.39$, unpaired t -test) or OFF-cell firing ($p = 0.38$, $t_{12} = 0.91$, unpaired t -test) between males and females. These data demonstrate that both ventral

and dorsal Vi/Vc can access pain-modulating neurons in RVM, but does not determine whether this is due to a direct projection to RVM, or via an indirect pathway, such as a relay through PB.

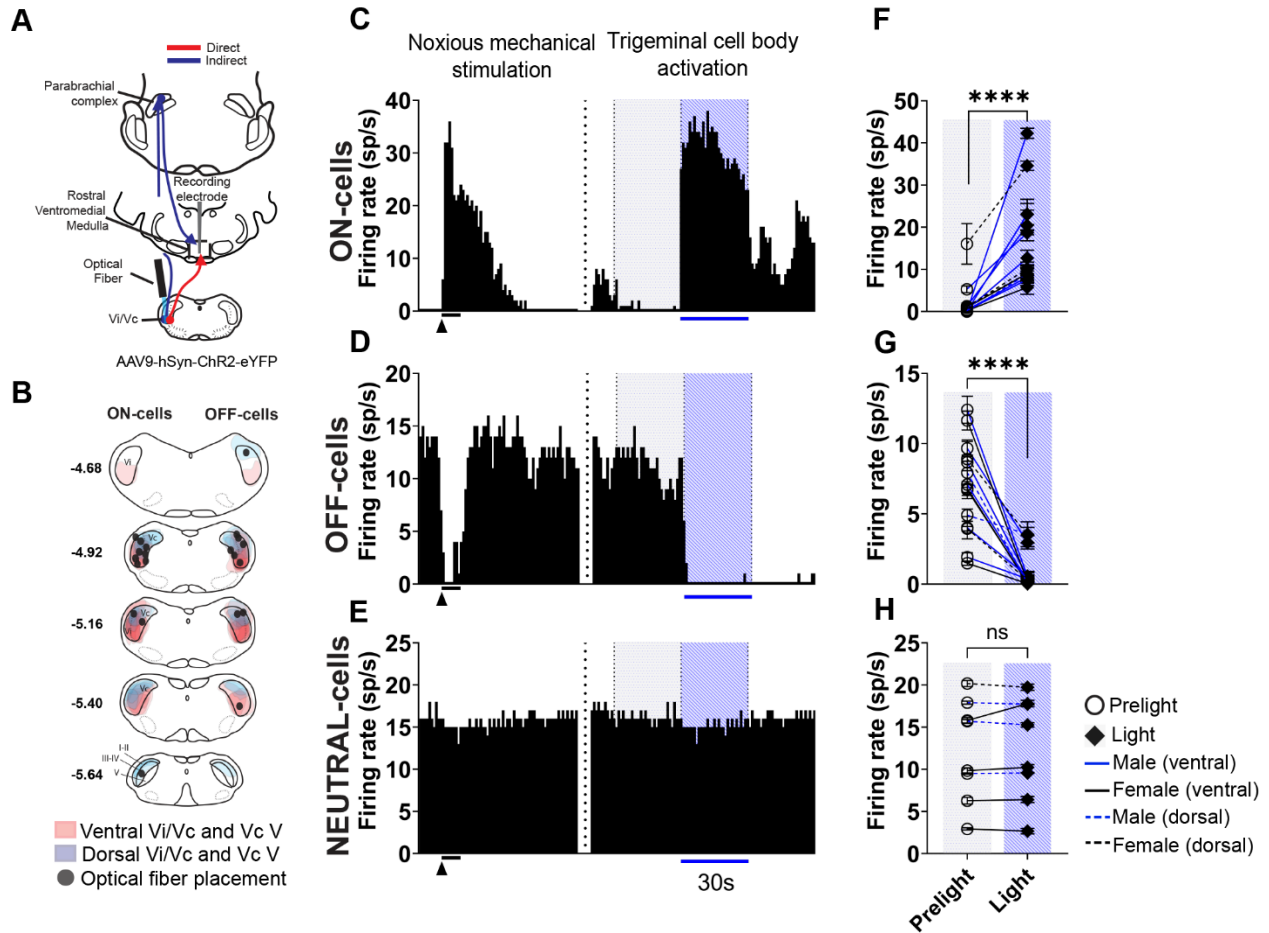


Figure 16. ChR2-induced activation of trigeminal cell bodies mimics noxious stimulation, activating ON-cells and suppressing the firing of OFF-cells.

(A) Light was delivered to Vi/Vc cell bodies while recording from RVM neurons. (B) Vector expression was found throughout the trigeminal complex and grouped by placement (ventral = red, dorsal = blue). Optical fiber placements are also mapped (gray circles). (C) ON- (D) OFF- and (E) NEUTRAL-cell responses to noxious mechanical stimulation of face and light delivered to Vi/Vc cell bodies. Ratemeter records (1-s bins) with mechanical stimulation of the whisker pad (left, black triangle) and light stimulation (right, blue bar and shading, 30 s) show mechanical-related and optogenetically-evoked responses recorded from RVM. (F) Group data show trigeminal cell body activation significantly increased the firing rate of ON-cells ($p < 0.0001$, $t_{13} = 9.64$, Cohen's $d = 1.76$), and significantly decreased the firing rate of (G) OFF-cells as compared to pre-light firing rates ($p < 0.0001$, $t_{13} = 8.55$, Cohen's $d = 2.35$). (H) NEUTRAL-cells showed no significant change in firing rate upon trigeminal cell body activation ($p = 0.59$, $t_7 = 0.57$). **** $p < 0.0001$ compared with pre-light firing rate, paired t -test. Blue lines = cells from male animals, black lines = cells from female animals. sp/s = spikes per second, dotted lines = cells from animals with virus restricted to dorsal Vi/Vc.

3.4.3. Ventral, but not dorsal, Vi/Vc projections to RVM recruit pain-modulating neurons

We next tested whether RVM pain-modulating neurons receive *direct* input from the Vi/Vc and Vc regions by optogenetically activating trigeminal terminals in the RVM itself (Fig. 17A). We compared the pre-light firing rate to light-evoked firing rate in 45 ON-cells (in 16 female, 17 male animals) and 40 OFF-cells (in 14 female, 19 male animals) with vector injected throughout the trigeminal complex at the level of the Vi/Vc junction (Fig. 17B). Because RVM-projecting *dorsal* Vi/Vc and Vc I-IV neurons are not activated by noxious stimulation, while those in *ventral* Vi/Vc are activated [22], animals were grouped by the location of vector expression. In animals with vector expressed in ventral Vi/Vc and lamina V of Vc, both ON- and OFF-cells responded to light directed to RVM to activate trigeminal terminals. Of 30 ON-cells, all but six showed an increase in activity of at least 50%. Of 26 OFF-cells tested, 18 exhibited a decrease in firing of at least 25%. By contrast, in animals with expression restricted to dorsal Vi/Vc and laminae I – IV of Vc, ON- and OFF-cells were less likely to respond to light in RVM (Figs. 17C and D). Only one of 15 OFF-cells showed a decrease in firing during light delivery, and only five of 14 ON-cells showed an increase.

ON- and OFF-cell responses to stimulation of trigeminal terminals in RVM are further quantified in Figures 17E – L. Light activation of RVM terminals in animals with vector expression in ventral Vi/Vc and lamina V of Vc mimicked noxious mechanical peripheral stimulation of the face, as seen in examples in Figs. 17E and G. In animals with vector expression in this location, ON-cells showed a significant increase in firing rate ($p < 0.0001$, $t_{29} = 6.39$, paired t -test, Cohen's $d = 0.48$, Fig. 17F), with a mean increase of 6.6 ± 1.7 spikes/s. OFF-cells showed a significant decrease in firing rate ($p < 0.0001$, $t_{25} = 4.84$, paired t -test, Cohen's $d = 0.69$, Fig. 17H), with a mean decrease of 2.8 ± 0.8 spikes/s. The direction of the response to RVM terminal stimulation was consistent in both sexes (Fig. 17F, H), and there was no significant difference in the percent change in ON-cell ($p = 0.79$, $t_{28} = 0.27$, unpaired t -test) or OFF-cell firing ($p = 0.37$, $t_{24} = 0.92$, unpaired t -test) between males and females.

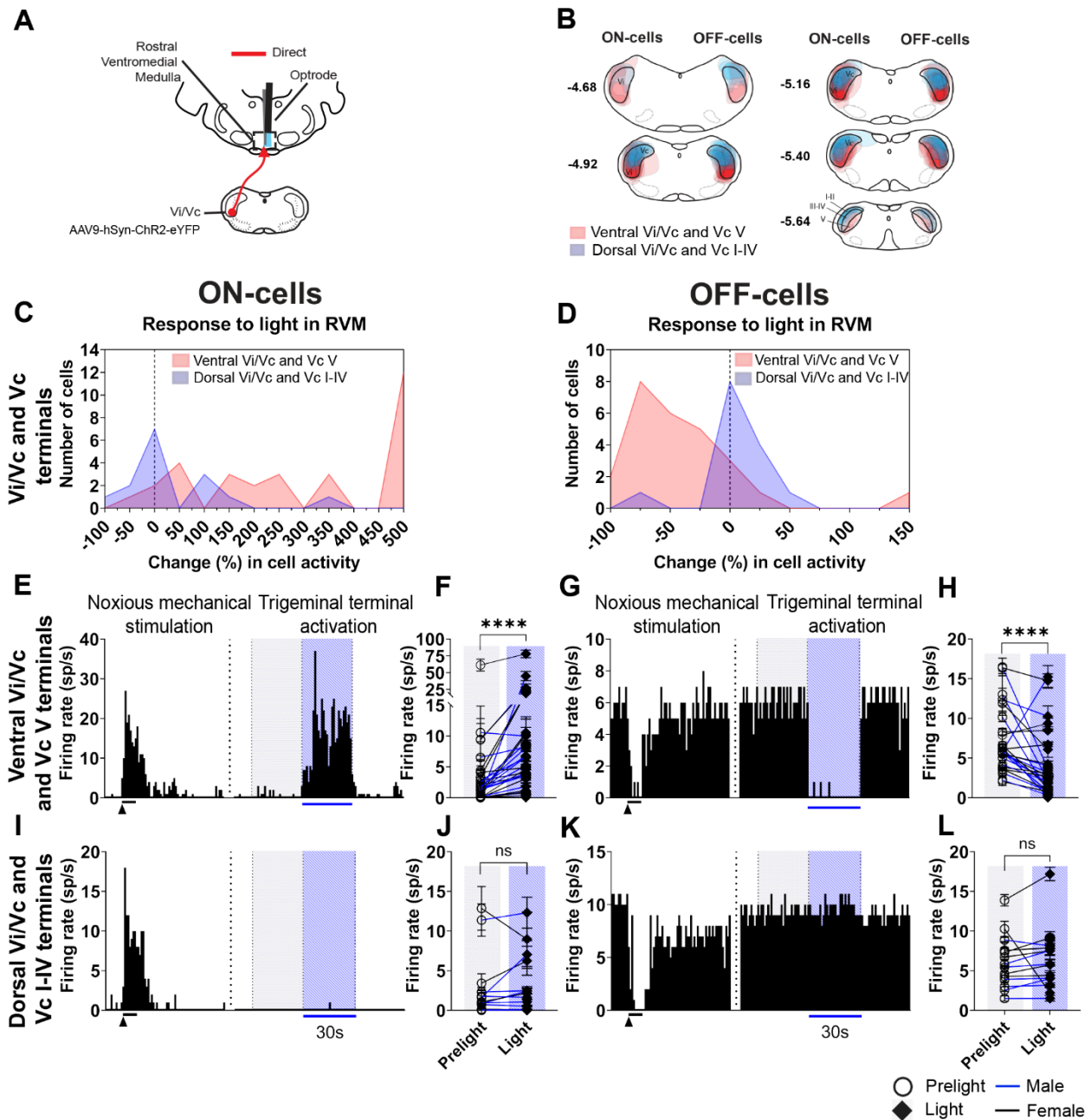


Figure 17. Chr2-induced activation of RVM terminals arising from ventral Vi/Vc and Vc lamina V neurons, but not dorsal Vi/Vc, mimics noxious stimulation, activating ON-cells and suppressing the firing of OFF-cells.

(A) Trigeminal terminals in RVM were activated while recording from RVM neurons. (B) Vector expression was found throughout the trigeminal complex and grouped by placement (ventral=red, dorsal=blue). (C) ON- and (D) OFF-cells were more likely to respond to light in RVM in animals with vector found in ventral Vi/Vc and Vc V than dorsal Vi/Vc and Vc I-IV. (E,G) Ratemeter records (1-s bins) with mechanical stimulation of the whisker pad (left, black triangle) and light stimulation (right, blue bar and shading, 30 s) show mechanical-related and optogenetically-evoked responses recorded from an RVM (E) ON-cell and (G) OFF-cell in animals with vector expression in ventral Vi/Vc. Activation of RVM terminals in animals injected

in ventral Vi/Vc and Vc V significantly increased (F) ON-cell firing ($p < 0.0001$, $t_{29} = 6.39$, Cohen's $d = 0.48$), and (H) significantly decreased OFF-cell firing ($p < 0.0001$, $t_{25} = 4.84$, $d = 0.69$) compared to pre-light firing rate. (I,K) Ratemeter records (1-s bins) with mechanical stimulation of the whisker pad (left, black triangle) and light stimulation (right, blue bar and shading, 30 s) show mechanical-related and optogenetically-evoked responses recorded from RVM (I) ON-cell and (K) OFF-cell in animals with vector expression in dorsal Vi/Vc. Light activation in animals with viral expression restricted to dorsal Vi/Vc resulted in no significant change on (J) ON-cell ($p = 0.20$, $t_{14} = 1.35$) or (L) OFF-cell firing ($p = 0.89$, $t_{13} = 0.14$). **** $p < 0.0001$ compared with pre-light firing rate, paired t -tests. Blue lines = cells from male animals, black lines = cells from female animals. sp/s = spikes per second.

In animals in which vector expression was restricted to the dorsal aspect of Vi/Vc and laminae I-IV of Vc, delivery of light to *terminals* in RVM did not recruit RVM pain-modulating neurons as seen in examples in Figs. 17I and K, despite the fact that activation of trigeminal *cell bodies* in animals with vector restricted to dorsal Vi/Vc recruited ON- and OFF-cells (see above, Fig. 16F and G). There was no change in the firing of either ON-cells ($p = 0.20$, $t_{14} = 1.35$, paired t -test, 0.5 ± 0.5 spikes/s, Fig. 17J) or OFF-cells ($p = 0.89$, $t_{13} = 0.14$, paired t -test, 0.2 ± 0.7 spikes/s, Fig. 17L) as compared to the pre-light firing rate. NEUTRAL-cells did not respond to stimulation of terminals in RVM arising from either ventral or dorsal Vi/Vc, and the mean change in firing rate was 0.04 ± 0.2 spikes/s, ($p = 0.69$, $t_{19} = 0.41$, paired t -test, data not shown).

These experiments using stimulation of Vi/Vc terminals in RVM demonstrate that ventral, but not dorsal, Vi/Vc can access RVM pain-modulating neurons via a direct trigeminal-to-RVM projection.

3.4.4. Optogenetic inhibition of ventral Vi/Vc terminals in RVM attenuates nociceptive responses of ON- and OFF-cells

The experiments outlined above demonstrate that ON- and OFF-cells receive input from Vi/Vc. We next determined whether the direct ventral Vi/Vc projections to RVM convey *nociceptive* information to the pain-modulating ON- and OFF-cells. To achieve this, an inhibitory opsin, ArchT, was expressed in ventral Vi/Vc and light was delivered to Vi/Vc terminals in RVM during noxious mechanical stimulation of the face (Fig. 18A). We compared the evoked activity

of nineteen ON-cells (in 4 female, 8 male animals) and 18 OFF-cells (in 6 female, 3 male animals) during trials with and without light introduced in RVM.

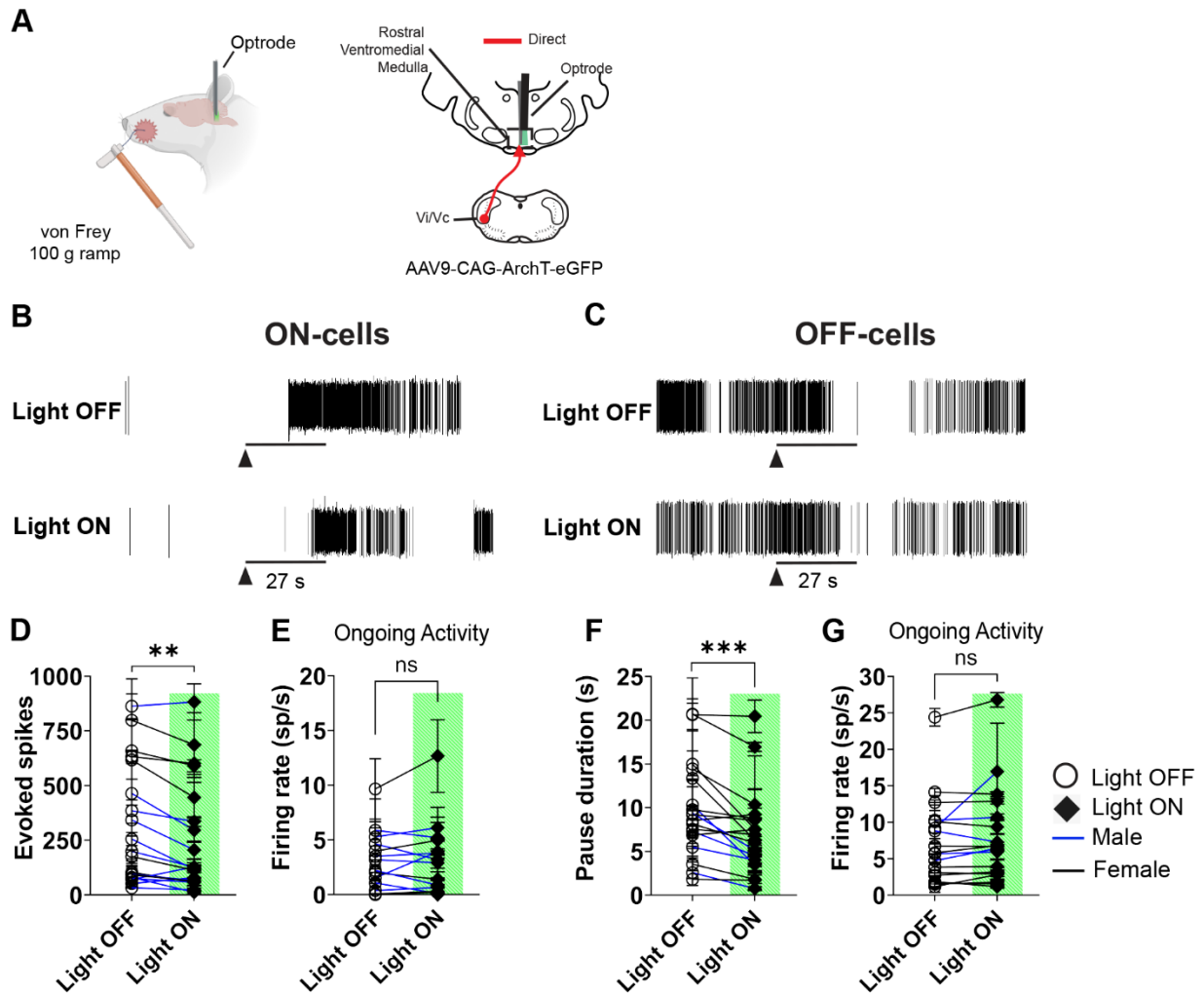


Figure 18. ArchT-induced inhibition of RVM terminals arising from ventral Vi/Vc attenuates ON- and OFF-cell noxious evoked activity.

(A) Ventral Vi/Vc terminals in RVM were inhibited during noxious mechanical stimulation of the face. Representative examples show (B) ON- and (C) OFF-cell activity during noxious mechanical stimulation during uninhibited trials (“Light OFF”), compared with during Arch-T induced inhibition of Vi/Vc terminals in RVM (“Light ON”). (D) ON-cell evoked spikes in response to noxious mechanical stimulation were significantly attenuated during terminal inhibition ($p = 0.0068$, $t_{18} = 3.06$, Cohen’s $d = 0.21$), while (E) ongoing activity was not affected ($p = 0.77$, $t_{18} = 0.30$). (F) The OFF-cell pause in response to noxious mechanical stimulation was significantly attenuated during terminal inhibition ($p = 0.0001$, $t_{17} = 4.97$, Cohen’s $d = 0.49$), while (G) ongoing activity was not affected ($p = 0.13$, $t_{17} = 1.58$). $**p < 0.01$ and $***p < 0.001$ compared with Light OFF trials, paired t -test. Blue lines = cells from male animals, black lines = cells from female animals. sp/s = spikes per second.

Optogenetic inhibition of ventral Vi/Vc terminals in RVM attenuated the noxious-evoked responses of both ON- and OFF-cells, as seen in examples in Figs. 18B and C. The number of evoked spikes for ON-cells ($p = 0.0068$, $t_{18} = 3.06$, paired t -test, Cohen's $d = 0.21$, Fig. 18B) and the duration of the pause for OFF-cells ($p = 0.0001$, $t_{17} = 4.97$, paired t -test, Cohen's $d = 0.49$, Fig. 18C) were significantly attenuated. The ON-cell burst was reduced by approximately 20%, while the OFF-cell pause duration was shortened by about 26%. By contrast with the attenuation of evoked responses, suppression of ventral Vi/Vc input to RVM did not result in a significant change in the ongoing activity of either cell class (ON-cells: $p = 0.77$, $t_{18} = 0.30$, paired t -test; OFF-cells: $p = 0.13$, $t_{17} = 1.58$, paired t -test, Fig. 18E, G). When the inhibitory opsin was expressed in dorsal Vi/Vc, optogenetic inhibition of terminals in RVM had no effect on evoked responses of either ON- ($p = 0.63$, $t_{13} = 0.49$, paired t -test) or OFF-cells ($p = 0.097$, $t_5 = 2.04$, paired t -test, data not shown).

These experiments using inhibition of Vi/Vc terminals in RVM demonstrate that a direct projection from ventral Vi/Vc to RVM conveys information to RVM pain-modulating neurons, and that this input is recruited during noxious stimulation.

3.4.5. Vi/Vc sends a GABAergic projection to RVM and PB neurons

Both GABAergic and glutamatergic neurons in the trigeminal complex are activated by noxious orofacial stimulation and likely are involved in orofacial nociceptive transmission [253-257]. Nonetheless, ascending nociceptive input from the dorsal horn to supraspinal targets is thought to be conveyed primarily by excitatory projections [258-260]. Optogenetic activation of ventral Vi/Vc terminals in RVM led to an increase in ON-cell firing and a decrease in OFF-cell firing. The increase in ON-cell firing is consistent with an excitatory ascending input to the brainstem. However, the decrease in OFF-cell firing, and the report that the OFF-cell pause is mediated by GABA [243], raises the possibility of a GABAergic input to RVM from ventral Vi/Vc that contributes to the OFF-cell pause. We therefore explored whether GABAergic trigeminal

cells that project to RVM can be identified. We also considered whether GABAergic neurons in Vi/Vc project to PB, since PB relays nociceptive information to RVM.

In 2 male and 2 female animals, AAV9-mGAD65(delE1)-GFP was injected in ventral Vi/Vc to allow us to visualize GAD65+ neurons in this region (Fig. 19Ai).

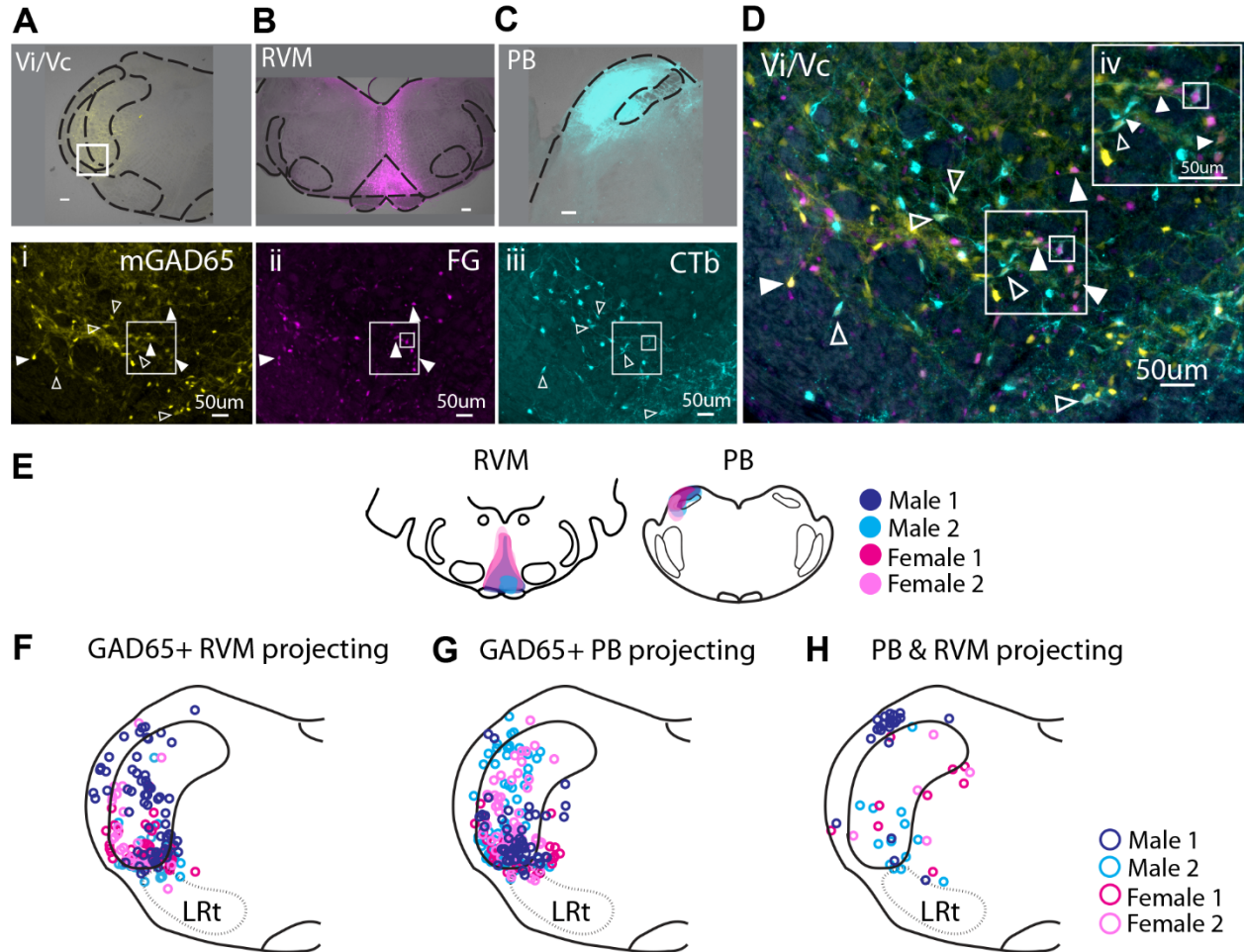


Figure 19. Both RVM and PB receive GABAergic projections from ventral Vi/Vc.

(A-D) Representative animal and (E-H) group data. (A) Vi/Vc was injected with AAV9-mGAD65(delE1)-GFP and (i) GFP labeled GABAergic cells were found in ventral Vi/Vc. (B) Injection of Fluorogold (FG) in RVM and (C) CTb in PB revealed cell bodies in ventral Vi/Vc (ii and iii, respectively). (D) GAD65+ Vi/Vc RVM projecting neurons (solid arrow) and PB projecting neurons (empty arrow) were identified (iv). Vi/Vc cells projecting to both RVM and PB could be identified (square). (E) Injection sites in RVM and in PB in 4 animals; 2 male and 2 female. (F) Anatomical maps showing co-localization of GAD65+ Vi/Vc neurons projecting to RVM, (G) GAD65+ Vi/Vc neurons projecting to PB, (H) and Vi/Vc neurons projecting to both PB and RVM in 4 animals. LRt = lateral reticular nucleus. Scale bars are 200 μm unless otherwise noted.

Retrograde tracers FG and CTb were injected into RVM and PB, respectively (Representative Figs. 19B, C and Fig.19E). FG-positive neurons in Vi/Vc (Fig. 19Bii) provided anatomical confirmation of our optogenetic/electrophysiological evidence that Vi/Vc neurons project to RVM. GFP+ cells co-labelled with FG (Representative Fig. 19Div, solid arrowhead, and Fig. 19F) were also identified, indicating that ventral Vi/Vc sends GABAergic input to RVM. While AAV9-mGAD65(delE1)-GFP was targeted to ventral Vi/Vc, vector leakage revealed the presence of GAD65+ neurons in dorsal Vi/Vc that project to RVM. It is unknown what role these neurons serve in the transfer of sensory information, as activation of dorsal Vi/Vc terminals in RVM did not influence OFF-cell activity in our electrophysiological recordings.

The well-documented projection from Vi/Vc to PB was also confirmed, with CTb-positive neurons in Vi/Vc [252] (Figs. 19Ciii). As with RVM-projecting Vi/Vc neurons, PB-projecting neurons co-labelled with GFP could be identified (Representative Fig. 19Diii, empty arrowhead and Fig. 19G), indicating that Vi/Vc also sends GABAergic projections to PB. Finally, Vi/Vc neurons double-labelled for FG and CTb were found throughout Vi/Vc, indicating that some Vi/Vc neurons project to both RVM and PB (Representative Fig. 19Div, square box and Fig. 19H).

3.4.6. *Vi/Vc also recruits RVM pain-modulating neurons via PB*

PB is known to convey nociceptive information to pain-modulating neurons in RVM [247, 248], and our anatomical data showed that at least some Vi/Vc neurons send projections to both PB and RVM. This raises the possibility that Vi/Vc can also influence activity of RVM pain-modulating neurons *indirectly*, via projections to PB. To address this possibility and the potential confound of antidromic activation, we investigated PB neuron activity in response to optogenetic activation of Vi/Vc neurons and RVM terminals (Fig 20A-C). We compared the pre-light firing rate to light-evoked firing rate during RVM terminal and Vi/Vc cell body activation in 7 PB neurons in 3 animals. PB neurons activated by noxious mechanical peripheral stimulation of the face did not change in cell activity when the light was introduced to RVM terminals. However,

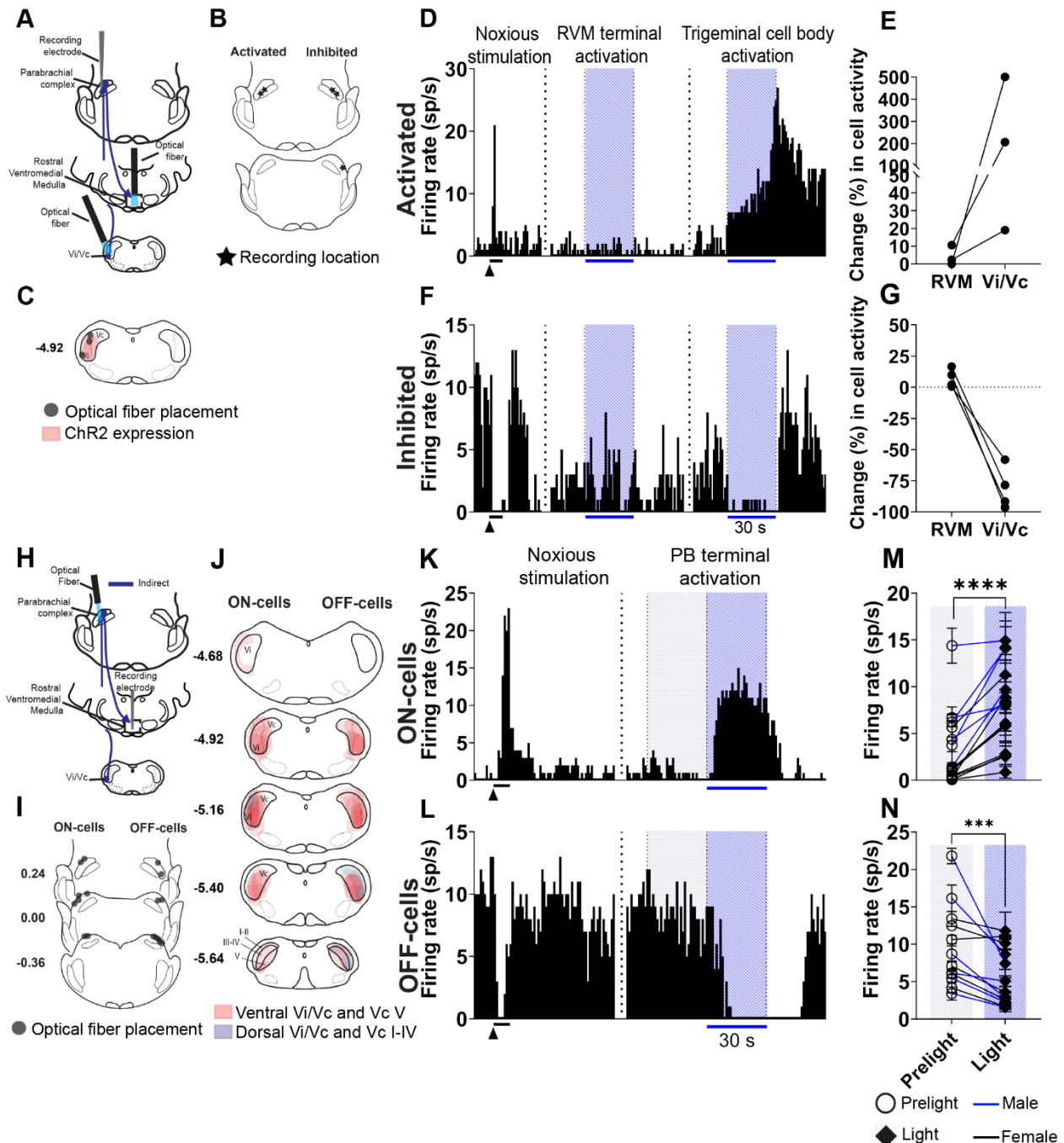


Figure 20. PB neurons are activated or inhibited by Vi/Vc cell body stimulation, while unaffected by RVM terminal activation.

ChR2-induced activation of trigeminal terminals in PB mimics noxious stimulation, activating ON-cells and suppressing OFF-cells. (A) Vi/Vc cell bodies and terminals in RVM were activated while recording from PB neurons. (B) Recording locations in PB and (C) optical fiber placements and vector expression in Vi/Vc were mapped. (D) Ratemeter records with mechanical stimulation of the whisker pad (left, black triangle) and light stimulation (right, blue bars and shading, 30 s) in RVM and Vi/Vc show mechanical-related and optogenetically-evoked responses recorded from PB neurons in cells that were (D) activated or (F) inhibited by noxious stimulation and Vi/Vc cell body activation. (E,G) PB neurons did not change in activity in

response to light in RVM, while activation of Vi/Vc cell bodies either (E) increased or (G) decreased PB neuron activity. (H) Vi/Vc terminals in PB were activated while recording from RVM neurons. (I) Optic fiber placements and (J) viral expression locations were mapped. (K,L) Ratemeter records with mechanical stimulation of the whisker pad (left, black triangle) and light stimulation (right, blue bar and shading, 30 s) in PB show mechanical-related and optogenetically-evoked responses recorded from RVM (K) ON and (L) OFF-cells. (M) Activation of terminals in PB significantly increased ON-cell firing ($p < 0.0001$, $t_{14} = 6.91$, Cohen's $d = 1.09$), and (N) significantly decreased OFF-cell firing ($p = 0.0002$, $t_{11} = 5.45$, Cohen's $d = 0.82$). *** $p < 0.001$ and **** $p < 0.0001$ compared with pre-light firing rate, paired t -test. Blue lines = cells from male animals, black lines = cells from female animals. sp/s = spikes per second.

Vi/Vc cell body activation increased the firing rate in these neurons (Figs. 20D, E). These 3 cells showed a mean increase of 3.3 ± 1.9 spikes/s in response to Vi/Vc cell body stimulation and mean percent increase in cell activity of approximately 242 %. Conversely, in these same cells, RVM terminal activation resulted in a mean change of only 0.03 ± 0.4 spikes/s.

PB neurons inhibited by noxious mechanical stimulation of the face also did not change in cell activity when the light was introduced to RVM terminals, but were inhibited during Vi/Vc cell body activation (Figs. 20F, G). These 4 cells showed a mean decrease of 8.0 ± 4.0 spikes/s in response to Vi/Vc cell body stimulation, a mean percent decrease of approximately 81%. Conversely, in these same cells, RVM terminal activation resulted in a mean change of only 0.3 ± 0.3 spikes/s.

These data indicate PB neurons are recruited during Vi/Vc cell body activation, but not during RVM terminal stimulation, confirming that Vi/Vc can influence the activity of RVM pain-modulating neurons indirectly through PB, and not through antidromic activation of Vi/Vc cell bodies via RVM terminal activation.

We then recorded from 15 ON-cells (in 3 female, and 3 male animals) and 12-OFF cells (in 5 female, 5 male animals) in RVM while stimulating Vi/Vc *terminals* in PB (Fig. 20H, I). Most animals had vector expression in both dorsal and ventral Vi/Vc (Fig. 20J). Optogenetic activation of PB terminals mimicked noxious mechanical peripheral stimulation of the face, as seen in examples in Figs. 20K and L. ON-cell firing rate was significantly increased ($p < 0.0001$, $t_{14} = 6.91$, paired t -test, Cohen's $d = 1.09$, 4.6 ± 0.8 spikes/s, Fig. 20M), while OFF-cell firing

was significantly suppressed ($p = 0.0002$, $t_{11} = 5.45$, paired t -test, Cohen's $d = 0.82$, -3.9 ± 1.1 spikes/s, Fig. 20N). This indicates that the Vi/Vc region can also access RVM indirectly, through its projections to PB.

3.4.7. Direct and indirect recruitment results in different RVM response profiles

Although Vi/Vc inputs to RVM itself and to PB were both capable of recruiting ON- and OFF-cells, the temporal profiles of the responses to activation of the RVM and PB projections were distinct, with optogenetic activation of Vi/Vc terminals in PB leading to a prolonged response compared to activation of terminals in RVM itself, as shown in the examples in 21A-D.

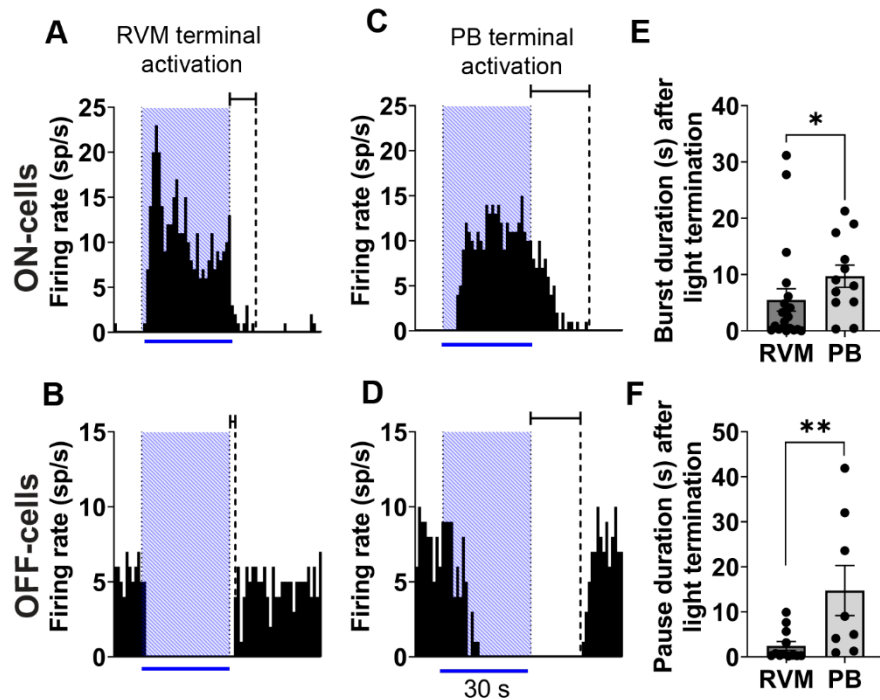


Figure 21. RVM cell response timing differs with activation of Vi/Vc terminals in RVM versus PB.

(A) Representative ON- and (B) OFF-cell responses to RVM terminal stimulation versus (C) ON- and (D) OFF-cell responses to PB terminal stimulation. Ratemeter records (1-s bins) show optogenetically-evoked responses (blue bar and shading, 30s) recorded from RVM. Line segment after light termination indicates the length of the after-response. (E) ON-cell after-responses were significantly longer with activation of Vi/Vc terminals in PB compared to activation of Vi/Vc terminals in RVM ($p = 0.0315$, $t_{30} = 2.26$, Cohen's $d = 0.53$). (F) The OFF-cell pause after-response was also longer with activation of terminals in PB ($p = 0.0085$, $t_{18} = 2.96$, Cohen's $d = 1.08$). * $p < 0.05$ and ** $p < 0.005$ compared between RVM and PB terminal activation, unpaired t -test. sp/s = spikes per second.

When RVM terminals were stimulated, ON-cell firing outlasted the period of stimulation by only 5.5 ± 2.0 s. By contrast, ON-cells continued to fire an average of 9.7 ± 2.0 s once stimulation of PB terminals was ended ($p = 0.0315$, $t_{30} = 2.26$, unpaired t -test, Cohen's $d = 0.53$, Fig. 21E). Similarly for OFF-cells, when PB terminal stimulation ended, OFF-cells did not resume firing for 14.7 ± 5.6 s. This after-response was substantially longer than when RVM terminals were activated (2.5 ± 1.0 s, $p = 0.0085$, $t_{18} = 2.96$, unpaired t -test, Cohen's $d = 1.08$, Fig. 21F). The response to stimulation of cell bodies in Vi/Vc itself was also prolonged relative to stimulation of RVM terminals (ON-cells: $p = 0.015$, $t_{31} = 2.57$, unpaired t -test, Cohen's $d = 0.63$, 16.3 ± 6.3 s; OFF-cells: $p = 0.0016$, $t_{21} = 3.61$, unpaired t -test, Cohen's $d = 1.13$, 9.5 ± 2.5 s).

3.5. DISCUSSION

These optogenetic and electrophysiological experiments revealed distinct direct and indirect pathways from Vi/Vc and Vc to RVM pain-modulating neurons. Ventral Vi/Vc and Vc lamina V neurons relay nociceptive information to RVM *directly*, while dorsal Vi/Vc and Vc laminae I-IV neurons send nociceptive information to RVM *indirectly*, possibly through PB. RVM responses to activation of the direct and indirect pathways exhibited different dynamics. Anatomical evidence combined with electrophysiological data suggests GABAergic neurons in ventral Vi/Vc project to RVM and contribute to the OFF-cell pause.

3.5.1. Direct pathway to RVM from ventral Vi/Vc and lamina V of Vc

RVM has functions beyond pain-modulation, including autonomic regulation, and contains cells, "NEUTRAL-cells," with no apparent involvement in pain-modulation [18, 238-240]. Therefore, the existence of trigeminal cells projecting to RVM does not necessarily mean that pain-modulating ON- and OFF-cells are engaged by this projection. The present study combined optogenetic manipulation of trigeminal inputs with *in vivo* electrophysiology of physiologically identified RVM neurons to address this question.

Activation of ventral Vi/Vc and lamina V terminals in RVM caused a significant increase in pain-facilitatory ON-cell firing and a significant decrease in pain-inhibitory OFF-cell firing,

mimicking noxious stimuli. NEUTRAL-cells did not respond to terminal or cell body activation. Inhibition of the direct pathway from ventral Vi/Vc during noxious mechanical stimulation of the whisker pad attenuated the ON-cell burst and OFF-cell pause. RVM terminal inhibition did not change ongoing activity, indicating that this direct input is likely recruited during noxious stimulation and does not contribute to the ongoing tone of RVM pain-modulating cells. These findings indicate that a direct projection from ventral Vi/Vc and lamina V of Vc to RVM specifically engages pain-modulating neurons in RVM.

3.5.2. Indirect pathway to RVM from dorsal Vi/Vc and more superficial laminae of Vc

Activation of RVM terminals arising from cell bodies in dorsal Vi/Vc and laminae I-IV of Vc had no effect on the activity of ON- and OFF-cells, and inhibition of these terminals during noxious stimulation of the whisker pad did not influence ON- and OFF-cell evoked responses. This suggests that these dorsal projections to RVM, unlike those from the more ventral aspect of the Vi/Vc transition zone, are not relevant to pain modulation. However, stimulation of cell bodies in dorsal Vi/Vc and more dorsally in Vc resulted in a significant increase in ON-cell firing and decrease in OFF-cell firing, indicating that these regions can influence RVM pain-modulating neurons through an indirect route. We therefore investigated indirect influences of Vi/Vc and considered PB as a potential relay.

Nociceptive neurons in Vi/Vc and Vc are known to send projections to PB [128, 145], and PB relays nociceptive information from the dorsal horn to RVM [247, 248]. In the present study, we found that activation of Vi/Vc terminals in PB significantly increased ON-cell firing and suppressed OFF-cell firing, indicating that Vi/Vc can modulate the activity of RVM pain-modulating neurons through PB. Whether these terminals arose from ventral or dorsal Vi/Vc cannot be determined. However, paired with the cell body stimulation data, it is likely that both regions can influence RVM indirectly through PB. While previous studies showed PB terminal activation in RVM caused an increase in both ON- and OFF-cell firing [247], the present finding that activation of trigeminal terminals in PB caused an increase in ON-cell firing and decrease in

OFF-cell firing is not contradictory. In the Chen et al. study, PB was shown to release both GABA and glutamate in RVM, and while activation of PB terminals in RVM recruited both ON- and OFF-cells, suppression of PB terminals in RVM interfered with the GABA-mediated OFF-cell pause. In the present study, we activated trigeminal input to PB, engaging the nociceptive circuitry in PB itself. It should thus not be surprising ON- and OFF-cell responses to this stimulation mirrored their responses to natural noxious stimuli.

While activation of Vi/Vc terminals in both RVM and PB recruited ON- and OFF-cells, the dynamics of the RVM responses recruited through these two pathways were distinct. Activation of Vi/Vc terminals in PB (and activation of Vi/Vc cell bodies) produced prolonged RVM responses compared to those observed with activation of Vi/Vc terminals in RVM. The differential after-response with stimulation of the direct and indirect pathways raises the possibility of distinct functions. The direct input from Vi/Vc to RVM might, for example, shift the balance between ON- and OFF-cell outputs to an ON-cell dominated pro-nociceptive state only as long as there is continuing sensory input. By contrast, the prolonged after-response with activation of the indirect pathway through PB could reflect recruitment by PB not only of RVM itself, but of other inputs to RVM, such as the amygdala or periaqueductal gray [126, 261, 262]. Therefore, PB and Vi/Vc cell body stimulation likely engages a greater population of cells within the RVM, at least over time. RVM pain-modulating cells demonstrate significant synchronization and integration of ongoing activity within and between cell classes [263, 264], which could contribute to the prolonged response. Thus, the direct and indirect pathways may have different functions and/or cooperate to modulate the processing of facial pain.

3.5.3. Contribution to the OFF-cell pause

The increase in ON-cell firing with activation of local trigeminal terminals is consistent with the classic understanding that the majority of ascending projections from the spinal cord are excitatory, although glycinergic and/or GABAergic spinoreticular projections have been identified [120, 258-260]. However, OFF-cell firing was consistently suppressed by activation of

these same Vi/Vc terminals. Because the OFF-cell pause is known to be mediated by GABA and not through local RVM interactions [148, 217, 243, 265], we also used an anatomical approach to explore whether Vi/Vc provides at least some direct, inhibitory input to RVM. Using AAV9-mGAD65-GFP combined with retrograde tracing, we determined that ventral Vi/Vc GABAergic neurons do project to RVM. Paired with the electrophysiological data, our observation that GAD65-expressing neurons can be found projecting to RVM supports our functional evidence that ventral Vi/Vc contribute directly to the OFF-cell pause. However, future studies could build on this, using selective optogenetic manipulation of GABAergic cells, as our approach nonspecifically activated and inhibited inputs to RVM.

We noted that some PB neurons were inhibited by activation of cell bodies in the Vi/Vc region, consistent with reports that some PB neurons are inhibited by noxious stimulation [146], and raises the possibility of an inhibitory projection to PB from the trigeminal dorsal horn. Prior anatomical studies of ascending GABAergic projections from Vc have been inconsistent, and it has been suggested that negative findings could be due to limited sensitivity of immunohistochemical approaches [266, 267]. However, the present studies combining electrophysiological and anatomical data suggest that PB, like RVM, receives a direct inhibitory input from the trigeminal complex.

3.6. SUMMARY AND CONCLUSIONS

Pain in the trigeminal distribution is often more impactful, both emotionally and physically, than body pain, and PB plays a well-documented role in the affective dimension of pain [262, 268, 269]. Stimuli applied to the face activate more PB neurons than comparable stimuli applied to the body [147], and persistent orofacial pain engages the Vc-PB pathway [144]. PB also coordinates withdrawal reflexes through reciprocal connections with the reticular formation [270]. Through these reciprocal connections, PB may be modulating RVM responses to direct trigeminal input, shaping how RVM modulates nocifensive behaviors, and linking RVM to the affective dimension of craniofacial pain. The direct pathway could engage RVM circuits to

permit the immediate nocifensive response. These pathways could also cooperate to determine information about pain, such as intensity, that is encoded by activation of multiple brain regions [271], highlighting the interrelationships within pain-modulating networks and of these modulatory networks with pain-transmission pathways. Our data also revealed that the effects of recruiting the direct and indirect pathway were consistent between the sexes. While women are more likely to be afflicted by trigeminal chronic pain conditions, it appears that the basal functional input from trigeminal nuclei to the pain-modulatory system is similar in both sexes.

In conclusion, the present study demonstrates that RVM pain-modulating circuits directly and indirectly receive nociceptive input from Vi/Vc. Activation experiments mimicked RVM cell responses to noxious stimuli, resulting an increase in ON-cell firing and decrease in OFF-cell firing. Inhibitory experiments revealed that Vi/Vc directly relays nociceptive information to RVM. Vi/Vc likely contributes to the OFF-cell pause evoked by noxious stimulation of the face by means of a direct GABAergic projection. A parallel indirect pathway from Vi/Vc to RVM via PB was also revealed. These data define two distinct pathways through which sensory input and modulating circuits can interact.

CHAPTER 4

MANUSCRIPT # 4

Comparative analysis of spike-sorters in large-scale brainstem recordings

Submitted.

Caitlynn C De Preter^{1,2}, Elizabeth M Leimer³, Alex Sonneborn^{1,4}, and Mary M Heinricher^{1,2}

¹Department of Neurological Surgery, Oregon Health & Science University, Portland, OR, 97239, USA. ²Department of Behavioral and Systems Neuroscience Graduate Program, Oregon Health & Science University, Portland, OR, 97239, USA. ³Department of Anesthesiology and Perioperative Medicine, Oregon Health & Science University, Portland, OR, 97239, USA. ⁴VA Portland Health Care System, Portland, OR, 97239, USA

CCDP-designed research, performed research, analyzed data, and wrote the paper.

EML, AS, and MH-analyzed data and wrote the paper.

4.1. ABSTRACT

Recent technological advancements in high-density multi-channel electrodes have made it possible to record large numbers of neurons from previously inaccessible regions. While the performance of automated spike-sorters has been assessed in recordings from cortex, dentate gyrus, and thalamus, the most effective and efficient approach for spike-sorting can depend on the target region due to differing morphological and physiological characteristics. We therefore assessed the performance of five sorters, Kilosort3 (KS3), MountainSort5 (MS5), Tridesclous (TDC), SpyKING CIRCUS (SC), and IronClust (IC), in rostral ventromedial medulla recordings, a region that has been characterized using single-electrode recordings but that is essentially unexplored at the high-density network level. As demonstrated in other brain regions, each sorter produced unique results. Manual curation preferentially eliminated units detected by only one sorter. KS3 and IC required the least curation while maintaining the largest number of units, whereas SC and MS5 required substantial curation. TDC consistently identified the smallest number of units. Nonetheless, all sorters successfully identified classically defined RVM physiological cell types. These findings suggest that while the level of manual curation needed may vary across sorters, each can extract meaningful data from this deep brainstem site.

4.2. SIGNIFICANCE STATEMENT

High-density multichannel recording probes that can access deep brainstem structures have only recently become commercially available, but the performance of open-source spike-sorting packages applied to recordings from these regions has not yet been evaluated. The present findings demonstrate that KS3, MS5, TDC, SC, and IC can all be reasonably used to identify units in a deep brainstem structure, the rostral ventromedial medulla (RVM). However, manual curation of the output was essential for all sorters. Importantly, all sorters identified the known, physiologically defined RVM cell classes, confirming their utility for deep brainstem recordings. Our findings provide suggestions for processing parameters to use for brainstem recordings and highlight considerations when using high-density silicon probes in the brainstem.

4.3. INTRODUCTION

“Spike-sorting” refers to the process of assigning extracellularly recorded action potential waveforms, or “spikes” to distinct individual neurons. Historically, extracellular recordings have been performed using a single electrode, recording a small number of neurons, followed by semi-automated sorting based on template matching and waveform features (shape, amplitude, or width) and extensive manual curation on an individual spike basis [272, 273]. However, the advent of multichannel recording technologies has increased data output by several orders of magnitude, making this method of sorting increasingly infeasible [273, 274]. More fully automated spike-sorting approaches have consequently been introduced, with the goal of reducing the time, effort, and human subjectivity associated with earlier sorting techniques [275]. Newer sorters employ a combination of template matching, density-based approaches, and clustering, with manual curation verifying the resulting clusters [275-277].

The most accurate and efficient approach for sorting a given dataset likely depends on the morphological and physiological properties of the brain region of interest. For example, recordings from brain regions with densely-packed cells with high firing rates suffer from overlapping spikes that can be assigned incorrectly during unit identification [278]. Sorters that rely on density-based approaches have been shown to fail at resolving overlapping spikes at a higher rate than those using template-matching [279, 280]. Conversely, low firing rates can impact the performance of template-based sorters, which rely on an average waveform shape to distinguish units [281, 282]. Therefore, the specific neuron populations in a region and corresponding firing rate distributions must be considered when choosing a spike-sorting package.

While the performance of a number of automated sorters has been evaluated and compared in recordings from the cortex, hippocampus, dentate gyrus, and thalamus [283, 284], the defined morphological cell types and layered structure in these regions gives neurons distinct electrical properties that result in distinguishable waveforms [285]. In contrast, brainstem

regions, which have only recently begun to be explored at the high-density network level, have received less attention, partly due to technological challenges. Multielectrode arrays are too large to be inserted into deep brainstem structures without serious injury, and high-density silicon probes long enough to reach deep structures have only recently become commercially available (e.g. [286, 287]). To date, few multichannel recordings have been reported from this region [e.g., 288, 289-292]. It is therefore important to systemically assess the performance of different automated sorters in the brainstem to help identify the most effective strategies for sorting.

Given that there are differences in neuronal size, density, and firing patterns across different brain regions [293], and that these might impact sorter performance, the present study compared the performance of different sorters applied to recordings from a deep brainstem region, the rostral ventromedial medulla (RVM). The RVM is a ventral brainstem region, encompassing the ventromedial aspects of gigantocellular and magnocellular reticular formation and medullary raphe, that has been well characterized using single-electrode approaches [242, 263, 294, 295]. The different cell classes lack distinct morphology [296], but are defined by firing changes associated with noxious-evoked withdrawal behaviors: “ON”-cells exhibit a burst of activity and “OFF”-cells a pause in activity associated with behavioral withdrawal from the stimulus [297]. The third class of cells, “NEUTRAL”-cells, do not exhibit any change in activity in response to noxious stimuli. Over the last 30 years, RVM spike waveforms have been sorted using software template matching, cluster analysis, and manual verification on an individual spike-to-spike basis [61, 298], a time- and labor-intensive approach that would be impossible in multi-channel recordings.

Here we took advantage the novel application of silicon-probe technology in RVM and the well-defined firing patterns to assess performance of these different sorters. We used SpikeInterface, a Python toolkit that integrates multiple sorters [283], to compare performance of five different sorters, with and without manual curation.

4.4. METHODS

All animal procedures were performed in accordance with Oregon Health & Science University's animal care committee's regulations and followed the guidelines of the National Institutes of Health and the Committee for Research and Ethical Issues of the International Association for the Study of Pain. Male and female Sprague Dawley rats were housed in a 12-hour light-dark cycle environment with free access to water and food for at least one week prior to experiments.

4.4.1. *Electrophysiological recordings*

Rats were briefly anesthetized (4-5% isoflurane) for external jugular vein catheter implantation. Animals were then transferred to a stereotactic frame and anesthetic plane was maintained with continuous methohexital infusion. A small craniotomy was made to gain access to the RVM and dura was removed. Following preparatory surgery, the anesthetic plane was set to maintain a stable heat-evoked paw withdrawal threshold. Heart rate and body temperature were monitored and maintained throughout the experiment. Testing was performed in low ambient light conditions (< 5 lux).

A 64-channel, high-density silicon probe was used to record RVM neuronal activity (Cambridge Neurotech M1, Cambridge, UK). Prior to placement, the probe was painted with Dil to identify probe location (Sigma-Aldrich: Cat. #42364). The probe was lowered at a rate of 1.25 micron/s using a hydraulic microdrive (David Kopf Instruments, Tujunga, CA) until the entire length (632 μm) of the contact distribution was within the RVM.

Probes were paired with a RHD 64-channel recording headstage (Intan Technologies, Los Angeles, CA) using an adaptor (ADPT A64-Om32x2, Cambridge Neurotech), and connected to both the Intan Recording Systems (RHD 1024-channel) and, in parallel, to a CED Spike2 (Cambridge Electronic Design, Cambridge, UK) data acquisition system. Signals were band-pass filtered (500 Hz to 15 kHz), sampled at 30 kHz, and stored for offline analysis.

A 25-min recording from each of six animals was used in this study. Noxious stimulation was delivered at 5-min intervals: three heat stimulations followed by a hindpaw pinch with toothed forceps. Noxious heat stimuli were applied to the plantar surface of the hindpaw using a custom-built Peltier device. The surface temperature was increased at a rate of 1.5 °C/s from 35 °C to a maximum of 53 °C. Withdrawal was determined from hamstring rectified and smoothed (0.05 s) electromyographic (EMG). EKG and core temperature were also collected.

4.4.2. Histology

At the conclusion of the experiment, rats were deeply anesthetized using methohexital before being perfused intracardially with 0.9% saline followed by 4% formalin. Brains were extracted and fixed in a 4% formalin solution for 24 hours, then stored in 30% sucrose. Brains were sectioned (60 µm), and probe placement confirmed by location of Dil tracks using a fluorescence microscope (BZ-X710, Keyence Corporation of America, Itasca, IL) and plotted according to the Paxinos & Watson rat brain atlas [299]. Only recordings in which the entire length of the contacts (632 µm) were in the RVM were used.

4.4.3. Spike sorters

We compared the performance of five established sorters on the RVM recordings: MountainSort5 (MS5) [300], IronClust (IC) [301], Kilosort3 (KS3) [302], Tridesclous (TDC) [303], and SpyKING CIRCUS (SC) [304]. KS3 assigns units as “good” or “mua” (multi-unit activity), and only the units labeled “good” were considered in further analyses. MS5 and IC employ a clustering algorithm, KS3 and TDC template matching, and SC a combination of clustering and template matching. Each of these sorters has been validated against “ground-truth” datasets [283, 284]. Outputs from each sorter were loaded into SpikeInterface for post-processing and comparison.

4.4.4. Post-processing of sorter output and comparison

The raw output of each sorter (1241 units) was post-processed (SpikeInterface postprocessing module) to eliminate units unlikely to correspond to a valid neuronal signal

based on low signal-to-noise ratio (< 4.0), a high (> 0.5) interspike interval violations ratio [305], or few spikes (< 500). This resulted in a reduction in the of total number of unique units found by the five sorters to 671 that were used for all analyses. The post-processed output of each sorter was also manually curated in Phy [306]. Sorted units were accepted, rejected, and split or merged to form new units [283, 306]. Units were rejected if they were not present throughout the recording (e.g. drifted in or out during the recording), if they had contamination (e.g. two units colliding), or if they were a duplicate (e.g. units recorded from the same contacts with similar waveforms and a zero-lag cross-correlogram peak). For duplicates, only the unit with the greater number of spikes was accepted for further analysis. The curated output was then reloaded into SpikeInterface for analysis of the impact of curation.

Spike trains were compared using the SpikeComparison package of SpikeInterface. A 50% spike train match was used to extract matched units (Buccino et al., 2020). Sorter performance was compared using a Chi-square test, *t*-test, or ANOVA with Holm-Sidak *post-hoc* tests in GraphPad Prism.

Table 1. Statistical analysis results for effect of sorter and manual curation on number of units for brainstem recordings.

Comparison	Type of test	Effect of sorter	<i>p</i>-value	n
Number of units identified:	One-way ANOVA	$F_{4,25} = 14.2$	$p < 0.0001$	30
Percentage of consensus units:	One-way ANOVA	$F_{4,25} = 42.1$	$p < 0.0001$	30
Percentage of unique units:	One-way ANOVA	$F_{4,25} = 31.9$	$p < 0.0001$	30
Effect of curation on output from different sorters:	One-way ANOVA	$F_{4,25} = 10.1$	$p < 0.0001$	30
Number of UNCLASSIFIABLE units eliminated during curation	<i>t</i> -test	$t_{29} = 5.8$	$p < 0.0001$	30

Number of cells eliminated during curation or surviving, two or more sorters vs. single sorter:	Chi-squared	$\chi^2_{(1)} = 200.2$	$p < 0.0001$	671
Interaction of curation with classifiability:	Two-way ANOVA	$F_{4,40} = 0.90$	$p = 0.47$	60

4.4.5. RVM neuron functional classification

Units were classified as ON-, OFF-, or NEUTRAL-like based on change in firing rate in the 5-s interval immediately before and after onset of noxious-evoked withdrawal [242]. A unit was classified as OFF-like if it exhibited an average percent *decrease* in firing rate greater than 40%, and ON-like if it showed an average firing rate *increase* greater than 100%. For units without ongoing activity, those exhibiting an increase of at least 5 spikes in the 5 s after EMG onset were also classified as ON-cells. NEUTRAL-like units had a minimum of 0.1 spikes/s and displayed no average change in firing rate greater than 50% overall, and no single trial with a decrease greater than 40% or increase greater than 100%. Units that did not match these criteria and inconsistently responded across trials were considered UNCLASSIFIABLE units.

4.5. RESULTS

4.5.1. Comparison of five sorters

To assess the agreement between the outputs of the five tested sorters, we compared performance on six RVM recordings, from 3 male and 3 female rats. An example of units identified on 18 probe channels before and after delivery of noxious pinch to the hindpaw is shown in Figure 22A. Units had discriminable waveforms (Figure 22A, inserts) and the recording location in RVM was confirmed (Figure 22B). Of 117 units identified by at least one sorter in this recording, different sorters identified different numbers of units. SC identified the greatest number of units (70) and TDC the fewest (24). MS5, KS3, and IC identified intermediate numbers of units, with 47, 45, and 38 respectively (Figure 22C). There was also substantial variation in the degree of agreement across sorters. Of 117 total units detected by at least one

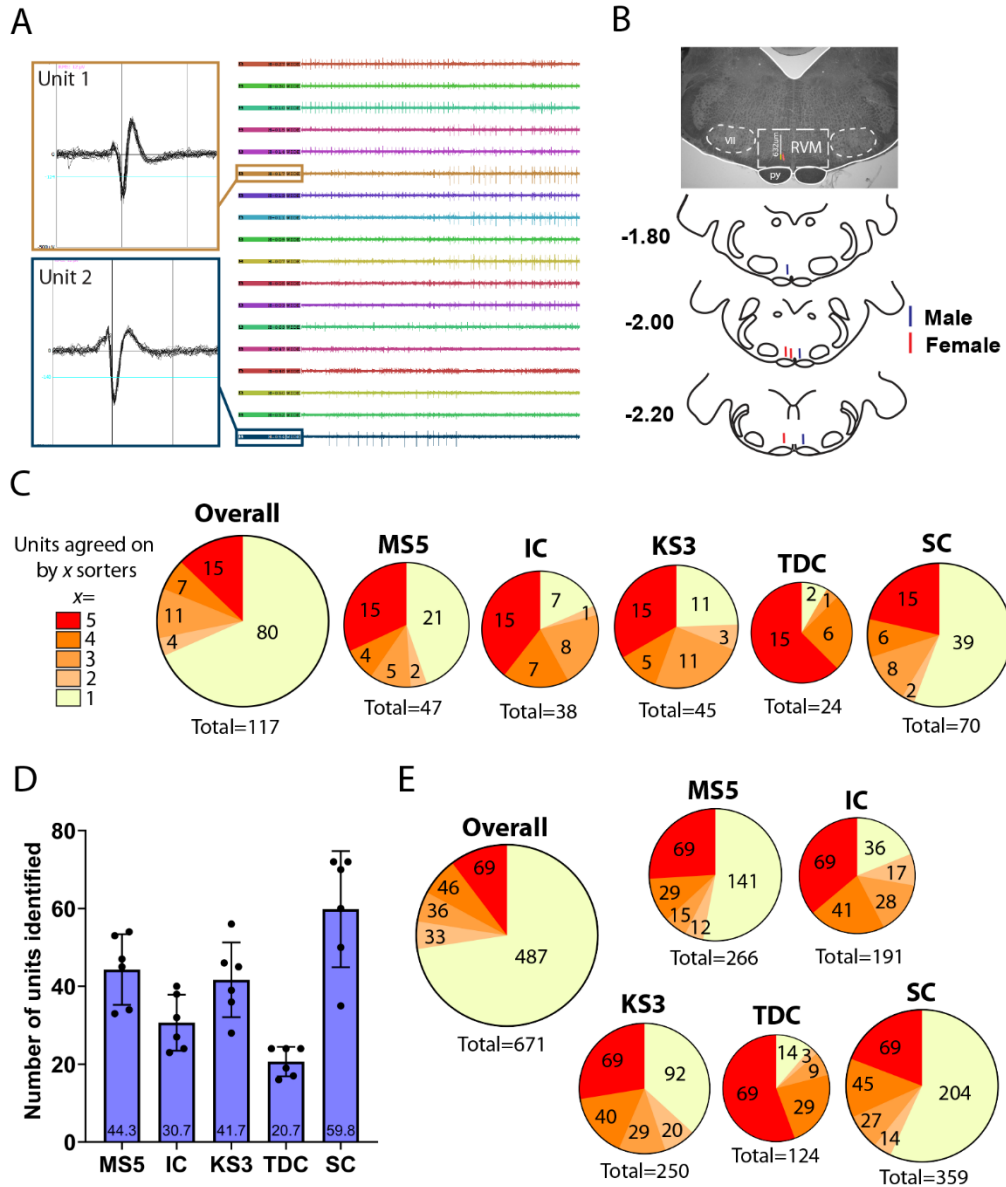


Figure 22. Performance of different automated sorters in brainstem recording.

(A) Example recording. 3-s sample of spiking activity seen on 18 channels. Two example waveforms in insets. (B) Location of the probe. The probe was confirmed to be in RVM (632 μm , probe tip was coated with Dil (red) for visualization). py: pyramid, VII: facial nucleus. (C) Number of units identified by each individual sorter and across all five sorters for the example recording. Of 117 units identified by at least one sorter, 15 were agreed upon by all five, whereas 80 were found by only a single sorter. Number of sorters that agreed upon a given unit ranged from all five (red, $x = 5$), to only a single sorter (yellow, $x = 1$). Pie charts are scaled to the total number of units identified by each sorter. (D) Mean (\pm SD) number of units identified by each sorter across all 6 recordings. (E) Number of units identified by each individual sorter and across all five sorters summed over the six recordings. Of 671 units identified by at least one sorter, 69 were agreed upon by all five (red), whereas 487 were found by only a single sorter (yellow).

sorter in this recording, 15 were identified by all five, 13% of the total (Figure 22C, red). However, these consensus units represented different proportions of the number identified by the different sorters. That is, these 15 represented almost 63% of the total identified by TDC, 39% of those found by IC, about a third of those identified by MS5 and KS3, and only 21% of those found by SC. However, another 22 units were agreed upon by two to four sorters (19% of total cells identified, Figure 22C, orange). Conversely, each sorter also identified unique units only found by that sorter (Figure 22C, yellow). TDC, which identified the fewest units overall, also identified the fewest unique units (2). IC and KS3 yielded a similar number of units not found by other sorters (7 and 11, respectively), and MS5 identified 21 unique units. SC identified 39 units that were not found by any other sorter, consistent with the large number of units identified by this sorter relative to the others. Of the 117 units identified, 80 (68%) were reported by only a single sorter, and almost half of those 80 were reported by SC.

Comparison of sorter outputs across all six recordings showed that these trends seen in the example recording were consistent (Figure 22D). SC reported significantly more units than any of the other four sorters, whereas TDC identified fewer than any of the other sorters except IC ($F_{4,25} = 14.2$, $p < 0.0001$, $n = 30$). MS, KS, and IC identified intermediate numbers of units.

Of the 671 total units across all recordings that were detected by at least one sorter, 69 (10%) were agreed upon by all five sorters (Figure 22E, red, 9 to 15 units per recording). As with the example recording, these consensus units represented different proportions of the number identified by the different sorters. That is, these 69 represented over half of the total identified by TDC (57%), 36.4% of those found by IC and, 26% of identified by MS5 and 28.6% of those found by KS3, but only 20% of those found by SC. The percentage of all units identified by TDC that were consensus units was significantly greater than that for any of the other sorters, while the percentage that were consensus units was significantly less for SC than for any of the other sorters ($F_{4,25} = 42.1$, $p < 0.0001$, $n = 30$, Holm-Sidak *post-hoc* test). Another 115 (17%) were agreed upon by two to four sorters (Figure 1E, orange). By contrast, 487 (73%)

were identified by only one sorter (Figure 1E, yellow). The percentage of unique units was different for the five sorters, and paralleled the total number of units identified ($F_{4,25} = 31.9$, $p < 0.0001$, $n = 30$, Holm-Sidak *post-hoc* test). That is, over half of the units identified by SC were found only by SC, whereas only about 10% of the units identified by TDC were unique to TDC.

4.5.2. Effect of manual curation

A stated goal of most automated sorters is to reduce the need for manual curation. Therefore, the automated output was compared to curated output to determine which sorter likely yielded the greatest number of true units. During curation, a unit was accepted or rejected based on whether it was present throughout the recording, whether it was contaminated by a second waveform, or whether it was a duplicate unit. An example of a duplicate unit identified during curation is shown in Figure 23A. Units 21 and 22 in this example recording demonstrated similar waveform shapes and a zero-lag peak on the cross-correlogram. Unit 21 had fewer spikes and was consequently rejected as a duplicate of Unit 22.

Of the 671 units identified in the automated output from the five sorters, 248 (37%) survived curation. Comparison of the effect of curation on the output from the different sorters showed substantial variability (Figure 23B, $F_{4,25} = 10.1$, $p < 0.0001$, $n = 30$). Thus, while TDC initially reported the smallest number of units, almost 72% of these were accepted during curation. By contrast, less than half of the units identified by MS5 and SC were accepted as valid units during curation. Considering only the 69 units originally agreed upon by all five sorters in the automated output, 52 (75%) survived curation (Figure 23C, Overall Curated, red). Of 184 units identified by at least two sorters, 136 survived curation (74%). By comparison, of the 487 unique units reported in the automated output, only 108 (22%) survived curation (Figure 23C, Overall Curated, yellow). Thus, units uniquely identified by a single sorter are less likely to survive curation than those identified by two or more sorters ($\chi(1) = 200.2$, $p < 0.0001$). SC and

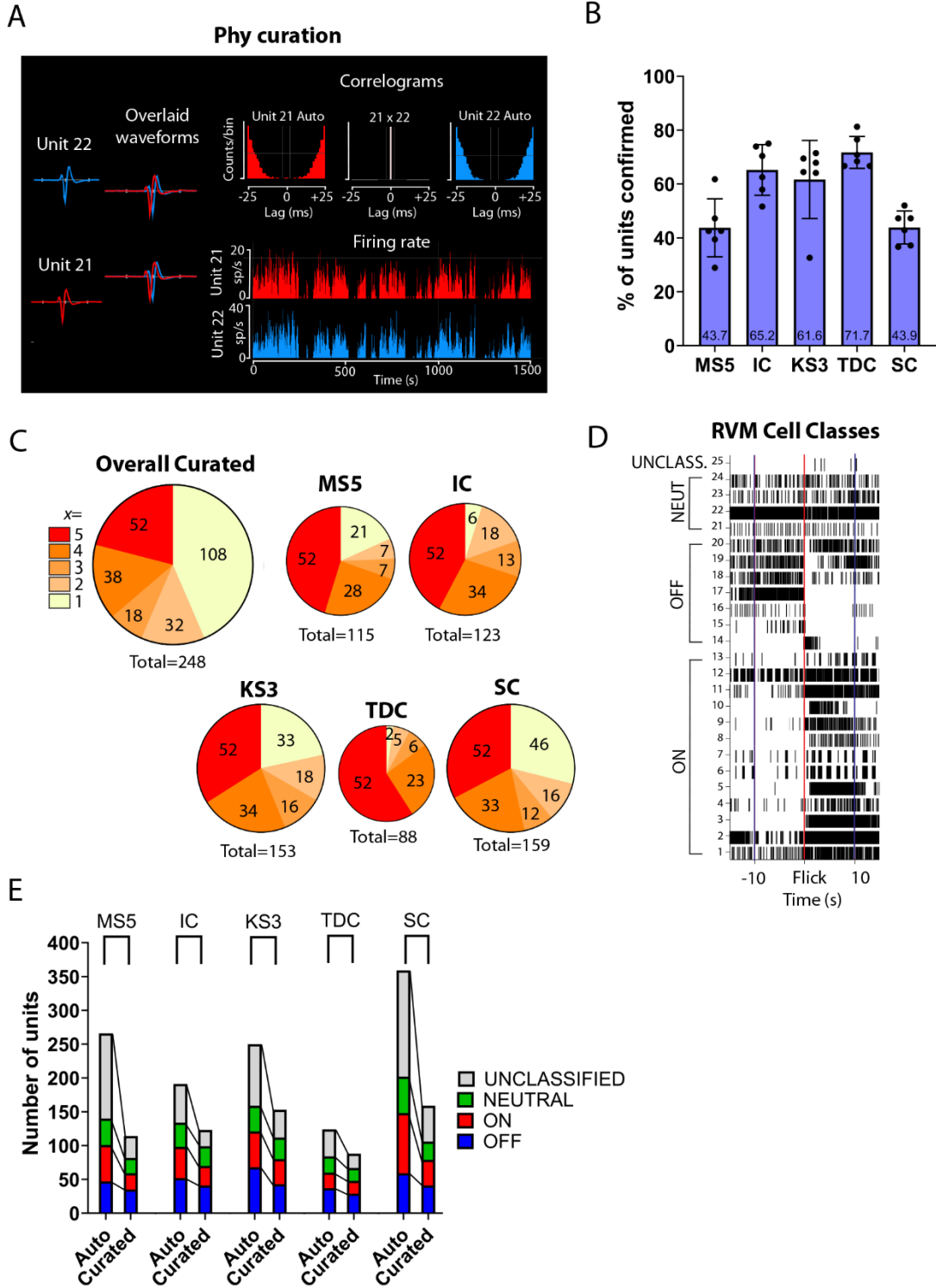


Figure 23. Effect of curation and interaction with physiological classification.

(A) Example of curation of duplicate units. Unit 21 and 22 are identified as duplicates based not only on the overlapping waveform shape but on zero-lag peak in the cross-correlogram (top row, middle). Autocorrelograms (top row, left and right) show expected absence of coincident

spikes. **(B)** Percentage of units (mean \pm SD) identified by each sorter that survived curation. **(C)** Number of units identified by each individual sorter and across all five sorters that survived curation. Number of units agreed upon by all five sorters (red), by 4, 3, or 2 sorters (orange), or unique to a single sorter (yellow). **(D)** Example of classification of individual neurons as UNCLASSIFIED, NEUTRAL-, OFF- and ON-like. Rasterplot shows activity for 25 units identified in the curated output of KS3 during the 10 seconds before and after noxious evoked withdrawal (Flick, red line). **(E)** All sorters were able to identify neurons in the three classically defined RVM classes. UNCLASSIFIED units were disproportionately eliminated during curation. MS5 and SC identified the greatest number of UNCLASSIFIABLE units.

KS3 identified the greatest total number of units that remained after curation, with 159 and 153, respectively (Figure 23C). IC and MS5 identified a similar number of units after curation, 123 and 115, respectively, and TDC identified 88 total units after curation (Figure 23C).

4.5.3. All five sorters identify physiologically classifiable units

We next determined the ability of each sorter to identify RVM units that could be classified as ON-, OFF-, or NEUTRAL-like units. Units that exhibited changes in activity associated with noxious-evoked withdrawal can be seen in the example trials shown in raster plots (Figure 23D) before and after curation. All sorters identified both UNCLASSIFIED and classifiable RVM units (Figure 23E). Between 54% and 70% of the cells identified in the automated output were classifiable, and assigned to the ON-, OFF-, OR NEUTRAL-like classes. In the curated output, between 75% and 80% of the cells were classifiable. There was no difference amongst sorters in the percentage of classifiable units identified in the automated or curated output (two-way ANOVA, $p > 0.05$).

Although all sorters identified classifiable units, curation differentially eliminated UNCLASSIFIABLE units. As shown in Figure 2E, the numbers of both classifiable and unclassifiable units were reduced by curation. SC identified the greatest number of classifiable RVM units, with 202 total ON-, OFF-, and NEUTRAL-like units. However, curation reduced this number by almost half, to 106. The number of UNCLASSIFIABLE units was reduced by about 66%, from 157 units to 53. KS3 identified the next highest number of classifiable units with a total of 159 ON-, OFF-, NEUTRAL-like units in the automated output. Curation reduced this

number by 30%, resulting in a total number of 112 units, 6 more units than SC. The number of UNCLASSIFIABLE units was reduced by about 55%, from 91 to 41. IC and MS5 reported similar numbers of classifiable units, 134 and 140 units, respectively. However, MS5 identified a much greater number of UNCLASSIFIABLE units, with 126 compared to the 57 UNCLASSIFIABLE units found by IC. After curation, the number of MS5 classifiable units was reduced by about 41% and UNCLASSIFIABLE units by around 75%, while for IC, curation resulted in a reduction of about 26% for classifiable units and 58% for UNCLASSIFIABLE units. TDC was the least impacted by curation compared to the other sorters, although it identified only 84 classifiable units prior to curation. This was reduced to 67 units after curation. The number of UNCLASSIFIABLE units was reduced by about 48%, from 40 to 21 units.

On average across sorters, there was about a 64% reduction in UNCLASSIFIABLE units but only about a 35% reduction in classifiable units following curation. Thus, across all sorters and all six recordings, curation substantially reduced the number of UNCLASSIFIABLE units, with a much smaller impact on classifiable units ($t_{29} = 5.8$, $p < 0.0001$, $n = 30$). In sum, all five sorters successfully identified RVM units that exhibit changes in firing that have been defined using single-electrode approaches.

4.6. DISCUSSION

The advent of high-density, multi-channel recording technologies has enabled the study of network level activity across brain regions. However, these advances also bring challenges for traditional spike-sorting approaches, as the increased data volume and signal complexity require new spike-sorting methods to most accurately identify individual units. The performance of different open-source sorters has been systematically evaluated and compared in recordings from cortex, hippocampus, dentate gyrus, and thalamus [283, 284]. However, the relative performance of various sorters may differ in other brain regions, given that performance can be influenced by both firing patterns and the anatomical properties of the target brain region, including cell morphology, density, and arrangement of neurons [279, 281, 282, 293]. Therefore,

the current study addressed this knowledge gap by evaluating the performance of five open-source sorters in recordings from the rostral ventromedial medulla (RVM), a pain-modulating brainstem structure with well-characterized physiological cell classes and multiple decades of single-unit definition. Using the SpikeInterface framework, Kilosort3 (KS3), MountainSort5 (MS5), Tridesclous (TDC), IronClust (IC), and SpyKING CIRCUS (SC) were each applied to RVM recordings. Although prior studies have applied both KS3 and SC to brainstem recordings [288-292], the current study took advantage of the well-characterized physiology of RVM neurons and used the SpikeInterface framework to compare the performance of five different sorters, MS5, IC, KS3, SC, and TDC, in brainstem recordings.

4.6.1. Agreement among output of different sorters applied to RVM recordings

Sorters varied widely in the total number of units identified. SC, which uses a combination of clustering and template matching [304], identified the most units, whereas TDC, which relies mostly on template matching with minimal clustering [303], consistently identified the smallest number of units. IC and MS5, which employ a clustering approach [300, 301], and KS3, which uses template learning [302], yielded similar numbers of units.

The five sorters also identified variable numbers of *unique* units – units not identified by any other sorter. SC not only identified the largest number of units, it also identified the largest number of unique units. Although IC, KS3, and MS5 yielded similar numbers of units overall, MS5 found more unique units.

Performance of sorters might be influenced by anatomical and physiological differences that contribute to either too few spikes to resolve a unit, which impacts template-based sorters, or overlapping spikes, which impacts density-based clustering sorters. The medial reticular core differs significantly from cortical and hippocampal regions in terms of cellular organization. Unlike the layered cortical and hippocampal structures with distinct morphological cell types creating varied electrical properties that result in relatively distinguishable waveforms [285], the RVM is marked by medium to large multipolar neurons compressed in the rostro-caudal plane,

giving a “stacked poker chip” organization [307, 308]. Additionally, the RVM functional classes do not have distinct morphological features that would contribute to characteristic extracellular action potential waveforms [296]. Nonetheless, the variation in the total number of units, agreement amongst sorters, and number of unique units found by each sorter is not inconsistent with a previous analysis of sorters applied to a single recording spanning cortex, hippocampus, dentate gyrus, and thalamus [283]. Based on both manual curation of their sample recording and on analysis of a simulated dataset, for which ground-truth was available, these authors argued that units agreed upon by more than one sorter are likely real, whereas unique units are more likely false positives. In the present study, about 27% of all units identified in the automated output from the five sorters were detected by at least two of the sorters, and units agreed upon by at least two sorters were more likely to survive manual curation, suggesting these units likely correspond to real units.

One false-positive that was observed across sorters was the identification of duplicate units. Duplicate units arise when a spike is assigned to multiple clusters, due to slight shifts in waveform shape [309]. This is problematic in densely packed regions like the brainstem, where spikes from neighboring neurons or from different parts of the same neuron (e.g. somata, dendrites) overlap frequently. The presence of duplicates in all sorter outputs highlights the necessity of careful manual curation to prevent duplicate units from artificially inflating unit counts and distorting interpretations of firing dynamics.

An additional factor that could influence the sortability of recordings from different brain regions is probe geometry, as contact spacing and layout influence the ability to resolve distinct units. Indeed, while the goal of the present study was to compare performance of different sorters applied to recordings from a brainstem site with well-characterized physiological properties, it could be useful to assess performance of these same sorters on recordings with this probe in different brain regions to determine whether and how probe geometry interacts with

the sorter. This could also help determine whether certain probes geometries are more effective in deep brain structures and guide future development of recording technologies.

4.6.2. All sorters identified classifiable RVM units

The mutually exclusive and exhaustive OFF/ON/NEUTRAL-cell framework for classification of RVM neurons is based on noxious event-related changes in firing, with OFF-cells exhibiting a pause in firing and ON-cells a burst associated with nocifensive withdrawal. NEUTRAL-cells are defined by exclusion, failing to show either a pause or a burst associated with nocifensive behaviors [242, 263]. Units corresponding to each of these three classes were identified by all sorters, and present in both the automated and curated output of each sorter.

Given the robust classification of RVM neurons in single-electrode recordings, and despite identification of OFF-, ON-, and NEUTRAL-like units in our multichannel recordings, it may be surprising that we also identified units that could not be classified. Units were considered UNCLASSIFIABLE either because they lacked sufficient activity to characterize possible responses or because apparent responses were inconsistent. The presence of UNCLASSIFIABLE units thus likely reflects the difficulty of fully characterizing each individual unit in a multi-channel recording. The single-electrode approach allows an investigator to optimize stimulus delivery so that changes in firing will be visible. That is, a “pause” in firing can only be seen during periods when the unit to be classified is spontaneously active, whereas a “burst” would be most evident only when the unit is not spontaneously active. The single-electrode approach allows full characterization of an individual unit, but is not feasible with a multi-channel recording, in which spontaneous firing can vary across different channels at different times. We therefore used a relatively insensitive measure, average change in firing rate, to classify an individual unit as OFF-, ON-, or NEUTRAL-like. With that approach, an OFF-cell with low ongoing activity or an ON-cell with high ongoing activity would have at best inconsistent changes in firing rate, causing it to be categorized as UNCLASSIFIABLE here. More sustained noxious stimulation or pharmacological interventions, such as morphine, which

reliably activates OFF-cells and suppresses firing of ON-cells [40, 61], may be necessary to fully and accurately classify RVM neurons in high-density recordings.

Interestingly, the number of UNCLASSIFIABLE units was preferentially reduced by curation: overall, by about two-third. By contrast, the number of classified (OFF/ON/NEUTRAL-like) units was reduced by only about a third. This suggests that UNCLASSIFIABLE units more frequently represented false-positives, whereas “real” units more commonly exhibit firing patterns consistent with what has been reported with single-electrode approaches. The slight reduction in classifiable units during curation was not a limitation. Indeed, one false-positive that was observed in both classifiable and UNCLASSIFIABLE groups and across sorters was duplication, which could lead to incorrect conclusions about population coding and dynamics in this region. Duplicate units arise when a spike is assigned to multiple clusters, presumably due to slight shifts in waveform shape. If not ruled out in curation, duplicate units would artificially inflate the total unit count and distort interpretations of firing dynamics.

4.6.3. MS5, IC, KS3, SC, and TDC can all be used to sort high-density RVM recordings

In the present study, MS5 required the most amount of curation, with 57% reduction in classified units, and about 75% of UNCLASSIFIABLE units eliminated during curation. SC required a similar level of curation, with more than half of all units eliminated during curation. IC, KS3, and TDC required less curation. Almost three-quarters of units identified by TDC survived curation, and this sorter also identified the smallest number of UNCLASSIFIABLE units. However, it also consistently identified the smallest number of units compared to the other sorters. IC identified the second-smallest number of UNCLASSIFIABLE units and curation resulted in a relatively small decrease in the number of classifiable units. For KS3, over a third of units were eliminated during curation. However, this sorter identified the greatest number of classifiable units that survived curation. KS3 and IC thus produced the greatest number of classifiable RVM units with less intense curation.

4.6.4. Conclusions

Any method for assessing activity of a neuronal population necessarily samples a subset of that population. Extracellular recording reveals only neurons that are active or for which there is a search stimulus, and with action potentials that can be resolved with a particular electrode technology. This depends both on the properties of the electrode and of the cell population under study including packing density, morphology of individual cells, and their arrangement [310, 311]. Choice of sorter is thus one of many factors that will influence which cells are “seen” using a given experimental protocol. Parallel limitations apply in use of calcium imaging, where expression of the indicator, optical constraints, thresholding, and selection based on activity define the subset of the relevant population that is sampled [312]. Thus, although different sorters tested here revealed different subsets of the RVM population, any of the sorters in this study could reasonably be used to sort high-density brainstem recordings, albeit with varying degrees of curation efforts.

The present study highlights some considerations that will be important in any application of multi-channel recording technologies. Investigators should explicitly report how units were accepted for further study. Further, analyses of both ongoing and evoked firing patterns will be more accurate if the experimental protocol is informed by “ground truth” understanding of the neurophysiological properties of system under study. However, focusing on those units thought to be relevant to the research question should be balanced by consideration of units that might exhibit potentially interesting, but new, firing patterns. Finally, consensus amongst sorters appears to improve confidence in results in brainstem recordings, as shown previously in forebrain [283].

CHAPTER 5

DISCUSSION

5.1. KEY FINDINGS

- Systemic morphine administration in female animals at an analgesic dose comparable in male animals influences RVM cell activity. Similar to males, ON-cell activity decreases, OFF-cell activity increases, and NEUTRAL-cells remain unchanged (Fig. 12). Nociception-related responses in ON- and OFF-cells are attenuated (Fig. 13).
- Vi/Vc relays nociceptive information from the ipsilateral side of the face to RVM via direct and indirect projections. This information contributes to the noxious-related evoked responses of ON- and OFF-cells in both male and female animals (Fig. 16).
- The direct Vi/Vc pathway is spatially segregated. Activation of terminals arising from ventral Vi/Vc influences RVM cell activity while activation of terminals arising from dorsal Vi/Vc does not. In response to activation of terminals arising from ventral Vi/Vc, ON-cell activity is significantly increased, OFF-cell activity is significantly decreased, and NEUTRAL-cells remain unchanged in both male and female animals (Fig. 17). Inhibition of the OFF-cell is likely mediated through a direct ascending GABAergic projection (Fig. 19). Inhibition of the direct input attenuates the noxious-related response of ON- and OFF-cells (Fig. 18).
- The PB receives input from Vi/Vc, resulting in either an increase or decrease in activity (Fig. 20). The indirect pathway through PB also influences RVM cell activity, similar to activation of the direct ventral Vi/Vc pathway, mimicking RVM cell responses to noxious stimulation of the face (Fig. 20). Activation of dorsal Vi/Vc cell bodies revealed a similar influence, suggesting dorsal Vi/Vc cells relay information to RVM indirectly via PB (Fig. 16).
- Activation of the two pathways result in different RVM response profiles, with prolonged activation of ON-cells and prolonged inhibition of OFF-cells in response to indirect recruitment. Activation of the direct pathway is time-locked to the stimulus duration,

suggesting the indirect and direct pathway from Vi/Vc to RVM may serve different functional roles in the response to acute noxious pain (Fig. 21).

- Outputs of different spike-sorters were not identical, as seen in other brain regions (Fig. 22).
- High-density silicon probes can be used to record from multiple ON-, OFF-, and NEUTRAL-cells in a single recording and location in RVM, increasing data output significantly and supporting the use of high-density silicon probes to record from deep brainstem structures (Fig. 23).
- Multiple spike sorters can be used in high-density silicon probe recordings of the rat brainstem, with varying degrees of curation efforts. Manual curation was critical to reducing the number of false positives, and reduced the total number of units that could not be assigned to classically defined categories (Fig. 23).

5.2. OVERVIEW

The RVM exerts bidirectional control of nociceptive transmission via projections to the spinal and trigeminal dorsal horns. This is accomplished via two physiologically defined cell classes: pain-facilitating “ON-cells” and pain-inhibiting “OFF-cells.” These cells are defined based on changes in their activity during nociceptive withdrawal. ON-cells have a “burst” of firing, while OFF-cells “pause” any ongoing activity. These cells are also defined by their response to endogenous opioids. ON-cells decrease in firing via post-synaptic μ -opioid receptors and exhibit a decrease in the total amount of spikes fired, while OFF-cells increase in firing and exhibit a reduction in the pause duration via disinhibition of inhibitory presynaptic input. While the opioid response of RVM neurons has been well-characterized in male animals, there is very little known about the behavior of these cells in female animals in response to morphine. Differences in pharmacological responses between the sexes has been observed in both human and rat studies, therefore, one goal of this dissertation was to determine whether the opioid response of RVM neurons are similar in males and females. Additionally, the direct pathways through which nociceptive signals reach the RVM to produce the characteristic “burst” and “pause” has not been identified, leaving a gap in our knowledge of how peripheral inputs engage descending pain-modulating systems. The second goal of this dissertation was to test the hypothesis that the trigeminal transition zone, Vi/Vc, relays nociceptive information to RVM. Lastly, RVM recordings have relied on single-electrode recording techniques that result in low data yield, biased search approaches, and the inability to capture RVM population activity. The final goal of this dissertation was to establish the high-density silicon probe technology in the RVM for future interrogation of RVM population dynamics.

The experiments in this dissertation demonstrate that RVM neurons in female animals respond to systemic morphine administration in the same direction as in male animals at doses that produce analgesia. This indicates that RVM neurons can be identified similarly in males and females, and that under normal conditions, opioid-manipulated output of the RVM functions

similarly between the sexes. Secondly, Vi/Vc was demonstrated to be a major relay of direct ascending nociceptive input to RVM ON- and OFF-cells. Optogenetic experiments revealed that Vi/Vc can access RVM directly, likely through ventral Vi/Vc neurons, and indirectly through PB, a major relay of ascending nociceptive information previously shown to indirectly relay dorsal horn nociceptive information to RVM. Dorsal Vi/Vc neurons were unable to access RVM directly, but cell-body stimulation experiments revealed this population could still influence RVM indirectly, again likely through PB. Tract tracing experiments strongly suggest that the OFF-cell pause is mediated by direct ascending GABAergic projections from ventral Vi/Vc. These findings demonstrate a functional link between an ascending nociceptive transmission relay (Vi/Vc) and the primary output node (RVM) of a descending pain-modulating circuit. Lastly, high-density silicon probe technology was successfully used to record from RVM functional cell classes. Multiple spike-sorters were compared and required varying degrees of curation efforts. However, while all sorters can be used successfully in RVM, curation efforts are still necessary to reduce the number of false positive units.

5.3. RVM NEURONS IN FEMALE ANIMALS RESPOND TO MORPHINE

Sexual dimorphisms in pain circuitry and opioid metabolism have been reported in both humans and rats. In Chapter 2, I demonstrated that when morphine was given systemically in female rats at a dose within the range reported to produce analgesia in male rats, OFF-cells shifted to an active state, with a reduction in the OFF-cell pause, while ON-cells shifted to an inactive state, with a reduction in the evoked response. This indicates that under normal conditions, the basal functioning of RVM in both males and females is comparable, with no differences in the response direction to systemic morphine administration in the two physiologically defined cell classes. Furthermore, this indicates that RVM neurons can be classified similarly in both males and females, and supports future brainstem pain-modulating studies using both male and female animals.

While the functional output of RVM after morphine was comparable, it is plausible that under chronic pain conditions, morphine administration would reveal sex differences. Changes to the modulating circuit would then influence morphine output and potentially reveal sex differences. Future studies should investigate the effects of morphine on RVM ON- and OFF-cell activity in persistent inflammatory states in both males and females.

5.4. VI/Vc INPUT TO RVM

5.4.1 Direct Vi/Vc input to RVM (Chapter 3)

RVM neurons are identified and defined by their nocifensive reflex-related change in activity. ON-cells are activated, exhibiting a “burst” in activity, while OFF-cells exhibit a “pause” in ongoing firing. RVM neurons are part of a reciprocal circuit, to allow ongoing and new nociceptive information to travel into the pain-transmission and pain-modulating system. Therefore, nociceptive inputs to RVM exert a major influence on the activity of ON- and OFF-cells, in turn changing how the pain-modulating circuit responds to new incoming pain. However, sensory inputs to RVM are only now being defined. Previously, the lab revealed that the parabrachial complex can indirectly relay nociceptive information from the spinal dorsal horn to RVM through its direct projections to RVM [247, 248]. However, direct inputs from the spinal and trigeminal dorsal horn have only been anatomically confirmed, and the functional significance of these direct inputs on RVM cell activity have not been investigated. In this dissertation, I investigated the trigeminal transition zone, Vi/Vc, and showed it to be a major relay of direct nociceptive input to RVM pain-modulating neurons, with a parallel indirect route through PB.

In Chapter 3, I demonstrated that Vi/Vc is a primary relay of direct nociceptive information to RVM ON- and OFF-cells under basal conditions. Studies using immunohistochemistry and retrograde tracing indicate Vi/Vc contains nociceptive neurons in the ventral region that respond to inflammation of the face, and that these neurons send direct projections to RVM. However, given that RVM contains multiple cell classes, involved in more

than just pain-modulation (i.e. NEUTRAL-cells, respiration, heart-rate, etc.), it was unknown what functional role this input had on RVM neuron activity. Using optogenetic methods, I demonstrated that the direct projection from ventral Vi/Vc neurons can influence ON- and OFF-cells. ON-cells significantly increased in firing or were activated, while OFF-cells significantly decreased in firing or were inhibited in both male and female animals. NEUTRAL-cells, which do not have any known role in pain-modulation, remained unchanged. This indicated the input from ventral Vi/Vc specifically transmits nociceptive information to RVM, since only the activity of pain-modulating cells in RVM were impacted.

These studies also confirmed the previous anatomical tracing experiments. Few neurons were found in dorsal Vi/Vc that projected to RVM directly and were activated by inflammation of the face. Similarly, in animals with ChR2 expression restricted to dorsal Vi/Vc, activation of terminals in these animals did not significantly change RVM pain-modulating activity, while activation of dorsal Vi/Vc cell bodies did. This indicates Vi/Vc nociceptive projections to RVM are spatially organized, and that multiple output pathways from Vi/Vc exist to reach RVM.

ArchT-induced inhibition of terminals from ventral Vi/Vc did not change the ongoing firing of ON- and OFF-cells, indicating Vi/Vc does not contribute to the ongoing “tone” of RVM ON- and OFF-cell pain modulating output. However, inhibition of Vi/Vc terminals in RVM reduced the nociceptive responses of RVM pain-modulating neurons: the OFF-cell “pause” and ON-cell “burst” was attenuated. This response was moderately reduced, since other pathways, likely PB which was previously demonstrated to relay nociceptive information to RVM, are still active during optogenetic inhibition of the direct Vi/Vc terminals in RVM. These data indicate that the Vi/Vc pathway is activated during acute nociceptive stimulation of the face, and only relays nociceptive information when activated. Given that the projection from Vi/Vc to RVM is sparse, this indicates that the density of the connection is not a measurement of its functional importance and highlights the need to further investigate the functional contribution of these projections.

5.4.2. Indirect Vi/Vc input to RVM (Chapter 3)

Stimulation of dorsal Vi/Vc neurons influenced RVM cell activity, while stimulation of direct terminals arising from these neurons did not. This pointed to a potential indirect relay of nociceptive information to RVM. Previous tract tracing studies have revealed potential nociceptive inputs from Vi/Vc neurons to PB, and previous studies from the lab demonstrated a direct connection between PB and RVM. Therefore, I hypothesized that Vi/Vc could also access RVM indirectly through PB.

In Chapter 3, it was demonstrated that Vi/Vc can access RVM indirectly via a pathway through PB. First, PB neurons were shown to respond to stimulation of Vi/Vc cell bodies. ON- and OFF-like behaving cells were previously reported to respond to noxious stimulation of the face. These neurons were identified, and Vi/Vc cell body stimulation resulted in an increase or decrease in the firing rate of PB neurons. Importantly, PB neuron activity remained unchanged in response to stimulation of Vi/Vc terminals in RVM, indicating Vi/Vc cell bodies were not recruited via antidromic activation. Stimulation of Vi/Vc terminals in PB while recording from identified RVM neurons caused a significant increase in ON-cell firing and significant decrease in OFF-cell firing, mimicking the direct circuit and RVM responses to noxious stimulation of the face.

In previous studies, activation of PB terminals in RVM resulted in an increase in both ON- and OFF-cell firing [247], rather than an increase ON-cell firing and decrease in OFF-cell firing. However, activation of PB terminals in RVM did not necessarily specifically engage nociceptive circuitry, recruiting all PB input to RVM, while manipulation of the Vi/Vc input in these experiments specifically recruited nociceptive transmission pathways. Additionally, PB was shown to release both GABA and glutamate in RVM, and inhibition of PB terminals in RVM interfered with the GABA-mediated OFF-cell pause [247]. Therefore, the present findings are not inconsistent since the previous experiment recruited all PB inputs to RVM, while the current experiments specifically recruited nociceptive circuitry in PB.

5.4.3. Differences in the direct and indirect circuits

The existence of two discrete nociceptive transmission pathways from Vi/Vc indicates how the body is critically set up so that pain cannot be ignored. The two pathways may explain why pain in the trigeminal distribution is often more debilitating both emotionally and physically than body pain. In Chapter 3, it was found that activation of Vi/Vc terminals in PB and activation of Vi/Vc cell bodies produced prolonged RVM responses compared with those observed with activation of Vi/Vc terminals in RVM. More PB neurons respond to stimuli applied to the face than the body [147], and PB links RVM to the affective dimension of pain. It is possible that activation of PB neurons by Vi/Vc terminal stimulation recruited other inputs to RVM, such as the amygdala or the PAG. Activation of the direct pathway may permit the immediate nocifensive response, as the output shifts to an ON-cell dominated pro-nociceptive state only if continuing sensory input is coming into the system.

Activation of Vi/Vc cell bodies also likely engaged multiple top-down brain regions that modulate RVM responses, contributing to the prolonged response. Additionally, it is likely that a greater population of cells within RVM were activated, and since RVM pain-modulating cells synchronize with each other, this could have contributed to the prolonged activity. It is also likely that the difference in response dynamic reflects different functional roles of the pain-transmission pathways. However, they are not mutually exclusive and could be cooperating to determine information about pain, such as intensity of the stimulation. Furthermore, RVM projections back down to Vi/Vc further complicates the relationship. The studies in Chapter 3 highlight the intricate and complex relationship between pain-transmission and pain-modulating pathways.

5.4.4. Contribution to the OFF-cell pause

The OFF-cell pause is known to be mediated by GABA and not through local RVM interactions. Ionophoretically applied GABAA receptor antagonist bicuculline methiodide during *in vivo* single-unit recordings blocks the OFF-cell pause, with no consistent effect on the firing of

ON- and NEUTRAL-cells [313]. Manipulations that affect the ON-cell firing rate, such as microinjection of morphine in RVM which directly acts on the μ -opioid receptor expressing ON-cells, does not impact the firing rate or pause of OFF-cells [265]. Similarly, excitatory amino acid neurotransmission is critical for producing the ON-cell burst, and broad-spectrum antagonism of excitatory amino acid receptors with kynurenate decreases ON-cell firing and suppresses the ON-cell burst, while OFF-cells continue to exhibit their reflex-related pause [217]. Lastly, paired recordings of ON- and OFF-cells demonstrate that the ON-cell burst regularly follows the OFF-cell pause, supporting the evidence that the ON-cell does not function as inhibitory interneurons within RVM controlling OFF-cell activity [148].

In Chapter 3, I provided tract tracing evidence that ventral Vi/Vc neurons that project to RVM directly are GAD65+. These cells may be contributing to the OFF-cell pause and are directly relaying this information to OFF-cells. However, *in vivo* optogenetic methods cannot conclude whether the suppression of the OFF-cell is due to local or direct action. Given the previous evidence collected by the lab, however, it is likely the functional role of GAD65+ neurons is to control the OFF-cell pause in response to acute noxious stimulation. GAD65+ Vi/Vc neurons also projected to PB. However, the current studies cannot make conclusions about the functional role of these neurons, as the direction of RVM cell responses remained the same regardless of terminal stimulation location. For example, it is possible that GAD65+ projecting neurons are inhibiting GABAergic projections from PB to RVM given that PB neurons were inhibited by Vi/Vc stimulation. This would then result in an increase in ON-cell firing. It is also possible these neurons do not play a nociceptive role in the indirect circuit, and PB interprets excitatory information before deciding to employ inhibitory or facilitatory output to RVM neurons. Future studies using GAD-Cre rats or other molecular and genetic tools should investigate the contribution of these neurons in the separate pathways.

5.5. HIGH-DENSITY SILICON PROBE RECORDINGS

In Chapter 4, I established the use of high-density silicon probe technology in RVM. Traditional RVM recordings have relied on single- or dual-electrode recordings to characterize RVM functional cell classes. While this has led to a thorough definition of these cell classes, this method yields 1-3 neurons at a time, and the animal can be stimulated at opportune times to evoke the ON-cell burst or OFF-cell pause. Additionally, questions concerning population level activity and interaction cannot be answered using a single-electrode. Therefore, the use of high-density silicon probe could overcome these challenges, greatly increasing the number of cells recorded from in one session and eliminating the biased search approach.

The primary goal of Chapter 4 was to identify RVM neurons using this new technology and identify appropriate spike sorters, since high-channel count recordings cannot be sorted in the same way as the traditional single-channel RVM recording. Using a Python package that allowed me to compare multiple sorter outcomes in the same recording, I found that Kilosort3, Mountainsort5, SpyKING CIRCUS, Tridesclous, and IronClust all identified unique units not shared by any other sorter output, consistent with previous results in cortex. While SpyKING CIRCUS identified the highest number of units, many of these were shown to be false positives after curation. Tridesclous resulted in the least number of units, but most of these units were found to be real. Kilosort3, Mountainsort5, and IronClust all found a similar number of units, but Mountainsort5 was found to have the highest number of false positive units between these sorters. Importantly, all sorters were able to identify RVM functional cell classes and could reasonably be used for RVM high-density recordings. Each sorter had their advantages and disadvantages, with some identifying more units, but then requiring more curation. It was found that curation is still a crucial step in sorting and should be used in future high-density recordings.

5.6. TECHNICAL CONSIDERATIONS

5.6.1. Anesthesia

All experiments were performed in lightly anesthetized animals. This allows us to precisely study the physiology of an isolated neuron within an intact circuit, while measuring the behavioral output. The lightly anesthetized protocol and model has been well established in descending pain-modulating studies, using a spinal reflex to noxious stimuli as the behavioral outcome. RVM neurons exhibit similar physiological characteristics under various anesthetics and in awake animals [65, 294, 314-319]. In these studies, stimulus intensities comparable to those used in awake animals were used. While the magnitude of the RVM response may be dampened in a lightly anesthetized animal, the relationship between RVM descending modulation and nociceptive transmission in awake animals is preserved in lightly anesthetized animals [71, 72, 78, 109, 320-322].

Female rats were not previously used in the electrophysiological studies that established the role of RVM in pain-modulation. Therefore, the anesthetic plane that was comparable between male and female rats had to be established. Male rats have more visceral fat than females, which can impact anesthetic metabolism [323, 324]. Therefore, we found that female rats in these studies had to run at a lower dose rate than males to achieve similar anesthetic planes. We found that the reflex-related response to nociceptive stimulation under acute conditions were similar between the sexes, indicating we achieved a comparable anesthetic plane. However, we did observe a very small number of cells that responded differently to morphine in female animals. This could have been an effect of morphine-brevital interaction, or a true difference between male and female animals. Due to the dosing regimen differing as well, this cannot be concluded at this time and future studies should continue to use female animals to establish if there is a true sex difference.

5.6.2. *Optogenetic methods*

Channel expression and distance of light travel can affect neuronal responses, causing over- or under-stimulation of terminals and cell bodies [325, 326]. Therefore, light stimulation protocols were optimized to ensure the reproducibility of the light response by avoiding terminal fatigue from overstimulation. Animals where no terminals were found in RVM or PB were not included in analysis. Cell bodies in Vi/Vc expressing ArchT or ChR2 were recorded from to ensure channel expression and reliability of the evoked light response. There was no difference in the response magnitude due to the diameter of the fiber used or location of the fiber in Vi/Vc, supporting the light stimulation protocol employed in these studies.

One concern with optogenetics is antidromic activation of cell-bodies in Vi/Vc, creating inaccurate conclusions on the contribution of the direct circuit on RVM cell activity. Given the complicated circuit between RVM, PB, and Vi/Vc and potential activation of fibers of passage through RVM, several cell-body recording control experiments were performed. I recorded from PB neurons while activating Vi/Vc terminals in RVM or activating Vi/Vc cell-bodies. PB neuron activity was unaffected by Vi/Vc terminal stimulation in RVM, even though these PB neurons responded to Vi/Vc cell body stimulation. This indicates that Vi/Vc cell bodies are not antidromically activated, since Vi/Vc terminal stimulation did not indirectly recruit Vi/Vc cell bodies, which would have recruited PB neurons. Additionally, stimulation of terminals in RVM that originated from dorsal Vi/Vc did not influence RVM cell activity. Activation of dorsal Vi/Vc cell bodies still influenced RVM cell activity, indicating light in RVM did not indirectly recruit dorsal Vi/Vc cell bodies via antidromic activation. Lastly, the response profile of RVM neurons to direct and indirect pathway recruitment differed significantly, indicating the two potential pathways did not influence each other and confuse the conclusions.

Finally, RVM neuron responses to terminal stimulation represent input to RVM in general. The effects reported in this dissertation could reflect local RVM interactions, since we

are unable to directly conclude whether an individual RVM neuron receives direct input. This can only be addressed in slice recordings.

5.6.3. Withdrawal in a stereotaxic frame

The RVM functional cell classification scheme is dependent on the withdrawal response as recorded by EMG signal. In the whisker pad stimulation experiments, EMG could not be recorded, as animals that are head-fixed cannot withdraw from stimulation on the face and head. In these experiments, cells were characterized and classified based on their response to noxious stimulation of the foot before stimulation of the face occurred. Previous studies have been successful using the jaw motor reflex and support the hypothesis that RVM neurons respond in the same direction regardless of the somatic site of stimulation [32]. Future studies could investigate how cell activity changes depending on stimulation site, however, finding comparable stimuli to the foot and head is challenging. Therefore, it is necessary to classify RVM neurons either based on the response to stimulation of the foot or capturing withdrawal reflexes from the jaw.

5.6.4. Pause and burst activity in high-density silicon probe recordings

The defining characteristic of ON- and OFF-cells are the burst and pause, respectively. Single-unit recordings with spike-to-spike manual curation allows the experimenter to mark the exact beginning and ending of the burst and pause. However, given the high number of recording channels, it is infeasible and impossible to ask of the experimenter to hand sort units on a spike-to-spike basis in a high-density silicon probe recording. While spike-sorters are adapting and can capture changes in activity, single spikes that end the pause or burst may be impossible to identify and cannot be manually identified as they are during single-unit sorting. This may not necessarily be a limitation, but a consideration. While changes in the ON-cell burst and OFF-cell pause are functionally significant, it has not been demonstrated that a certain percent change of the burst or pause must be reached for behavioral significance. It may be suitable enough to capture the change without needed spike-to-spike level of accuracy.

5.7. FUTURE DIRECTIONS

5.7.1. Role of GAD65+ neurons in the direct and indirect pathway

Chapter 3 revealed Vi/Vc GAD65+ neurons project to both RVM and PB. Currently, inhibitory specific cell type promoters for the brainstem are lacking. The GAD65+ promoter used in the experiments described above could not be combined with ChR2 in the open reading frame into an AAV package due to the size of the promoter. Development of a shorter promoter sequence or use of GAD-Cre rats would allow one to optogenetically manipulate GAD65+ neurons and determine the contribution of this cell type specific projection on RVM cell activity. Likewise, given that the indirect pathway maintained the same effect as the direct pathway, use of the GAD65+ promoter would allow one to determine the functional contribution of this projection on PB neuron activity.

5.7.2. Synaptic characteristics of the Vi/Vc-RVM circuit

The *in vivo* electrophysiological experiments described in the above chapters cannot conclude whether Vi/Vc neurons project directly to individual RVM neurons, only to RVM locally. *In vitro* patch recordings using Dermorphin-Alexa594 to label μ -opioid expressing ON-cells combined with optogenetic stimulation would allow one to determine if Vi/Vc inputs synapse directly onto individual RVM ON- or OFF-cells, or if local circuitry within the RVM is mediating the Vi/Vc-dependent responses. Combined with viral tools that selectively target GAD65+ neurons, optogenetic activation while recording from Dermorphin-Alexa594 negative cells could determine if these neurons directly contribute to the OFF-cell pause.

5.7.3. Identification of RVM cell types in slice

RVM neurons currently can only be identified by their physiological response to noxious stimuli. In slice recordings, it is assumed that the μ -opioid positive neurons are ON-cells, but currently no specific molecular marker for OFF- and NEUTRAL-cells exist. Given that ON- and OFF- cells consistently responded to Vi/Vc stimulation across all recordings, one could theoretically discern RVM cell types *in vitro* using Dermorphin-Alexa594 and optogenetic

stimulation of Vi/Vc terminals. One could assume ON-cells were labeled and infer the OFF- and NEUTRAL-cells were the unlabeled cells. It would then be useful to perform single-cell RNA sequencing on these patched neurons to determine if molecular markers exist. It is likely that discrete molecular cell types will not be found, and rather represent a subset of ON- or OFF-CELLS. Additionally, not every cell in RVM will receive direct input from the trigeminal dorsal horn, so one would only be able to make conclusions about cells that receive trigeminal nociceptive information. Nonetheless, future treatments will likely target molecular cell types, and the ability to manipulate ON- and OFF-cell output would revolutionize pain therapies and brainstem pain-modulating research.

5.7.4. The role of Vi/Vc neurons in chronic inflammation

The transition from acute to chronic pain induces physiological changes in the RVM. It is unknown how the function of the direct projection to RVM from Vi/Vc evolves over the course of persistent inflammation. Vi/Vc neurons that project to RVM are activated by chronic inflammation of the masseter muscle, and lesioning RVM or Vi/Vc attenuates hyperalgesia early after CFA exposure. Given that chronic pain reflects a dysfunction of the descending modulatory output, long after peripheral injuries have healed and ascending nociceptive information has halted, it is unknown if the direct Vi/Vc pathway is still employed during chronic pain. It would be useful to test the effects of blocking Vi/Vc input to RVM both early and late in the development of inflammation to determine when the direct Vi/Vc input to RVM is necessary for the formation of chronic pain. Additionally, if one investigated the indirect pathway through PB, which is known to play a role in sensitization of RVM neurons in response to persistent inflammation, one may be able to determine which pathway contributes more to the development of chronic pain. Given that chronic pain represents dysfunction in top down input, I hypothesize that the direct pathway may play a very small role in the transition from acute to chronic pain, and rather the pathway through PB from Vi/Vc changes under persistent inflammatory conditions.

5.8. CONCLUSIONS

In this dissertation, I demonstrated that the opioid-facilitated output of the descending pain-modulation system has similar responses in male and female animals under basal conditions. Additionally, I established a functional link between a pain-transmission system (Vi/Vc) and a pain-modulating system (RVM). Vi/Vc can influence RVM activity through direct and indirect pathways, and the two circuits may play different functional roles in the response to noxious input. Furthermore, evidence for a direct ascending GABAergic input from Vi/Vc likely contributes to the OFF-cell pause before nocifensive withdrawal. Lastly, I established the use of high-density silicon probe recording technology for future RVM population studies. Identifying potential noxious transmission pathways may identify potential targets to treat pain, and continuing to use both male and females in research will lead to improved treatments and understanding of pain conditions.

REFERENCES

1. Berta, A., E.G. Ekdale, and T.W. Cranford, *Review of the cetacean nose: form, function, and evolution*. *Anat Rec (Hoboken)*, 2014. **297**(11): p. 2205-15.
2. Niemiller, M.L., D.M. Higgs, and D. Soares, *Evidence for hearing loss in amblyopsid cavefishes*. *Biol Lett*, 2013. **9**(3): p. 20130104.
3. Policarpo, M., J. Fumey, P. Lafargeas, D. Naquin, C. Thermes, M. Naville, C. Dechaud, J.N. Volff, C. Cabau, C. Klopp, P.R. Moller, L. Bernatchez, E. Garcia-Machado, S. Retaux, and D. Casane, *Contrasting Gene Decay in Subterranean Vertebrates: Insights from Cavefishes and Fossorial Mammals*. *Mol Biol Evol*, 2021. **38**(2): p. 589-605.
4. Smith, E.S. and G.R. Lewin, *Nociceptors: a phylogenetic view*. *J Comp Physiol A Neuroethol Sens Neural Behav Physiol*, 2009. **195**(12): p. 1089-106.
5. Dib-Hajj, S.D. and S.G. Waxman, *Sodium Channels in Human Pain Disorders: Genetics and Pharmacogenomics*. *Annu Rev Neurosci*, 2019. **42**: p. 87-106.
6. Heinricher, M.M., I. Tavares, J.L. Leith, and B.M. Lumb, *Descending control of nociception: specificity, recruitment and plasticity*. *Brain Res Rev*, 2009. **60**: p. 214-225.
7. Heinricher, M.M. and H.L. Fields, *Central nervous system mechanisms of pain modulation.*, in *Wall and Melzack's Textbook of Pain, 6th ed.*, S. McMahon, et al., Editors. 2013, Elsevier: London. p. 129-142.
8. Heinricher, M.M., *Pain Modulation and the Transition from Acute to Chronic Pain*. *Adv Exp Med Biol*, 2016. **904**: p. 105-15.
9. Fields, H., *State-dependent opioid control of pain*. *Nat Rev Neurosci*, 2004. **5**(7): p. 565-75.
10. Xue, Y., S. Mo, Y. Li, Y. Cao, X. Xu, and Q. Xie, *Dissecting neural circuits from rostral ventromedial medulla to spinal trigeminal nucleus bidirectionally modulating craniofacial mechanical sensitivity*. *Prog Neurobiol*, 2023. **232**: p. 102561.

11. Bushnell, M.C., M. Ceko, and L.A. Low, *Cognitive and emotional control of pain and its disruption in chronic pain*. Nat Rev Neurosci, 2013. **14**(7): p. 502-11.
12. Fields, H.L. and M.M. Heinricher, *Anatomy and physiology of a nociceptive modulatory system*. Philos Trans of the R Soc Lond B Biol Sci, 1985. **308**: p. 361-374.
13. Porreca, F., M.H. Ossipov, and G.F. Gebhart, *Chronic pain and medullary descending facilitation*. Tr Neurosci, 2002. **25**(6): p. 319-25.
14. Morrison, S.F. and K. Nakamura, *Central Mechanisms for Thermoregulation*. Annu Rev Physiol, 2019. **81**: p. 285-308.
15. Blessing, W.W., *The lower brainstem and bodily homeostasis*. 1997, New York: Oxford University Press. 575.
16. Mason, P., *Deconstructing endogenous pain modulations*. J Neurophysiol, 2005. **94**(3): p. 1659-63.
17. Rathner, J.A., N.C. Owens, and R.M. McAllen, *Cold-activated raphe-spinal neurons in rats*. J Physiol (Lond), 2001. **535**(3): p. 841-854.
18. Martenson, M.E., J.S. Cetas, and M.M. Heinricher, *A possible neural basis for stress-induced hyperalgesia*. Pain, 2009. **142**(3): p. 236-44.
19. Vianna, D.M., C. Allen, and P. Carrive, *Cardiovascular and behavioral responses to conditioned fear after medullary raphe neuronal blockade*. Neuroscience, 2008. **153**(4): p. 1344-53.
20. Basbaum, A.I., C.H. Clanton, and H.L. Fields, *Three bulbospinal pathways from the rostral medulla of the cat: an autoradiographic study of pain modulating systems*. J Comp Neurol, 1978. **178**(2): p. 209-24.
21. Aicher, S.A., S.M. Hermes, K.L. Whittier, and D.M. Hegarty, *Descending projections from the rostral ventromedial medulla (RVM) to trigeminal and spinal dorsal horns are morphologically and neurochemically distinct*. J Chem Neuroanat, 2012. **43**(2): p. 103-11.

22. Sugiyo, S., M. Takemura, R. Dubner, and K. Ren, *Trigeminal transition zone/rostral ventromedial medulla connections and facilitation of orofacial hyperalgesia after masseter inflammation in rats*. J Comp Neurol, 2005. **493**(4): p. 510-23.
23. Ruda, M.A., B. Allen, and S. Gobel, *Ultrastructural analysis of medial brain stem afferents to the superficial dorsal horn*. Brain Res, 1981. **205**(1): p. 175-80.
24. Fields, H.L., A. Malick, and R. Burstein, *Dorsal horn projection targets of ON and OFF cells in the rostral ventromedial medulla*. J Neurophysiol, 1995. **74**(4): p. 1742-59.
25. Lovick, T.A. and J.H. Wolstencroft, *Projections from brain stem nuclei to the spinal trigeminal nucleus in the cat*. Neuroscience, 1983. **9**(2): p. 411-20.
26. Huisman, A.M., H.G. Kuypers, and C.A. Verburgh, *Quantitative differences in collateralization of the descending spinal pathways from red nucleus and other brain stem cell groups in rat as demonstrated with the multiple fluorescent retrograde tracer technique*. Brain Res, 1981. **209**(2): p. 271-86.
27. Fields, H.L., A.I. Basbaum, C.H. Clanton, and S.D. Anderson, *Nucleus raphe magnus inhibition of spinal cord dorsal horn neurons*. Brain Res, 1977. **126**(3): p. 441-53.
28. Heinricher, M.M., I. Tavares, J.L. Leith, and B.M. Lumb, *Descending control of nociception: Specificity, recruitment and plasticity*. Brain Res Rev, 2009. **60**(1): p. 214-25.
29. Fields, H.L., J. Bry, I. Hentall, and G. Zorman, *The activity of neurons in the rostral medulla of the rat during withdrawal from noxious heat*. J Neurosci, 1983. **3**: p. 2545-2552.
30. Heinricher, M.M. and M.J. Neubert, *Neural basis for the hyperalgesic action of cholecystinin in the rostral ventromedial medulla*. J Neurophysiol, 2004. **92**(4): p. 1982-9.

31. Carlson, J.D., J.J. Maire, M.E. Martenson, and M.M. Heinricher, *Sensitization of pain-modulating neurons in the rostral ventromedial medulla after peripheral nerve injury*. J Neurosci, 2007. **27**(48): p. 13222-31.
32. Tang, J.S., C.Y. Chiang, J.O. Dostrovsky, D. Yao, and B.J. Sessle, *Responses of neurons in rostral ventromedial medulla to nociceptive stimulation of craniofacial region and tail in rats*. Brain Res, 2021. **1767**: p. 147539.
33. Vanegas, H., N.M. Barbaro, and H.L. Fields, *Tail-flick related activity in medullospinal neurons*. Brain Research, 1984. **321**: p. 135-41.
34. Fields, H.L., A. Malick, and R. Burstein, *Dorsal horn projection targets of ON and OFF cells in the rostral ventromedial medulla*. J Neurophysiol, 1995. **74**: p. 1742-59.
35. Devonshire, I.M., C.H. Kwok, A. Suvik, A.R. Haywood, A.H. Cooper, and G.J. Hathway, *A quantification of the relationship between neuronal responses in the rat rostral ventromedial medulla and noxious stimulation-evoked withdrawal reflexes*. Eur J Neurosci, 2015. **42**(1): p. 1726-37.
36. Jinks, S.L., E.E. Carstens, and J.F. Antognini, *Glutamate receptor blockade in the rostral ventromedial medulla reduces the force of multisegmental motor responses to supramaximal noxious stimuli*. Neurosci Lett, 2007. **426**(3): p. 175-80.
37. Heinricher, M.M. and H.J. Kaplan, *GABA-mediated inhibition in rostral ventromedial medulla: role in nociceptive modulation in the lightly anesthetized rat*. Pain, 1991. **47**(1): p. 105-113.
38. Proudfit, H.K., *Reversible inactivation of raphe magnus neurons: effects on nociceptive threshold and morphine-induced analgesia*. Brain Res, 1980. **201**(2): p. 459-64.
39. Young, E.G., L.R. Watkins, and D.J. Mayer, *Comparison of the effects of ventral medullary lesions on systemic and microinjection morphine analgesia*. Brain Res, 1984. **290**(1): p. 119-29.

40. Fields, H.L. and M.M. Heinricher, *Anatomy and physiology of a nociceptive modulatory system*. Philos Trans R Soc Lond B Biol Sci, 1985. **308**(1136): p. 361-74.
41. Heinricher, M.M., N.M. Barbaro, and H.L. Fields, *Putative nociceptive modulating neurons in the rostral ventromedial medulla of the rat: firing of on- and off-cells is related to nociceptive responsiveness*. Somatosens Mot Res, 1989. **6**: p. 427-39.
42. De Felice, M., N. Eyde, D. Dodick, G.O. Dussor, M.H. Ossipov, H.L. Fields, and F. Porreca, *Capturing the aversive state of cephalic pain preclinically*. Ann Neurol, 2013. **74**(2): p. 257-65.
43. De Felice, M., R. Sanoja, R. Wang, L. Vera-Portocarrero, J. Oyarzo, T. King, M.H. Ossipov, T.W. Vanderah, J. Lai, G.O. Dussor, H.L. Fields, T.J. Price, and F. Porreca, *Engagement of descending inhibition from the rostral ventromedial medulla protects against chronic neuropathic pain*. Pain, 2011. **152**(12): p. 2701-2709.
44. King, T., L. Vera-Portocarrero, T. Gutierrez, T.W. Vanderah, G. Dussor, J. Lai, H.L. Fields, and F. Porreca, *Unmasking the tonic-aversive state in neuropathic pain*. Nat Neurosci, 2009. **12**(11): p. 1364-6.
45. Chen, Q. and M.M. Heinricher, *Descending Control Mechanisms and Chronic Pain*. Curr Rheumatol Rep, 2019. **21**(5): p. 13.
46. Hentall, I.D., G. Zorman, S. Kansky, and H.L. Fields, *Relations among threshold, spike height, electrode distance, and conduction velocity in electrical stimulation of certain medullospinal neurons*. J Neurophysiol, 1984. **51**: p. 968-77.
47. Hentall, I.D., G. Zorman, S. Kansky, and H.L. Fields, *An estimate of minimum number of brain stem neurons required for inhibition of a flexion reflex*. J Neurophysiol, 1984. **51**: p. 978-85.
48. Neubert, M.J., W. Kincaid, and M.M. Heinricher, *Nociceptive facilitating neurons in the rostral ventromedial medulla*. Pain, 2004. **110**: p. 158-165.

49. Meng, I.D., D. Dodick, M.H. Ossipov, and F. Porreca, *Pathophysiology of medication overuse headache: insights and hypotheses from preclinical studies*. *Cephalalgia*, 2011. **31**(7): p. 851-60.
50. Ossipov, M.H., J. Lai, T. King, T.W. Vanderah, T.P. Malan, Jr., V.J. Hruby, and F. Porreca, *Antinociceptive and nociceptive actions of opioids*. *J Neurobiol*, 2004. **61**(1): p. 126-48.
51. Heinricher, M.M., M.M. Morgan, and H.L. Fields, *Direct and indirect actions of morphine on medullary neurons that modulate nociception*. *Neuroscience*, 1992. **48**: p. 533-43.
52. Heinricher, M.M., C.M. Haws, and H.L. Fields, *Opposing actions of norepinephrine and clonidine on single pain-modulating neurons in rostral ventromedial medulla*, in *Pain Res Clin Mgt*, R. Dubner, G.F. Gebhart, and M.R. Bond, Editors. 1988, Elsevier: Amsterdam. p. 590-594.
53. Meng, I.D., B.H. Manning, W.J. Martin, and H.L. Fields, *An analgesia circuit activated by cannabinoids*. *Nature*, 1998. **395**(6700): p. 381-3.
54. Meng, I.D. and J.P. Johansen, *Antinociception and modulation of rostral ventromedial medulla neuronal activity by local microinfusion of a cannabinoid receptor agonist*. *Neuroscience*, 2004. **124**(3): p. 685-93.
55. Selden, N.R., J.D. Carlson, J. Cetas, L.N. Close, and M.M. Heinricher, *Purinergic actions on neurons that modulate nociception in the rostral ventromedial medulla*. *Neuroscience*, 2007. **146**(4): p. 1808-16.
56. Harasawa, I., H.L. Fields, and I.D. Meng, *Delta opioid receptor mediated actions in the rostral ventromedial medulla on tail flick latency and nociceptive modulatory neurons*. *Pain*, 2000. **85**: p. 255-262.
57. Meng, I.D., J.P. Johansen, I. Harasawa, and H.L. Fields, *Kappa opioids inhibit physiologically identified medullary pain modulating neurons and reduce morphine antinociception*. *J Neurophysiol*, 2005. **93**(3): p. 1138-44.

58. Marabese, I., F. Rossi, E. Palazzo, V. de Novellis, K. Starowicz, L. Cristino, D. Vita, L. Gatta, F. Guida, V. Di Marzo, F. Rossi, and S. Maione, *Periaqueductal gray metabotropic glutamate receptor subtype 7 and 8 mediate opposite effects on amino acid release, rostral ventromedial medulla cell activities, and thermal nociception*. J Neurophysiol, 2007. **98**(1): p. 43-53.
59. de Novellis, V., L. Mariani, E. Palazzo, D. Vita, I. Marabese, M. Scafuro, F. Rossi, and S. Maione, *Periaqueductal grey CB1 cannabinoid and metabotropic glutamate subtype 5 receptors modulate changes in rostral ventromedial medulla neuronal activities induced by subcutaneous formalin in the rat*. Neuroscience, 2005. **134**(1): p. 269.
60. de Novellis, V., L. Negri, R. Lattanzi, F. Rossi, E. Palazzo, I. Marabese, E. Giannini, D. Vita, P. Melchiorri, and S. Maione, *The prokineticin receptor agonist Bv8 increases GABA release in the periaqueductal grey and modifies RVM cell activities and thermoceptive reflexes in the rat*. Eur J Neurosci, 2007. **26**(11): p. 3068-78.
61. Hryciw, G., C.C. De Preter, J. Wong, and M.M. Heinricher, *Physiological properties of pain-modulating neurons in rostral ventromedial medulla in female rats, and responses to opioid administration*. Neurobiol Pain, 2021. **10**: p. 100075.
62. Heinricher, M.M., M.M. Morgan, V. Tortorici, and H.L. Fields, *Disinhibition of off-cells and antinociception produced by an opioid action within the rostral ventromedial medulla*. Neuroscience, 1994. **63**: p. 279-288.
63. McGaraughty, S., S. Reinis, and J. Tsoukatos, *Two distinct unit activity responses to morphine in the rostral ventromedial medulla of awake rats*. Brain Research, 1993. **604**: p. 331-3.
64. Clarke, R.W., M.M. Morgan, and M.M. Heinricher, *Identification of nocifensor reflex-related neurons in the rostroventromedial medulla of decerebrated rats*. Brain Research, 1994. **636**: p. 169-74.

65. Foo, H. and P. Mason, *Movement-related discharge of ventromedial medullary neurons*. J Neurophysiol, 2005. **93**(2): p. 873-83.
66. Hellman, K.M., T.S. Brink, and P. Mason, *Activity of murine raphe magnus cells predicts tachypnea and on-going nociceptive responsiveness*. J Neurophysiol, 2007. **98**(6): p. 3121-3133.
67. Ellrich, J., C. Ulucan, and C. Schnell, *Are 'neutral cells' in the rostral ventro-medial medulla subtypes of on- and off-cells?* Neurosci Res, 2000. **38**(4): p. 419-423.
68. Ellrich, J., C. Ulucan, and C. Schnell, *Is the response pattern of on- and off-cells in the rostral ventromedial medulla to noxious stimulation independent of stimulation site?* Exp Brain Res, 2001. **136**(3): p. 394-9.
69. Hurley, R.W. and D.L. Hammond, *The analgesic effects of supraspinal m and d opioid receptor agonists are potentiated during persistent inflammation*. J Neurosci, 2000. **20**(3): p. 1249-59.
70. Smith, D.J., A.A. Hawranko, P.J. Monroe, D. Gully, M.O. Urban, C.R. Craig, J.P. Smith, and D.L. Smith, *Dose-dependent pain-facilitatory and -inhibitory actions of neurotensin are revealed by SR 48692, a nonpeptide neurotensin antagonist: influence on the antinociceptive effect of morphine*. J Pharmacol Exp Ther, 1997. **282**(2): p. 899-908.
71. Kovelowski, C.J., M.H. Ossipov, H. Sun, J. Lai, T.P. Malan, and F. Porreca, *Supraspinal cholecystokinin may drive tonic descending facilitation mechanisms to maintain neuropathic pain in the rat*. Pain, 2000. **87**(3): p. 265-273.
72. Edelmayer, R.M., T.W. Vanderah, L. Majuta, E.T. Zhang, B. Fioravanti, M. De Felice, J.G. Chichorro, M.H. Ossipov, T. King, J. Lai, S.H. Kori, A.C. Nelsen, K.E. Cannon, M.M. Heinricher, and F. Porreca, *Medullary pain facilitating neurons mediate allodynia in headache-related pain*. Ann Neurol, 2009. **65**(2): p. 184-93.

73. Porreca, F., S.E. Burgess, L.R. Gardell, T.W. Vanderah, T.P. Malan, Jr., M.H. Ossipov, D.A. Lappi, and J. Lai, *Inhibition of neuropathic pain by selective ablation of brainstem medullary cells expressing the m-opioid receptor*. J Neurosci, 2001. **21**(14): p. 5281-8.
74. Francois, A., S.A. Low, E.I. Sypek, A.J. Christensen, C. Sotoudeh, K.T. Beier, C. Ramakrishnan, K.D. Ritola, R. Sharif-Naeini, K. Deisseroth, S.L. Delp, R.C. Malenka, L. Luo, A.W. Hantman, and G. Scherrer, *A brainstem-spinal cord inhibitory circuit for mechanical pain modulation by GABA and enkephalins*. Neuron, 2017. **93**(4): p. 822-839.e6.
75. Zhang, Y., S. Zhao, E. Rodriguez, J. Takatoh, B.X. Han, X. Zhou, and F. Wang, *Identifying local and descending inputs for primary sensory neurons*. J Clin Invest, 2015. **125**(10): p. 3782-94.
76. Jiao, Y., P. Gao, L. Dong, X. Ding, Y. Meng, J. Qian, T. Gao, R. Wang, T. Jiang, Y. Zhang, D. Kong, Y. Wu, S. Chen, S. Xu, D. Tang, P. Luo, M. Wu, L. Meng, D. Wen, C. Wu, G. Zhang, X. Shi, W. Yu, and W. Rong, *Molecular identification of bulbospinal ON neurons by GPER, which drives pain and morphine tolerance*. J Clin Invest, 2023. **133**(1): p. e154588.
77. Kim, J.H., G. Gangadharan, J. Byun, E.J. Choi, C.J. Lee, and H.S. Shin, *Yin-and-yang bifurcation of opioidergic circuits for descending analgesia at the midbrain of the mouse*. Proc Natl Acad Sci USA, 2018. **115**(43): p. 11078-11083.
78. Nguyen, E., K.M. Smith, N. Cramer, R.A. Holland, I.H. Bleimeister, K. Flores-Felix, H. Silberberg, A. Keller, C.E. Le Pichon, and S.E. Ross, *Medullary kappa-opioid receptor neurons inhibit pain and itch through a descending circuit*. Brain, 2022. **145**(7): p. 2586-2601.
79. Nguyen, E., J.G. Grajales-Reyes, R.W. Gereau, and S.E. Ross, *Cell type-specific dissection of sensory pathways involved in descending modulation*. Trends Neurosci, 2023.

80. Oliva, V., R. Hartley-Davies, R. Moran, A.E. Pickering, and J.C. Brooks, *Simultaneous brain, brainstem, and spinal cord pharmacological-fMRI reveals involvement of an endogenous opioid network in attentional analgesia*. *eLife*, 2022. **11**.
81. Brooks, J.C., W.E. Davies, and A.E. Pickering, *Resolving the brainstem contributions to attentional analgesia*. *J Neurosci*, 2017. **37**(9): p. 2279-2291.
82. Mills, E.P., F. Di Pietro, Z. Alshelh, C.C. Peck, G.M. Murray, E.R. Vickers, and L.A. Henderson, *Brainstem Pain-Control Circuitry Connectivity in Chronic Neuropathic Pain*. *J Neurosci*, 2018. **38**(2): p. 465-473.
83. Mills, E.P., K.A. Keay, and L.A. Henderson, *Brainstem Pain-Modulation Circuitry and Its Plasticity in Neuropathic Pain: Insights From Human Brain Imaging Investigations*. *Front Pain Res*, 2021. **2**(34): p. 705345.
84. Khasabov, S.G., P. Malecha, J. Noack, J. Tabakov, K. Okamoto, D.A. Bereiter, and D.A. Simone, *Activation of rostral ventromedial medulla neurons by noxious stimulation of cutaneous and deep craniofacial tissues*. *J Neurophysiol*, 2015. **113**(1): p. 14-22.
85. Gao, K. and P. Mason, *Serotonergic raphe magnus cells that respond to noxious tail heat are not ON or OFF cells*. *J Neurophysiol*, 2000. **84**(4): p. 1719-25.
86. Gao, K., Y.H. Kim, and P. Mason, *Serotonergic pontomedullary neurons are not activated by antinociceptive stimulation in the periaqueductal gray*. *J Neurosci*, 1997. **17**: p. 3285-92.
87. Gao, K., D.O. Chen, J.R. Genzen, and P. Mason, *Activation of serotonergic neurons in the raphe magnus is not necessary for morphine analgesia*. *J Neurosci*, 1998. **18**(5): p. 1860-8.
88. Gau, R., C. Sevoz-Couche, M. Hamon, and J.F. Bernard, *Noxious stimulation excites serotonergic neurons: a comparison between the lateral paragigantocellular reticular and the raphe magnus nuclei*. *Pain*, 2012. **154**: p. 647-659.

89. LeBars, D., *Serotonin and pain*, in *Neuronal serotonin*, N.N. Osborne and M. Hamond, Editors. 1988, Wiley: New York. p. 171-226.
90. Cai, Y.Q., W. Wang, Y.Y. Hou, and Z.Z. Pan, *Optogenetic activation of brainstem serotonergic neurons induces persistent pain sensitization*. *Mol Pain*, 2014. **10**: p. 70.
91. Mo, S.Y., Y. Xue, Y. Li, Y.J. Zhang, X.X. Xu, K.Y. Fu, B.J. Sessle, Q.F. Xie, and Y. Cao, *Descending serotonergic modulation from rostral ventromedial medulla to spinal trigeminal nucleus is involved in experimental occlusal interference-induced chronic orofacial hyperalgesia*. *J Headache Pain*, 2023. **24**(1): p. 50.
92. Cooper, A.H., N.S. Hedden, P. Prason, Y. Qi, and B.K. Taylor, *Postsurgical Latent Pain Sensitization Is Driven by Descending Serotonergic Facilitation and Masked by μ -Opioid Receptor Constitutive Activity in the Rostral Ventromedial Medulla*. *J Neurosci*, 2022. **42**(30): p. 5870-5881.
93. Cramer, N., Y. Ji, M.A. Kane, N.R. Pilli, A. Castro, L. Posa, G. Van Patten, R. Masri, and A. Keller, *Elevated Serotonin in Mouse Spinal Dorsal Horn Is Pronociceptive*. *eNeuro*, 2023. **10**(12): p. ENEURO.0293-23.202.
94. Suzuki, R., L.J. Rygh, and A.H. Dickenson, *Bad news from the brain: descending 5-HT pathways that control spinal pain processing*. *Trends Pharmacol Sci*, 2004. **25**(12): p. 613-617.
95. Gautier, A., D. Geny, S. Bourgoin, J.F. Bernard, and M. Hamon, *Differential innervation of superficial versus deep laminae of the dorsal horn by bulbo-spinal serotonergic pathways in the rat*. *IBRO Rep*, 2017. **2**: p. 72-80.
96. Ganley, R.P., M.M. de Sousa, K. Werder, T. Öztürk, R. Mendes, M. Ranucci, H. Wildner, and H.U. Zeilhofer, *Targeted anatomical and functional identification of antinociceptive and pronociceptive serotonergic neurons that project to the spinal dorsal horn*. *Elife*, 2023. **12**.

97. Heinricher, M.M. and S. McGaraughty, *Brainstem pain modulating neurons and behavioral state*, in *State-Dependent Processing in Somatosensory Pathways*, P.J. Soja, Editor. 1999, CRC Press: San Diego. p. 487-503.
98. Winkler, C.W., S.M. Hermes, C.I. Chavkin, C.T. Drake, S.F. Morrison, and S.A. Aicher, *Kappa opioid receptor (KOR) and GAD67 immunoreactivity are found in OFF and NEUTRAL cells in the rostral ventromedial medulla*. *J Neurophysiol*, 2006. **96**(6): p. 3465-3473.
99. Bowker, R.M., K.N. Westlund, M.C. Sullivan, and J.D. Coulter, *Organization of descending serotonergic projections to the spinal cord*. *Prog Brain Res*, 1982. **57**: p. 239-65.
100. Bowker, R.M., K.N. Westlund, M.C. Sullivan, J.F. Wilber, and J.D. Coulter, *Descending serotonergic, peptidergic and cholinergic pathways from the raphe nuclei: a multiple transmitter complex*. *Brain Research*, 1983. **288**: p. 33-48.
101. Bowker, R.M., L.C. Abbott, and R.P. Dilts, *Peptidergic neurons in the nucleus raphe magnus and the nucleus gigantocellularis: their distributions, interrelationships, and projections to the spinal cord*. *Progress in Brain Research*, 1988. **77**: p. 95-127.
102. Rampon, C., P.H. Luppi, P. Fort, C. Peyron, and M. Jouvet, *Distribution of glycine-immunoreactive cell bodies and fibers in the rat brain*. *Neuroscience*, 1996. **75**(3): p. 737-55.
103. Hossaini, M., J.A.C. Goos, S.K. Kohli, and J.C. Holstege, *Distribution of Glycine/GABA Neurons in the Ventromedial Medulla with Descending Spinal Projections and Evidence for an Ascending Glycine/GABA Projection*. *PLoS ONE*, 2012. **7**(4): p. e35293.
104. Holmes, C.J., L.S. Mainville, and B.E. Jones, *Distribution of cholinergic, GABAergic and serotonergic neurons in the medial medullary reticular formation and their projections studied by cytotoxic lesions in the cat*. *Neuroscience*, 1994. **62**: p. 1155-78.

105. Heinricher, M.M. and S.L. Ingram, *The brainstem and nociceptive modulation*, in *The Science of Pain*, M.C. Bushnell and A.I. Basbaum, Editors. 2008, Academic Press: San Diego. p. 593-626.
106. Xu, J.J., P. Gao, Y. Wu, S.Q. Yin, L. Zhu, S.H. Xu, D. Tang, C.W. Cheung, Y.F. Jiao, W.F. Yu, Y.H. Li, and L.Q. Yang, *G protein-coupled estrogen receptor in the rostral ventromedial medulla contributes to the chronification of postoperative pain*. *CNS Neurosci Ther*, 2021. **27**(11): p. 1313-1326.
107. Heinricher, M.M. and V. Tortorici, *Interference with GABA transmission in the rostral ventromedial medulla: disinhibition of off-cells as a central mechanism in nociceptive modulation*. *Neuroscience*, 1994. **63**: p. 533-46.
108. Jiao, Y., P. Gao, L. Dong, X. Ding, Y. Meng, J. Qian, T. Gao, R. Wang, T. Jiang, Y. Zhang, D. Kong, Y. Wu, S. Chen, S. Xu, D. Tang, P. Luo, M. Wu, L. Meng, D. Wen, C. Wu, G. Zhang, X. Shi, W. Yu, and W. Rong, *Molecular identification of bulbospinal ON neurons by GPER, which drives pain and morphine tolerance*. *J Clin Invest*, 2023. **133**(1).
109. Gao, T., L. Dong, J. Qian, X. Ding, Y. Zheng, M. Wu, L. Meng, Y. Jiao, P. Gao, P. Luo, G. Zhang, C. Wu, X. Shi, and W. Rong, *G-Protein-Coupled Estrogen Receptor (GPER) in the Rostral Ventromedial Medulla Is Essential for Mobilizing Descending Inhibition of Itch*. *J Neurosci*, 2021. **41**(37): p. 7727-7741.
110. Skagerberg, G. and A. Björklund, *Topographic principles in the spinal projections of serotonergic and non-serotonergic brainstem neurons in the rat*. *Neuroscience*, 1985. **15**: p. 445-80.
111. Aicher, S.A., S.M. Hermes, K.L. Whittier, and D.M. Hegarty, *Descending projections from the rostral ventromedial medulla (RVM) to trigeminal and spinal dorsal horns are morphologically and neurochemically distinct*. *J Chem Neuroanat*, 2012. **43**(2): p. 103-111.

112. De Felice, M., R. Sanoja, R. Wang, L. Vera-Portocarrero, J. Oyarzo, T. King, M.H. Ossipov, T.W. Vanderah, J. Lai, G.O. Dussor, H.L. Fields, T.J. Price, and F. Porreca, *Engagement of descending inhibition from the rostral ventromedial medulla protects against chronic neuropathic pain*. Pain, 2011. **152**(12): p. 2701-9.
113. Hirakawa, N., S.A. Tershner, H.L. Fields, and B.H. Manning, *Bi-directional changes in affective state elicited by manipulation of medullary pain-modulatory circuitry*. Neuroscience, 2000. **100**(4): p. 861-871.
114. Gomtsian, L., K. Bannister, N. Eyde, D. Robles, A.H. Dickenson, F. Porreca, and E. Navratilova, *Morphine effects within the rodent anterior cingulate cortex and rostral ventromedial medulla reveal separable modulation of affective and sensory qualities of acute or chronic pain*. Pain, 2018. **159**(12): p. 2512-2521.
115. Antal, M., M. Petko, E. Polgar, C.W. Heizmann, and J. Storm-Mathisen, *Direct evidence of an extensive GABAergic innervation of the spinal dorsal horn by fibres descending from the rostral ventromedial medulla*. Neuroscience, 1996. **73**: p. 509-18.
116. Light, A.R. and A.M. Kavookjian, *The ultrastructure and synaptic connections of the spinal terminations from single, physiologically characterized axons descending in the dorsolateral funiculus from the midline, pontomedullary region*. Journal of Comparative Neurology, 1985. **234**: p. 549-60.
117. Otsu, Y. and K.R. Aubrey, *Kappa opioids inhibit the GABA/glycine terminals of rostral ventromedial medulla projections in the superficial dorsal horn of the spinal cord*. J Physiol, 2022. **600**(18): p. 4187-4205.
118. Willis, W.D., Jr., *Anatomy and physiology of descending control of nociceptive responses of dorsal horn neurons: comprehensive review*. Prog Brain Res, 1988. **77**: p. 1-29.
119. Lubejko, S.T., G. Livrizzi, S.A. Buczynski, J. Patel, J.C. Yung, T.L. Yaksh, and M.R. Banghart, *Inputs to the locus coeruleus from the periaqueductal gray and rostroventral*

- medulla shape opioid-mediated descending pain modulation*. Sci Adv, 2024. **10**(17): p. eadj9581.
120. Hossaini, M., J.A. Goos, S.K. Kohli, and J.C. Holstege, *Distribution of glycine/GABA neurons in the ventromedial medulla with descending spinal projections and evidence for an ascending glycine/GABA projection*. PLoS One, 2012. **7**(4): p. e35293.
 121. Bagley, E.E. and S.L. Ingram, *Endogenous opioid peptides in the descending pain modulatory circuit*. Neuropharmacology, 2020. **173**: p. 108131.
 122. Martenson, M.E., O.I. Halawa, K.J. Tonsfeldt, C.A. Maxwell, N. Hammack, S.D. Mist, M.E. Pennesi, R.M. Bennett, K.M. Mauer, K.D. Jones, and M.M. Heinricher, *A possible neural mechanism for photosensitivity in chronic pain*. Pain, 2016. **157**: p. 868-878.
 123. McGaraughty, S. and M.M. Heinricher, *Microinjection of morphine into various amygdaloid nuclei differentially affects nociceptive responsiveness and RVM neuronal activity*. Pain, 2002. **96**(1-2): p. 153-162.
 124. Hermann, D.M., P.H. Luzzi, C. Peyron, P. Hinckel, and M. Jouvet, *Afferent projections to the rat nuclei raphe magnus, raphe pallidus and reticularis gigantocellularis pars alpha demonstrated by iontophoretic application of cholera toxin (subunit b)*. J Chem Neuroanat, 1997. **13**(1): p. 1-21.
 125. Ramirez, F. and H. Vanegas, *Tooth pulp stimulation advances both medullary off-cell pause and tail flick*. Neurosci Lett, 1989. **100**: p. 153-6.
 126. Gauriau, C. and J.F. Bernard, *Pain pathways and parabrachial circuits in the rat*. Exp Physiol, 2002. **87**(2): p. 251-8.
 127. Todd, A.J., *Neuronal circuitry for pain processing in the dorsal horn*. Nat Rev Neurosci, 2010. **11**(12): p. 823-836.
 128. Saito, H., A. Katagiri, S. Okada, L. Mikuzuki, A. Kubo, T. Suzuki, K. Ohara, J. Lee, N. Gionhaku, T. Inuma, D.A. Bereiter, and K. Iwata, *Ascending projections of nociceptive*

- neurons from trigeminal subnucleus caudalis: A population approach.* Exp Neurol, 2017. **293**: p. 124-136.
129. Bernard, J.F., R. Dallel, P. Raboisson, L. Villanueva, and D. Le Bars, *Organization of the efferent projections from the spinal cervical enlargement to the parabrachial area and periaqueductal gray: a PHA-L study in the rat.* J Comp Neurol, 1995. **353**: p. 480-505.
130. Bourgeois, L., L. Monconduit, L. Villanueva, and J.F. Bernard, *Parabrachial internal lateral neurons convey nociceptive messages from the deep laminae of the dorsal horn to the intralaminar thalamus.* J Neurosci, 2001. **21**(6): p. 2159-65.
131. Beitz, A.J., J.R. Clements, L.J. Ecklund, and M.M. Mullett, *The nuclei of origin of brainstem enkephalin and cholecystokinin projections to the spinal trigeminal nucleus of the rat.* Neuroscience, 1987. **20**: p. 409-25.
132. Roeder, Z., Q. Chen, S. Davis, J.D. Carlson, D. Tupone, and M.M. Heinricher, *The parabrachial complex links pain transmission to descending pain modulation.* Pain, 2016. **157**: p. 2697-2708.
133. Verner, T.A., P.M. Pilowsky, and A.K. Goodchild, *Retrograde projections to a discrete apneic site in the midline medulla oblongata of the rat.* Brain Res, 2008. **1208**: p. 128-136.
134. Chen, Q. and M.M. Heinricher, *Plasticity in the link between pain-transmitting and pain-modulating systems in acute and persistent inflammation.* J Neurosci, 2019. **39**: p. 2065-2079.
135. Chaouch, A., D. Menetrey, D. Binder, and J.M. Besson, *Neurons at the origin of the medial component of the bulbopontine spinoreticular tract in the rat: an anatomical study using horseradish peroxidase retrograde transport.* J Comp Neurol, 1983. **214**: p. 309-20.

136. De Preter, C.C. and M.M. Heinricher, *Direct and indirect nociceptive input from the trigeminal dorsal horn to pain-modulating neurons in the rostral ventromedial medulla*. J Neurosci, 2023. **43**: p. 5779-5791.
137. Gu, X., Y.Z. Zhang, J.J. O'Malley, C.C. De Preter, M. Penzo, and M.A. Hoon, *Neurons in the caudal ventrolateral medulla mediate descending pain control*. Nat Neurosci, 2023. **26**(4): p. 594-605.
138. Olszewski, J., *On the anatomical and functional organization of the spinal trigeminal nucleus*. J Comp Neurol, 1950. **92**(3): p. 401-13.
139. Sessle, B.J., *Acute and chronic craniofacial pain: brainstem mechanisms of nociceptive transmission and neuroplasticity, and their clinical correlates*. Crit Rev Oral Biol Med, 2000. **11**(1): p. 57-91.
140. Matthews, D.W., M. Deschenes, T. Furuta, J.D. Moore, F. Wang, H.J. Karten, and D. Kleinfeld, *Feedback in the brainstem: an excitatory disynaptic pathway for control of whisking*. J Comp Neurol, 2015. **523**(6): p. 921-42.
141. Strassman, A.M. and B.P. Vos, *Somatotopic and laminar organization of fos-like immunoreactivity in the medullary and upper cervical dorsal horn induced by noxious facial stimulation in the rat*. J Comp Neurol, 1993. **331**(4): p. 495-516.
142. Ren, K. and R. Dubner, *The role of trigeminal interpolaris-caudalis transition zone in persistent orofacial pain*. Int Rev Neurobiol, 2011. **97**: p. 207-25.
143. Bereiter, D.A., C.B. Hathaway, and A.P. Benetti, *Caudal portions of the spinal trigeminal complex are necessary for autonomic responses and display Fos-like immunoreactivity after corneal stimulation in the cat*. Brain Res, 1994. **657**(1-2): p. 73-82.
144. Okada, S., A. Katagiri, H. Saito, J. Lee, K. Ohara, T. Iinuma, D.A. Bereiter, and K. Iwata, *Differential activation of ascending noxious pathways associated with trigeminal nerve injury*. Pain, 2019. **160**(6): p. 1342-1360.

145. Ikeda, T., R. Terayama, S.S. Jue, S. Sugiyo, R. Dubner, and K. Ren, *Differential rostral projections of caudal brainstem neurons receiving trigeminal input after masseter inflammation*. J Comp Neurol, 2003. **465**(2): p. 220-33.
146. Uddin, O., P. Studlack, T. Akintola, C. Raver, A. Castro, R. Masri, and A. Keller, *Amplified parabrachial nucleus activity in a rat model of trigeminal neuropathic pain*. Neurobiol Pain, 2018. **3**: p. 22-30.
147. Rodriguez, E., K. Sakurai, J. Xu, Y. Chen, K. Toda, S. Zhao, B.X. Han, D. Ryu, H. Yin, W. Liedtke, and F. Wang, *A craniofacial-specific monosynaptic circuit enables heightened affective pain*. Nat Neurosci, 2017. **20**(12): p. 1734-1743.
148. Cleary, D.R., M.J. Neubert, and M.M. Heinricher, *Are opioid-sensitive neurons in the rostral ventromedial medulla inhibitory interneurons?* Neuroscience, 2008. **151**(2): p. 564-71.
149. Heinricher, M.M. and S. McGaraughty, *Analysis of excitatory amino acid transmission within the rostral ventromedial medulla: Implications for circuitry*. Pain, 1998. **75**: p. 247-255.
150. Heinricher, M.M., C.M. Haws, and H.L. Fields, *Evidence for GABA-mediated control of putative nociceptive modulating neurons in the rostral ventromedial medulla: iontophoresis of bicuculline eliminates the off-cell pause*. Somatosens Mot Res, 1991. **8**: p. 215-25.
151. Silva, C. and N. McNaughton, *Are periaqueductal gray and dorsal raphe the foundation of appetitive and aversive control? A comprehensive review*. Prog Neurobiol, 2019. **177**: p. 33-72.
152. Keay, K.A. and R. Bandler, *Parallel circuits mediating distinct emotional coping reactions to different types of stress*. Neurosci Biobehav Rev, 2001. **25**(7-8): p. 669-78.

153. Koutsikou, S., T.C. Watson, J.J. Crook, J.L. Leith, C.L. Lawrenson, R. Apps, and B.M. Lumb, *The Periaqueductal Gray Orchestrates Sensory and Motor Circuits at Multiple Levels of the Neuraxis*. J Neurosci, 2015. **35**(42): p. 14132-47.
154. Barbaro, N.M., *Studies of PAG/PVG stimulation for pain relief in humans*. Prog. Brain Res., 1988. **77**: p. 165-173.
155. Barbaro, N.M., *Studies of PAG/PVG stimulation for pain relief in humans*. Prog Brain Res, 1988. **77**: p. 165-73.
156. Hosobuchi, Y., J.E. Adams, and R. Linchitz, *Pain relief by electrical stimulation of the central gray matter in humans and its reversal by naloxone*. Science, 1977. **197**(4299): p. 183-6.
157. Richardson, D.E. and H. Akil, *Pain reduction by electrical brain stimulation in man. Part 1: Acute administration in periaqueductal and periventricular sites*. J Neurosurg, 1977. **47**(2): p. 178-83.
158. Mayer, D.J., T.L. Wolfle, H. Akil, B. Carder, and J.C. Liebeskind, *Analgesia from electrical stimulation in the brainstem of the rat*. Science, 1971. **174**(4016): p. 1351-4.
159. Morgan, M.M., J.H. Sohn, and J.C. Liebeskind, *Stimulation of the periaqueductal gray matter inhibits nociception at the supraspinal as well as spinal level*. Brain Res, 1989. **502**(1): p. 61-6.
160. Samineni, V.K., J.G. Grajales-Reyes, B.A. Copits, D.E. O'Brien, S.L. Trigg, A.M. Gomez, M.R. Bruchas, and R.W.t. Gereau, *Divergent Modulation of Nociception by Glutamatergic and GABAergic Neuronal Subpopulations in the Periaqueductal Gray*. eNeuro, 2017. **4**(2): p. ENEURO.0129-16.201.
161. Assareh, N., C. Fenech, R. Power, M.N. Uddin, Y. Otsu, and K.R. Aubrey, *Bidirectional Modulation of Nociception by GlyT2(+) Neurons in the Ventrolateral Periaqueductal Gray*. eNeuro, 2023. **10**(6): p. ENEURO.0069-23.2023.

162. Drake, R.A., J.L. Leith, F. Almahasneh, J. Martindale, A.W. Wilson, B. Lumb, and L.F. Donaldson, *Periaqueductal Grey EP3 Receptors Facilitate Spinal Nociception in Arthritic Secondary Hypersensitivity*. J Neurosci, 2016. **36**(35): p. 9026-40.
163. McPherson, K.B. and S.L. Ingram, *Cellular and circuit diversity determines the impact of endogenous opioids in the descending pain modulatory pathway*. Front Syst Neurosci, 2022. **16**: p. 963812.
164. Samineni, V.K., J.G. Grajales-Reyes, S.S. Sundaram, J.J. Yoo, and R.W.t. Gereau, *Cell type-specific modulation of sensory and affective components of itch in the periaqueductal gray*. Nat Commun, 2019. **10**(1): p. 4356.
165. Xie, L., H. Wu, Q. Chen, F. Xu, H. Li, Q. Xu, C. Jiao, L. Sun, R. Ullah, and X. Chen, *Divergent modulation of pain and anxiety by GABAergic neurons in the ventrolateral periaqueductal gray and dorsal raphe*. Neuropsychopharmacology, 2023. **48**(10): p. 1509-1519.
166. Morgan, M.M., K.L. Whittier, D.M. Hegarty, and S.A. Aicher, *Periaqueductal gray neurons project to spinally projecting GABAergic neurons in the rostral ventromedial medulla*. Pain, 2008. **140**(2): p. 376-386.
167. Reichling, D.B. and A.I. Basbaum, *Contribution of brainstem GABAergic circuitry to descending antinociceptive controls: II. Electron microscopic immunocytochemical evidence of GABAergic control over the projection from the periaqueductal gray to the nucleus raphe magnus in the rat*. J Comp Neurol, 1990. **302**: p. 378-93.
168. Kalyuzhny, A.E. and M.W. Wessendorf, *Relationship of m- and d-opioid receptors to GABAergic neurons in the central nervous system, including antinociceptive brainstem circuits*. J Comp Neurol, 1998. **392**(4): p. 528-47.
169. Lau, B.K. and C.W. Vaughan, *Descending modulation of pain: the GABA disinhibition hypothesis of analgesia*. Curr Opin Neurobiol, 2014. **29C**: p. 159-164.

170. Osborne, P.B., C.W. Vaughan, H.I. Wilson, and M.J. Christie, *Opioid inhibition of rat periaqueductal grey neurones with identified projections to rostral ventromedial medulla in vitro*. J Physiol (Lond), 1996. **490**(Pt 2): p. 383-9.
171. Kalyuzhny, A.E., U. Arvidsson, W. Wu, and M.W. Wessendorf, *m-Opioid and d-opioid receptors are expressed in brainstem antinociceptive circuits: studies using immunocytochemistry and retrograde tract-tracing*. Journal of Neuroscience, 1996. **16**: p. 6490-503.
172. Du, Y., K. Yu, C. Yan, C. Wei, Q. Zheng, Y. Qiao, Y. Liu, J. Han, W. Ren, and Z. Liu, *The Contributions of Mu-Opioid Receptors on Glutamatergic and GABAergic Neurons to Analgesia Induced by Various Stress Intensities*. eNeuro, 2022. **9**(3): p. ENEURO.0487-21.2022.
173. Xie, J.Y., D.S. Herman, C.O. Stiller, L.R. Gardell, M.H. Ossipov, J. Lai, F. Porreca, and T.W. Vanderah, *Cholecystokinin in the rostral ventromedial medulla mediates opioid-induced hyperalgesia and antinociceptive tolerance*. J Neurosci, 2005. **25**(2): p. 409-16.
174. Smith, H.S., *Opioid metabolism*. Mayo Clin Proc, 2009. **84**(7): p. 613-24.
175. Miller, P.L. and A.A. Ernst, *Sex differences in analgesia: a randomized trial of mu versus kappa opioid agonists*. South Med J, 2004. **97**(1): p. 35-41.
176. Craft, R.M., *Sex differences in opioid analgesia: "from mouse to man"*. Clin J Pain, 2003. **19**(3): p. 175-86.
177. Doyle, H.H. and A.Z. Murphy, *Sex-dependent influences of morphine and its metabolites on pain sensitivity in the rat*. Physiol Behav, 2018. **187**: p. 32-41.
178. Loyd, D.R., X. Wang, and A.Z. Murphy, *Sex differences in micro-opioid receptor expression in the rat midbrain periaqueductal gray are essential for eliciting sex differences in morphine analgesia*. J Neurosci, 2008. **28**(52): p. 14007-17.

179. Loyd, D.R., M.M. Morgan, and A.Z. Murphy, *Sexually dimorphic activation of the periaqueductal gray-rostral ventromedial medullary circuit during the development of tolerance to morphine in the rat*. Eur J Neurosci, 2008. **27**(6): p. 1517-24.
180. Lomas, L.M., J.M. Turner, and M.J. Picker, *Sex differences in NMDA antagonist enhancement of morphine antihyperalgesia in a capsaicin model of persistent pain: comparisons to two models of acute pain*. Pharmacol Biochem Behav, 2008. **89**(2): p. 127-36.
181. Wang, X., R.J. Traub, and A.Z. Murphy, *Persistent pain model reveals sex difference in morphine potency*. Am J Physiol Regul Integr Comp Physiol, 2006. **291**(2): p. R300-6.
182. Ji, Y., A.Z. Murphy, and R.J. Traub, *Sex differences in morphine-induced analgesia of visceral pain are supraspinally and peripherally mediated*. Am J Physiol Regul Integr Comp Physiol, 2006. **291**(2): p. R307-14.
183. Boyer, J.S., M.M. Morgan, and R.M. Craft, *Microinjection of morphine into the rostral ventromedial medulla produces greater antinociception in male compared to female rats*. Brain Res, 1998. **796**(1-2): p. 315-8.
184. Cook, C.D. and M.D. Nickerson, *Nociceptive sensitivity and opioid antinociception and antihyperalgesia in Freund's adjuvant-induced arthritic male and female rats*. J Pharmacol Exp Ther, 2005. **313**(1): p. 449-59.
185. Bobeck, E.N., A.L. McNeal, and M.M. Morgan, *Drug dependent sex-differences in periaqueductal gray mediated antinociception in the rat*. Pain, 2009. **147**(1-3): p. 210-6.
186. Tershner, S.A., J.M. Mitchell, and H.L. Fields, *Brainstem pain modulating circuitry is sexually dimorphic with respect to mu and kappa opioid receptor function*. Pain, 2000. **85**(1-2): p. 153-9.
187. Linnman, C., J.C. Beucke, K.B. Jensen, R.L. Gollub, and J. Kong, *Sex similarities and differences in pain-related periaqueductal gray connectivity*. Pain, 2012. **153**(2): p. 444-454.

188. Kong, J., P.C. Tu, C. Zyloney, and T.P. Su, *Intrinsic functional connectivity of the periaqueductal gray, a resting fMRI study*. Behav Brain Res, 2010. **211**(2): p. 215-9.
189. Loyd, D.R. and A.Z. Murphy, *Sex differences in the anatomical and functional organization of the periaqueductal gray-rostral ventromedial medullary pathway in the rat: a potential circuit mediating the sexually dimorphic actions of morphine*. J Comp Neurol, 2006. **496**(5): p. 723-38.
190. Loyd, D.R. and A.Z. Murphy, *The role of the periaqueductal gray in the modulation of pain in males and females: are the anatomy and physiology really that different?* Neural Plast, 2009. **2009**: p. 462879.
191. Bernal, S.A., M.M. Morgan, and R.M. Craft, *PAG mu opioid receptor activation underlies sex differences in morphine antinociception*. Behav Brain Res, 2007. **177**(1): p. 126-33.
192. Doyle, H.H., L.N. Eidson, D.M. Sinkiewicz, and A.Z. Murphy, *Sex Differences in Microglia Activity within the Periaqueductal Gray of the Rat: A Potential Mechanism Driving the Dimorphic Effects of Morphine*. J Neurosci, 2017. **37**(12): p. 3202-3214.
193. Tonsfeldt, K.J., K.L. Suchland, K.A. Beeson, J.D. Lowe, M.H. Li, and S.L. Ingram, *Sex Differences in GABAA Signaling in the Periaqueductal Gray Induced by Persistent Inflammation*. J Neurosci, 2016. **36**(5): p. 1669-81.
194. Rojas-Piloni, G., I. Duran, and R. Cueva-Rolon, *The activity of ON and OFF cells at the rostroventromedial medulla is modulated by vagino-cervical stimulation*. Pain, 1998. **74**(1): p. 29-34.
195. Craft, R.M., M.M. Morgan, and D.A. Lane, *Oestradiol dampens reflex-related activity of on- and off-cells in the rostral ventromedial medulla of female rats*. Neuroscience, 2004. **125**(4): p. 1061-8.
196. Hardy, S.G., *Analgesia elicited by prefrontal stimulation*. Brain Res, 1985. **339**(2): p. 281-4.

197. Drake, R.A., K.A. Steel, R. Apps, B.M. Lumb, and A.E. Pickering, *Loss of cortical control over the descending pain modulatory system determines the development of the neuropathic pain state in rats*. *Elife*, 2021. **10**: p. e65156.
198. Cheriyan, J. and P.L. Sheets, *Altered Excitability and Local Connectivity of mPFC-PAG Neurons in a Mouse Model of Neuropathic Pain*. *J Neurosci*, 2018. **38**(20): p. 4829-4839.
199. Cheriyan, J. and P.L. Sheets, *Peripheral nerve injury reduces the excitation-inhibition balance of basolateral amygdala inputs to prelimbic pyramidal neurons projecting to the periaqueductal gray*. *Mol Brain*, 2020. **13**(1): p. 100.
200. Huang, J., V.M. Gadotti, L. Chen, I.A. Souza, S. Huang, D. Wang, C. Ramakrishnan, K. Deisseroth, Z. Zhang, and G.W. Zamponi, *A neuronal circuit for activating descending modulation of neuropathic pain*. *Nat Neurosci*, 2019. **22**(10): p. 1659-1668.
201. Tran, H., Y. Feng, D. Chao, Q.S. Liu, Q.H. Hogan, and B. Pan, *Descending mechanism by which medial prefrontal cortex endocannabinoid signaling controls the development of neuropathic pain and neuronal activity of dorsal root ganglion*. *Pain*, 2024. **165**(1): p. 102-114.
202. Chen, T., W. Taniguchi, Q.Y. Chen, H. Tozaki-Saitoh, Q. Song, R.H. Liu, K. Koga, T. Matsuda, Y. Kaito-Sugimura, J. Wang, Z.H. Li, Y.C. Lu, K. Inoue, M. Tsuda, Y.Q. Li, T. Nakatsuka, and M. Zhuo, *Top-down descending facilitation of spinal sensory excitatory transmission from the anterior cingulate cortex*. *Nat Commun*, 2018. **9**(1): p. 1886.
203. Navratilova, E., J.Y. Xie, D. Meske, C. Qu, K. Morimura, A. Okun, N. Arakawa, M. Ossipov, H.L. Fields, and F. Porreca, *Endogenous opioid activity in the anterior cingulate cortex is required for relief of pain*. *J Neurosci*, 2015. **35**(18): p. 7264-71.
204. Barbaro, N.M., M.M. Heinricher, and H.L. Fields, *Putative nociceptive modulatory neurons in the rostral ventromedial medulla of the rat display highly correlated firing patterns*. *Somatosens Mot Res*, 1989. **6**: p. 413-25.

205. Mason, P. and H.L. Fields, *Axonal trajectories and terminations of on- and off-cells in the cat lower brainstem*. J Comp Neurol, 1989. **288**: p. 185-207.
206. Fillingim, R.B., C.D. King, M.C. Ribeiro-Dasilva, B. Rahim-Williams, and J.L. Riley, 3rd, *Sex, gender, and pain: a review of recent clinical and experimental findings*. J Pain, 2009. **10**(5): p. 447-85.
207. Racine, M., Y. Tousignant-Laflamme, L.A. Kloda, D. Dion, G. Dupuis, and M. Choiniere, *A systematic literature review of 10 years of research on sex/gender and experimental pain perception - part 1: are there really differences between women and men?* Pain, 2012. **153**(3): p. 602-18.
208. Mogil, J.S., *Sex differences in pain and pain inhibition: multiple explanations of a controversial phenomenon*. Nat Rev Neurosci, 2012. **13**(12): p. 859-866.
209. Tershner, S.A., J.M. Mitchell, and H.L. Fields, *Brainstem pain modulating circuitry is sexually dimorphic with respect to mu and kappa opioid receptor function*. Pain, 2000. **85**(1-2): p. 153-9.
210. Nasser, S.A. and E.A. Afify, *Sex differences in pain and opioid mediated antinociception: Modulatory role of gonadal hormones*. Life Sci, 2019. **237**: p. 116926.
211. Mogil, J.S., *Qualitative sex differences in pain processing: emerging evidence of a biased literature*. Nat Rev Neurosci, 2020. **21**(7): p. 353-365.
212. Cleary, D.R. and M.M. Heinricher, *Adaptations in responsiveness of brainstem pain-modulating neurons in acute compared with chronic inflammation*. Pain, 2013. **154**(0): p. 845-855.
213. Merkel, G. and E.I. Eger, 2nd, *A comparative study of halothane and halopropane anesthesia including method for determining equipotency*. Anesthesiology, 1963. **24**: p. 346-57.
214. Ren, K., *An improved method for assessing mechanical allodynia in the rat*. Physiol Behav, 1999. **67**(5): p. 711-6.

215. Ren, K. and R. Dubner, *Inflammatory Models of Pain and Hyperalgesia*. ILAR J, 1999. **40**(3): p. 111-118.
216. Barbaro, N.M., M.M. Heinricher, and H.L. Fields, *Putative pain modulating neurons in the rostral ventral medulla: reflex-related activity predicts effects of morphine*. Brain Res, 1986. **366**(1-2): p. 203-10.
217. Heinricher, M.M., S. McGaraughty, and D.A. Farr, *The role of excitatory amino acid transmission within the rostral ventromedial medulla in the antinociceptive actions of systemically administered morphine*. Pain, 1999. **81**(1-2): p. 57-65.
218. Heinricher, M.M., S. McGaraughty, and V. Tortorici, *Circuitry underlying antiopioid actions of cholecystinin within the rostral ventromedial medulla*. J Neurophysiol, 2001. **85**(1): p. 280-6.
219. Fields, H.L., H. Vanegas, I.D. Hentall, and G. Zorman, *Evidence that disinhibition of brain stem neurones contributes to morphine analgesia*. Nature, 1983. **306**: p. 684-686.
220. Montagne-Clavel, J. and J.L. Oliveras, *Are ventromedial medulla neuronal properties modified by chronic peripheral inflammation? A single-unit study in the awake, freely moving polyarthritic rat*. Brain Research, 1994. **657**: p. 92-104.
221. Pinto-Ribeiro, F., O.B. Ansah, A. Almeida, and A. Pertovaara, *Influence of arthritis on descending modulation of nociception from the paraventricular nucleus of the hypothalamus*. Brain Res, 2008. **1197**: p. 63-75.
222. Ren, K. and R. Dubner, *Enhanced descending modulation of nociception in rats with persistent hindpaw inflammation*. J Neurophysiol, 1996. **76**(5): p. 3025-37.
223. Wei, F., R. Dubner, and K. Ren, *Nucleus reticularis gigantocellularis and nucleus raphe magnus in the brain stem exert opposite effects on behavioral hyperalgesia and spinal Fos protein expression after peripheral inflammation*. Pain, 1999. **80**(1-2): p. 127-41.

224. Okun, A., M. DeFelice, N. Eyde, J. Ren, R. Mercado, T. King, and F. Porreca, *Transient inflammation-induced ongoing pain is driven by TRPV1 sensitive afferents*. *Mol Pain*, 2011. **7**: p. 4.
225. Almarestani, L., M.A. Fitzcharles, G.J. Bennett, and A. Ribeiro-da-Silva, *Imaging studies in Freund's complete adjuvant model of regional polyarthritis, a model suitable for the study of pain mechanisms, in the rat*. *Arthritis Rheum*, 2011. **63**(6): p. 1573-81.
226. Guan, Y., W. Guo, S.-P. Zou, R. Dubner, and K. Ren, *Inflammation-induced upregulation of AMPA receptor subunit expression in brain stem pain modulatory circuitry*. *Pain*, 2003. **104**(1-2): p. 401-413.
227. Craft, R.M., R. Kandasamy, and S.M. Davis, *Sex differences in anti-allodynic, anti-hyperalgesic and anti-edema effects of Delta(9)-tetrahydrocannabinol in the rat*. *Pain*, 2013. **154**(9): p. 1709-17.
228. Bradshaw, H., J. Miller, Q. Ling, K. Malsnee, and M.A. Ruda, *Sex differences and phases of the estrous cycle alter the response of spinal cord dynorphin neurons to peripheral inflammation and hyperalgesia*. *Pain*, 2000. **85**(1-2): p. 93-9.
229. Armendariz, A. and A. Nazarian, *Morphine antinociception on thermal sensitivity and place conditioning in male and female rats treated with intraplantar complete freund's adjuvant*. *Behav Brain Res*, 2018. **343**: p. 21-27.
230. Niesters, M., A. Dahan, B. Kest, J. Zacny, T. Stijnen, L. Aarts, and E. Sarton, *Do sex differences exist in opioid analgesia? A systematic review and meta-analysis of human experimental and clinical studies*. *Pain*, 2010. **151**(1): p. 61-8.
231. Sarton, E., E. Olofsen, R. Romberg, J. den Hartigh, B. Kest, D. Nieuwenhuijs, A. Burm, L. Teppema, and A. Dahan, *Sex differences in morphine analgesia: an experimental study in healthy volunteers*. *Anesthesiology*, 2000. **93**(5): p. 1245-54; discussion 6A.
232. Cicero, T.J., B. Nock, and E.R. Meyer, *Gender-related differences in the antinociceptive properties of morphine*. *J Pharmacol Exp Ther*, 1996. **279**(2): p. 767-73.

233. Baker, L. and A. Ratka, *Sex-specific differences in levels of morphine, morphine-3-glucuronide, and morphine antinociception in rats*. Pain, 2002. **95**(1-2): p. 65-74.
234. Barbaro, N.M., M.M. Heinricher, and H.L. Fields, *Putative pain modulating neurons in the rostral ventral medulla: reflex-related activity predicts effects of morphine*. Brain Res, 1986. **366**: p. 203-10.
235. Racine, M., Y. Tousignant-Laflamme, L.A. Kloda, D. Dion, G. Dupuis, and M. Choiniere, *A systematic literature review of 10 years of research on sex/gender and pain perception - part 2: do biopsychosocial factors alter pain sensitivity differently in women and men?* Pain, 2012. **153**(3): p. 619-35.
236. Hashmi, J.A. and K.D. Davis, *Deconstructing sex differences in pain sensitivity*. Pain, 2014. **155**(1): p. 10-13.
237. Kennedy, J., J.M. Roll, T. Schraudner, S. Murphy, and S. McPherson, *Prevalence of persistent pain in the U.S. adult population: new data from the 2010 national health interview survey*. J Pain, 2014. **15**(10): p. 979-84.
238. Lovick, T.A., *The medullary raphe nuclei: a system for integration and gain control in autonomic and somatomotor responsiveness?* Exp Physiol, 1997. **82**(1): p. 31-41.
239. Dampney, R.A., *Functional organization of central pathways regulating the cardiovascular system*. Physiol Rev, 1994. **74**(2): p. 323-64.
240. Morrison, S.F., *Central neural control of thermoregulation and brown adipose tissue*. Auton Neurosci, 2016. **196**: p. 14-24.
241. Chen, Q. and M.M. Heinricher, *Shifting the balance: how top-down and bottom-up inputs modulate pain via the rostral ventromedial medulla*. Front Pain Res, 2022. **3**: p. 932476.
242. Fields, H.L., J. Bry, I. Hentall, and G. Zorman, *The activity of neurons in the rostral medulla of the rat during withdrawal from noxious heat*. J Neurosci, 1983. **3**(12): p. 2545-52.

243. Heinricher, M.M., C.M. Haws, and H.L. Fields, *Evidence for GABA-mediated control of putative nociceptive modulating neurons in the rostral ventromedial medulla: iontophoresis of bicuculline eliminates the off-cell pause*. Somatosens Mot Res, 1991. **8**(3): p. 215-25.
244. Todd, A.J., M.M. McGill, and S.A. Shehab, *Neurokinin 1 receptor expression by neurons in laminae I, III and IV of the rat spinal dorsal horn that project to the brainstem*. Eur J Neurosci, 2000. **12**(2): p. 689-700.
245. Craig, A.D., *Distribution of brainstem projections from spinal lamina I neurons in the cat and the monkey*. J Comp Neurol, 1995. **361**(2): p. 225-48.
246. Feil, K. and H. Herbert, *Topographic organization of spinal and trigeminal somatosensory pathways to the rat parabrachial and Kolliker-Fuse nuclei*. J Comp Neurol, 1995. **353**(4): p. 506-28.
247. Chen, Q., Z. Roeder, M.H. Li, Y. Zhang, S.L. Ingram, and M.M. Heinricher, *Optogenetic Evidence for a Direct Circuit Linking Nociceptive Transmission through the Parabrachial Complex with Pain-Modulating Neurons of the Rostral Ventromedial Medulla (RVM)*. eNeuro, 2017. **4**(3).
248. Roeder, Z., Q. Chen, S. Davis, J.D. Carlson, D. Tupone, and M.M. Heinricher, *Parabrachial complex links pain transmission to descending pain modulation*. Pain, 2016. **157**(12): p. 2697-2708.
249. Chaouch, A., D. Menetrey, D. Binder, and J.M. Besson, *Neurons at the origin of the medial component of the bulbopontine spinoreticular tract in the rat: an anatomical study using horseradish peroxidase retrograde transport*. J Comp Neurol, 1983. **214**(3): p. 309-20.
250. Hoshino, C., A. Konno, N. Hosoi, R. Kaneko, R. Mukai, J. Nakai, and H. Hirai, *GABAergic neuron-specific whole-brain transduction by AAV-PHP.B incorporated with a new GAD65 promoter*. Mol Brain, 2021. **14**(1): p. 33.

251. Martenson, M.E., O.I. Halawa, K.J. Tonsfeldt, C.A. Maxwell, N. Hammack, S.D. Mist, M.E. Pennesi, R.M. Bennett, K.M. Mauer, K.D. Jones, and M.M. Heinricher, *A possible neural mechanism for photosensitivity in chronic pain*. *Pain*, 2016. **157**(4): p. 868-878.
252. Cechetto, D.F., D.G. Standaert, and C.B. Saper, *Spinal and trigeminal dorsal horn projections to the parabrachial nucleus in the rat*. *J Comp Neurol*, 1985. **240**(2): p. 153-60.
253. Wang, D., Y.Q. Li, J.L. Li, T. Kaneko, S. Nomura, and N. Mizuno, *g-Aminobutyric acid- and glycine-immunoreactive neurons postsynaptic to substance P-immunoreactive axon terminals in the superficial layers of the rat medullary dorsal horn*. *Neurosci Lett*, 2000. **288**(3): p. 187-90.
254. Basbaum, A.I., E.J. Glazer, and W. Oertel, *Immunoreactive glutamic acid decarboxylase in the trigeminal nucleus caudalis of the cat: a light- and electron-microscopic analysis*. *Somatosens Res*, 1986. **4**(1): p. 77-94.
255. Zhang, C.K., Z.H. Li, Y. Qiao, T. Zhang, Y.C. Lu, T. Chen, Y.L. Dong, Y.Q. Li, and J.L. Li, *VGLUT1 or VGLUT2 mRNA-positive neurons in spinal trigeminal nucleus provide collateral projections to both the thalamus and the parabrachial nucleus in rats*. *Mol Brain*, 2018. **11**(1): p. 22.
256. Zhang, L., J. Wang, C. Niu, Y. Zhang, T. Zhu, D. Huang, J. Ma, H. Sun, N. Gamper, X. Du, and H. Zhang, *Activation of parabrachial nucleus - ventral tegmental area pathway underlies the comorbid depression in chronic neuropathic pain in mice*. *Cell Rep*, 2021. **37**(5): p. 109936.
257. Persson, S., J.L. Boulland, M. Aspling, M. Larsson, R.T. Fremeau, Jr., R.H. Edwards, J. Storm-Mathisen, F.A. Chaudhry, and J. Broman, *Distribution of vesicular glutamate transporters 1 and 2 in the rat spinal cord, with a note on the spinocervical tract*. *J Comp Neurol*, 2006. **497**(5): p. 683-701.

258. Todd, A.J., D.I. Hughes, E. Polgar, G.G. Nagy, M. Mackie, O.P. Ottersen, and D.J. Maxwell, *The expression of vesicular glutamate transporters VGLUT1 and VGLUT2 in neurochemically defined axonal populations in the rat spinal cord with emphasis on the dorsal horn*. Eur J Neurosci, 2003. **17**(1): p. 13-27.
259. Wozniak, K.M., C. Rojas, Y. Wu, and B.S. Slusher, *The role of glutamate signaling in pain processes and its regulation by GCP II inhibition*. Curr Med Chem, 2012. **19**(9): p. 1323-34.
260. D'Mello, R. and A.H. Dickenson, *Spinal cord mechanisms of pain*. Br J Anaesth, 2008. **101**(1): p. 8-16.
261. Tokita, K., T. Inoue, and J.D. Boughter, Jr., *Subnuclear organization of parabrachial efferents to the thalamus, amygdala and lateral hypothalamus in C57BL/6J mice: a quantitative retrograde double labeling study*. Neuroscience, 2010. **171**(1): p. 351-65.
262. Chiang, M.C., A. Bowen, L.A. Schier, D. Tupone, O. Uddin, and M.M. Heinricher, *Parabrachial Complex: A Hub for Pain and Aversion*. J Neurosci, 2019. **39**(42): p. 8225-8230.
263. Heinricher, M.M., N.M. Barbaro, and H.L. Fields, *Putative nociceptive modulating neurons in the rostral ventromedial medulla of the rat: firing of on- and off-cells is related to nociceptive responsiveness*. Somatosens Mot Res, 1989. **6**(4): p. 427-39.
264. Barbaro, N.M., M.M. Heinricher, and H.L. Fields, *Putative nociceptive modulatory neurons in the rostral ventromedial medulla of the rat display highly correlated firing patterns*. Somatosens Mot Res, 1989. **6**(4): p. 413-25.
265. Heinricher, M.M., M.M. Morgan, and H.L. Fields, *Direct and indirect actions of morphine on medullary neurons that modulate nociception*. Neuroscience, 1992. **48**(3): p. 533-43.
266. Haring, J.H., T.A. Henderson, and M.F. Jacquin, *Principalis- or parabrachial-projecting spinal trigeminal neurons do not stain for GABA or GAD*. Somatosens Mot Res, 1990. **7**(4): p. 391-7.

267. Furuta, T., E. Timofeeva, K. Nakamura, K. Okamoto-Furuta, M. Togo, T. Kaneko, and M. Deschenes, *Inhibitory gating of vibrissal inputs in the brainstem*. J Neurosci, 2008. **28**(8): p. 1789-97.
268. Neugebauer, V., *Amygdala pain mechanisms*. Handb Exp Pharmacol, 2015. **227**: p. 261-84.
269. Chiang, M.C., E.K. Nguyen, M. Canto-Bustos, A.E. Papale, A.M. Oswald, and S.E. Ross, *Divergent Neural Pathways Emanating from the Lateral Parabrachial Nucleus Mediate Distinct Components of the Pain Response*. Neuron, 2020. **106**(6): p. 927-939.e5.
270. Barik, A., J.H. Thompson, M. Seltzer, N. Ghitani, and A.T. Chesler, *A Brainstem-Spinal Circuit Controlling Nocifensive Behavior*. Neuron, 2018. **100**(6): p. 1491-1503.
271. Petre, B., P. Kragel, L.Y. Atlas, S. Geuter, M. Jepma, L. Koban, A. Krishnan, M. Lopez-Sola, E.A.R. Losin, M. Roy, C.W. Woo, and T.D. Wager, *A multistudy analysis reveals that evoked pain intensity representation is distributed across brain systems*. PLoS Biol, 2022. **20**(5): p. e3001620.
272. Gerstein, G.L. and W.A. Clark, *Simultaneous Studies of Firing Patterns in Several Neurons*. Science, 1964. **143**(3612): p. 1325-7.
273. Rey, H.G., C. Pedreira, and R. Quiñero, *Past, present and future of spike sorting techniques*. Brain Res Bull, 2015. **119**(Pt B): p. 106-17.
274. Stevenson, I.H. and K.P. Kording, *How advances in neural recording affect data analysis*. Nat Neurosci, 2011. **14**(2): p. 139-42.
275. Lefebvre, B., P. Yger, and O. Marre, *Recent progress in multi-electrode spike sorting methods*. J Physiol Paris, 2016. **110**(4 Pt A): p. 327-335.
276. Hennig, M.H., C. Hurwitz, and M. Sorbaro, *Scaling Spike Detection and Sorting for Next-Generation Electrophysiology*. Adv Neurobiol, 2019. **22**: p. 171-184.

277. Buccino, A.P., S. Garcia, and P. Yger, *Spike sorting: new trends and challenges of the era of high-density probes*. Progress in Biomedical Engineering, 2022. **4**(2): p. 022005.
278. Averbeck, B.B., P.E. Latham, and A. Pouget, *Neural correlations, population coding and computation*. Nat Rev Neurosci, 2006. **7**(5): p. 358-66.
279. Garcia, S., A.P. Buccino, and P. Yger, *How Do Spike Collisions Affect Spike Sorting Performance?* eNeuro, 2022. **9**(5).
280. Pillow, J.W., J. Shlens, E.J. Chichilnisky, and E.P. Simoncelli, *A model-based spike sorting algorithm for removing correlation artifacts in multi-neuron recordings*. PLoS One, 2013. **8**(5): p. e62123.
281. Pedreira, C., J. Martinez, M.J. Ison, and R. Quian Quiroga, *How many neurons can we see with current spike sorting algorithms?* J Neurosci Methods, 2012. **211**(1): p. 58-65.
282. Shoham, S., D.H. O'Connor, and R. Segev, *How silent is the brain: is there a "dark matter" problem in neuroscience?* J Comp Physiol A Neuroethol Sens Neural Behav Physiol, 2006. **192**(8): p. 777-84.
283. Buccino, A.P., C.L. Hurwitz, S. Garcia, J. Magland, J.H. Siegle, R. Hurwitz, and M.H. Hennig, *SpikeInterface, a unified framework for spike sorting*. Elife, 2020. **9**.
284. Magland, J., J.J. Jun, E. Lovero, A.J. Morley, C.L. Hurwitz, A.P. Buccino, S. Garcia, and A.H. Barnett, *SpikeForest, reproducible web-facing ground-truth validation of automated neural spike sorters*. Elife, 2020. **9**.
285. Trainito, C., C. von Nicolai, E.K. Miller, and M. Siegel, *Extracellular Spike Waveform Dissociates Four Functionally Distinct Cell Classes in Primate Cortex*. Curr Biol, 2019. **29**(18): p. 2973-2982 e5.
286. Ulyanova, A.V., C. Cottone, C.D. Adam, K.G. Gagnon, D.K. Cullen, T. Holtzman, B.G. Jamieson, P.F. Koch, H.I. Chen, V.E. Johnson, and J.A. Wolf, *Multichannel Silicon Probes for Awake Hippocampal Recordings in Large Animals*. Front Neurosci, 2019. **13**: p. 397.

287. Shoup, A.M., N. Porwal, M.A. Fakharian, P. Hage, S.P. Orozco, and R. Shadmehr, *Rejuvenating silicon probes for acute neurophysiology*. J Neurophysiol, 2024. **132**(1): p. 308-315.
288. Concha-Miranda, M., W. Tang, K. Hartmann, and M. Brecht, *Large-Scale Mapping of Vocalization-Related Activity in the Functionally Diverse Nuclei in Rat Posterior Brainstem*. J Neurosci, 2022. **42**(44): p. 8252-8261.
289. Strickland, J.A. and M.A. McDannald, *Brainstem networks construct threat probability and prediction error from neuronal building blocks*. Nat Commun, 2022. **13**(1): p. 6192.
290. Yang, W., H. Kanodia, and S. Arber, *Structural and functional map for forelimb movement phases between cortex and medulla*. Cell, 2023. **186**(1): p. 162-177.e18.
291. Tsunematsu, T., A.A. Patel, A. Onken, and S. Sakata, *State-dependent brainstem ensemble dynamics and their interactions with hippocampus across sleep states*. Elife, 2020. **9**.
292. Malfatti, T., B. Ciralli, M.M. Hilscher, R.N. Leao, and K.E. Leao, *Decreasing dorsal cochlear nucleus activity ameliorates noise-induced tinnitus perception in mice*. BMC Biol, 2022. **20**(1): p. 102.
293. Mochizuki, Y., T. Onaga, H. Shimazaki, T. Shimokawa, Y. Tsubo, R. Kimura, A. Saiki, Y. Sakai, Y. Isomura, S. Fujisawa, K. Shibata, D. Hirai, T. Furuta, T. Kaneko, S. Takahashi, T. Nakazono, S. Ishino, Y. Sakurai, T. Kitsukawa, J.W. Lee, H. Lee, M.W. Jung, C. Babul, P.E. Maldonado, K. Takahashi, F.I. Arce-McShane, C.F. Ross, B.J. Sessle, N.G. Hatsopoulos, T. Brochier, A. Riehle, P. Chorley, S. Grun, H. Nishijo, S. Ichihara-Takeda, S. Funahashi, K. Shima, H. Mushiake, Y. Yamane, H. Tamura, I. Fujita, N. Inaba, K. Kawano, S. Kurkin, K. Fukushima, K. Kurata, M. Taira, K. Tsutsui, T. Ogawa, H. Komatsu, K. Koida, K. Toyama, B.J. Richmond, and S. Shinomoto, *Similarity in Neuronal Firing Regimes across Mammalian Species*. J Neurosci, 2016. **36**(21): p. 5736-47.

294. Clarke, R.W., M.M. Morgan, and M.M. Heinricher, *Identification of nocifensor reflex-related neurons in the rostroventromedial medulla of decerebrated rats*. Brain Res, 1994. **636**(1): p. 169-74.
295. Heinricher, M.M., Z.F. Cheng, and H.L. Fields, *Evidence for two classes of nociceptive modulating neurons in the periaqueductal gray*. J Neurosci, 1987. **7**(1): p. 271-8.
296. Winkler, C.W., S.M. Hermes, C.I. Chavkin, C.T. Drake, S.F. Morrison, and S.A. Aicher, *Kappa opioid receptor (KOR) and GAD67 immunoreactivity are found in OFF and NEUTRAL cells in the rostral ventromedial medulla*. J Neurophysiol, 2006. **96**(6): p. 3465-73.
297. De Preter, C.C. and M.M. Heinricher, *The 'in's and out's' of descending pain modulation from the rostral ventromedial medulla*. Trends Neurosci, 2024. **47**(6): p. 447-460.
298. De Preter, C.C. and M.M. Heinricher, *Direct and Indirect Nociceptive Input from the Trigeminal Dorsal Horn to Pain-Modulating Neurons in the Rostral Ventromedial Medulla*. J Neurosci, 2023. **43**(32): p. 5779-5791.
299. Paxinos, G. and C. Watson, *The Rat Brain in Stereotaxic Coordinates*. 6 ed. 2009: Elsevier.
300. Chung, J.E., J.F. Magland, A.H. Barnett, V.M. Tolosa, A.C. Tooker, K.Y. Lee, K.G. Shah, S.H. Felix, L.M. Frank, and L.F. Greengard, *A Fully Automated Approach to Spike Sorting*. Neuron, 2017. **95**(6): p. 1381-1394 e6.
301. Jun, J.J., C. Mitelut, C. Lai, S. Gratiy, C.A. Anastassious, and T.D. Harris, *Real-time spike sorting platform for high-density extracellular probes with ground-truth validation and drift correction*. bioRxiv, 2017.
302. Pachitariu, M., S. Sridhar, and C. Stringer, *Solving the spike sorting problem with Kilosort*. bioRxiv, 2023.
303. Garcia, S. and C. Pouzat. *Tridesclous*. 2015; Available from: <https://github.com/tridesclous/tridesclous>.

304. Yger, P., G.L. Spampinato, E. Esposito, B. Lefebvre, S. Deny, C. Gardella, M. Stimberg, F. Jetter, G. Zeck, S. Picaud, J. Duebel, and O. Marre, *A spike sorting toolbox for up to thousands of electrodes validated with ground truth recordings in vitro and in vivo*. *Elife*, 2018. **7**.
305. Vincent, J.P. and M.N. Economo, *Assessing Cross-Contamination in Spike-Sorted Electrophysiology Data*. *eNeuro*, 2024. **11**(8).
306. Rossant, C. and K.D. Harris, *Hardware-accelerated interactive data visualization for neuroscience in Python*. *Front Neuroinform*, 2013. **7**: p. 36.
307. Humphries, M.D., K. Gurney, and T.J. Prescott, *The brainstem reticular formation is a small-world, not scale-free, network*. *Proc Biol Sci*, 2006. **273**(1585): p. 503-11.
308. Scheibel, M.E. and A.B. Scheibel, *Anatomical basis of attention mechanisms in vertebrate brains.*, in *The neurosciences, a study program*. 1967, The Rockefeller University Press: New York, NY. p. 577–602.
309. Dehnen, G., M.S. Kehl, A. Darcher, T.T. Muller, J.H. Macke, V. Borger, R. Surges, and F. Mormann, *Duplicate Detection of Spike Events: A Relevant Problem in Human Single-Unit Recordings*. *Brain Sci*, 2021. **11**(6).
310. Robinson, D.A., *The electrical properties of metal microelectrodes*. *Proceedings of the IEEE*, 1968. **56**(6): p. 1065-1071.
311. Lemon, R., *Methods for Neuronal Recording in Conscious Animals*. 1984, Chichester: John Wiley & Sons.
312. Papaioannou, S. and P. Medini, *Advantages, Pitfalls, and Developments of All Optical Interrogation Strategies of Microcircuits in vivo*. *Front Neurosci*, 2022. **16**: p. 859803.
313. Heinricher, M.M. and V. Tortorici, *Interference with GABA transmission in the rostral ventromedial medulla: disinhibition of off-cells as a central mechanism in nociceptive modulation*. *Neuroscience*, 1994. **63**(2): p. 533-46.

314. McGaraughty, S., S. Reinis, and J. Tsoukatos, *Two distinct unit activity responses to morphine in the rostral ventromedial medulla of awake rats*. Brain Res, 1993. **604**(1-2): p. 331-3.
315. McGaraughty, S., S. Reinis, and J. Tsoukatos, *Investigating the role of anaesthetics on the rostral ventromedial medulla: implications for a GABAergic link between ON and OFF cells*. Neurosci Lett, 1993. **149**(2): p. 119-22.
316. McGaraughty, S. and S. Reinis, *Simultaneous multi- and single-unit recordings in the rostral ventromedial medulla of ketamine-anaesthetized rats, and the cross-correlogram analysis of their interactions*. Exp Brain Res, 1993. **92**(3): p. 489-94.
317. McGaraughty, S. and M.M. Heinricher, *Microinjection of morphine into various amygdaloid nuclei differentially affects nociceptive responsiveness and RVM neuronal activity*. Pain, 2002. **96**(1-2): p. 153-62.
318. Morgan, M.M. and M.M. Heinricher, *Activity of neurons in the rostral medulla of the halothane-anesthetized rat during withdrawal from noxious heat*. Brain Res, 1992. **582**(1): p. 154-8.
319. Leung, C.G. and P. Mason, *Physiological properties of raphe magnus neurons during sleep and waking*. J Neurophysiol, 1999. **81**(2): p. 584-95.
320. Wagner, K.M., Z. Roeder, K. Desrochers, A.V. Buhler, M.M. Heinricher, and D.R. Cleary, *The dorsomedial hypothalamus mediates stress-induced hyperalgesia and is the source of the pronociceptive peptide cholecystinin in the rostral ventromedial medulla*. Neuroscience, 2013. **238**: p. 29-38.
321. Hurley, R.W. and D.L. Hammond, *The analgesic effects of supraspinal mu and delta opioid receptor agonists are potentiated during persistent inflammation*. J Neurosci, 2000. **20**(3): p. 1249-59.

322. Porreca, F., S.E. Burgess, L.R. Gardell, T.W. Vanderah, T.P. Malan, Jr., M.H. Ossipov, D.A. Lappi, and J. Lai, *Inhibition of neuropathic pain by selective ablation of brainstem medullary cells expressing the mu-opioid receptor*. J Neurosci, 2001. **21**(14): p. 5281-8.
323. Leshner, A.I. and G. Collier, *The effects of gonadectomy on the sex differences in dietary self-selection patterns and carcass compositions of rats*. Physiol Behav, 1973. **11**(5): p. 671-6.
324. Morimoto, Y., A. Matsumoto, Y. Koizumi, K. Ishida, T. Tamura, and T. Sakabe, [*Effect of body fat percentage on estimated propofol concentrations at awakening from anesthesia using target controlled infusion*]. Masui, 2003. **52**(9): p. 967-71.
325. Yizhar, O., L.E. Fenno, T.J. Davidson, M. Mogri, and K. Deisseroth, *Optogenetics in neural systems*. Neuron, 2011. **71**(1): p. 9-34.
326. Zimmermann, D., A. Zhou, M. Kiesel, K. Feldbauer, U. Terpitz, W. Haase, T. Schneider-Hohendorf, E. Bamberg, and V.L. Sukhorukov, *Effects on capacitance by overexpression of membrane proteins*. Biochem Biophys Res Commun, 2008. **369**(4): p. 1022-6.